Diss. ETH No. 17406

STEAM BURNS

MOISTURE MANAGEMENT IN FIREFIGHTER PROTECTIVE CLOTHING

A dissertation submitted to the

SWISS FEDERAL INSTITUTE OF TECHNOLOGY
ETH ZURICH

for the degree of
Doctor of Sciences

presented by

CORINNE KEISER
Dipl. Masch.-Ing. ETH
born January 26th, 1978
citizen of Hergiswil NW

accepted on the recommendation of
Prof. Dr. Ph. Rudolf von Rohr, examiner
Prof. Dr. L. Schlapbach, co-examiner
Dr. R. Rossi, co-examiner

St. Gallen, 2007

us dere bouschteu wird es fröidehuus
us em schnee vo geschter e fluss
& glychschtrom wird wächsuschtrom
die wyti wäut wartet voruss
d gruebe wird e garte
us dere knacknuss wachst e boum
& dä boum treit honigsüessi frücht
dert isch scho wieder dr wurm drin

ACKNOWLEDGEMENTS

in his laboratory. He competently introduced me into the X-ray technology and supported me with kind advice during the experiments and the evaluation of the data.

I owe a lot to all the colleagues at the laboratory, in particular to Martin Camenzind, Rolf Stämpfli, Benno Wüst, Roman Huber, Walter Bolli, Georg Bruggmann and Cordula Becker for their help for the setup and the performance of the experiments.

I would like to express my gratitude to Agnieszka and Katinka, my friends at the Laboratory, for sharing with me all the ups and downs of a PhD-student's life. Their friendship was always very important to me. And I want also to thank Yvonne Metzger who not only shared the office with me but also always advised and encouraged me in all circumstances of life.

I want to thank Giachem for his love and for always being there for me throughout those turbulent days.

A silent thought goes to Klara and Peter.

Most of all I want to thank my parents, who always believed in me and supported all of my decisions. And I thank also my brother who inspired me with the fascination of science when we were children.

TABLE OF CONTENTS

ABSTRACT

While working on a fire ground, firefighters are exposed to a hot and very moist environment. During an assignment they start to sweat heavily. A large amount of this sweat remains in the clothing layers and strongly affects the thermal insulation properties of the garment. Furthermore, new fire extinguishing techniques use small water droplets to smother the fire, producing a high water vapour partial pressure atmosphere. The protective clothing has to be able to absorb this moisture while keeping its heat protection. Additionally, when the garment is exposed to thermal hazard, moisture trapped in the clothing layers might evaporate and move towards the skin where it condenses. During the phase change of the moisture, high energy transfer to the skin takes place and second degree burns may occur. These injuries are generally referred to as steam burns which seem to emerge especially at low level radiant heat fluxes.

Aim of this thesis was to analyse the absorption and the transfer of moisture within the clothing layers and its effects on the heat transfer. The main emphasis was put on conditions for the formation of steam burns.

In a first step, the distribution of moisture in the layers of a firefighter protective clothing system (usually three layers of firefighter protective clothing plus the underwear and a work wear) was studied. The location and amount of moisture in the protective clothing affects the ability of hot steam to arise and also to move through the clothing layers towards the body. The moisture content of a single layer was found to be not only dependent on the material properties of that particular layer but mainly on properties of the neighbouring layers or even of the whole combination. Effects of the moisture absorption ability of the underwear and

wicking properties of the neighbouring layer were superimposed. Especially the second layer of the combination proved to be of high importance for the moisture distribution.

The aim of the subsequent study was to determine the speed of evaporation and vapour diffusion through protective clothing layers. As humidity sensors were too slow to measure fast changes of humidity inside the clothing layers, temperature changes were used to analyse the evaporation of moisture. The temperature courses of the measurements could be regarded as consisting of two superimposed curves. First, the curve of the textile including a moist layer from which the moisture is evaporating. Second, the curve of heating up the dry textiles after all moisture has evaporated out of the clothing layers. The end of the evaporation was clearly visible as the point at which the temperatures quickly changed after a phase with constant temperatures. Temperatures within the clothing layers containing a wet layer never rose higher than the temperatures within dry clothing. As soon as all moisture had evaporated, the temperature increase followed exactly the curves of the measurements of dry samples.

Steam burns are assumed to appear during fire fighters assignments especially at low level radiant heat fluxes. Heat fluxes measured in wet combinations were not higher than in dry combinations. Therefore, it may be assumed that steam burns might not occur due to a higher heat transfer in wet conditions but more likely due to the condensation of moisture on the skin.

In further study the moisture transfer within protective clothing layers at low level thermal radiation was analysed by using X-ray radiography. Moisture accumulation was found in the underwear and the inner layer of the firefighter jacket when one of the outer layers was initially wet. As the layers between the inner layer of the jacket and the initially wet layer stayed dry throughout the measurement, moisture transfer must have taken place by evaporation in the wet and condensation in the inner layers.

ZUSAMMENFASSUNG

Feuerwehrleute sind während ihrer Arbeit einer heissen und sehr feuchten Umgebung ausgesetzt. Dadurch schwitzen sie meist sehr stark. Ein grosser Teil des Schweisses sammelt sich in ihrer Schutzbekleidung an und beeinflusst dadurch die Wärmetransfereigenschaften der Bekleidung. Ausserdem werden in der Brandbekämpfung neue Techniken eingesetzt, bei denen das Feuer durch zerstäuben des Wasserstrahls bekämpft wird. Dadurch entsteht ein hoher Wasserdampfpartialdruck in der Atmosphäre. Die Schutzbekleidung muss in der Lage sein, diese grossen Feuchtigkeitsmengen aufzunehmen und trotzdem ihre Schutzfunktion nicht zu verlieren. Wenn die durchnässte Kleidung einem plötzlichen Hitzeeinfluss ausgesetzt ist, kann es geschehen, dass die Feuchtigkeit in der Kleidung verdampft. Der entstandene Dampf bewegt sich innerhalb der Kleidung Richtung Haut, wo er kondensiert. Während der Phasenumwandlung wird Energie abgegeben, welche auf der Haut Verbrennungen bis zu zweiten Grades verursachen kann. Solche Verbrennungen werden als Dampfverbrennungen bezeichnet. Sie scheinen besonders bei relativ tiefen Hitzestrahlungsintensitäten aufzutreten.

Ziel dieser Arbeit war es, die Absorption und den Transfer von Feuchtigkeit innerhalb von Feuerwehrschutzbekleidungen und ihren Einfluss auf den Wärmetransfer zu untersuchen. Hauptaugenmerk wurde auf Bedingungen die zur Entstehung von Dampfverbrennungen führen gelegt.

In einem ersten Schritt wurde die Absorption und Verteilung von Feuchtigkeit innerhalb der Feuerwehrschutzbekleidung (üblicherweise eine dreischichtige Feuerwehrschutzbekleidung in Kombination mit Unterwäsche und Arbeitskombi) untersucht. Die Lokalisation und die Menge der Feuchtigkeit in der Schutzbekleidung beeinflusst die Entstehung von Dampf und

den Transfer des Dampfes durch die Bekleidung in Richtung Haut. Es hat sich herausgestellt, dass die Feuchtigkeitsmenge, die sich in einer Schicht ansammelt, nicht nur von den Eigenschaften dieser einen Schicht abhängt, sondern besonders auch von den Eigenschaften der benachbarten Schichten oder sogar von der gesamten Bekleidungskombination. Das Feuchteabsorptionsvermögen der Unterwäsche und die Feuchteleitfähigkeit der darauf folgenden Schicht hängen stark zusammen. Es stellte sich heraus, dass besonders die zweite Schicht des Bekleidungssystems einen grossen Einfluss auf die Feuchtigkeitsverteilung in der gesamten Kombination hat.

Das Ziel der nächsten Studie war, herauszufinden, wie schnell die Feuchtigkeit in den Bekleidungsschichten verdampfen kann und wohin der entstandene Dampf diffundiert. Da sich bei Vorversuchen herausstellte, dass Feuchtigkeitssensoren zu langsam sind um schnelle Feuchtigkeitsveränderungen zu messen, wurde die Verdampfung anhand von Temperaturmessungen bestimmt. Die gemessenen Temperaturkurven bestanden aus zwei überlagerten Kurven. Einerseits waren dies die Kurven während der Verdampfungsphase und andererseits die Kurven in denen die Temperaturen stark ansteigen, nachdem alle Feuchtigkeit verdampft ist. Das Ende der Verdampfungsphase ist klar ersichtlich, da zu diesem Zeitpunkt die Temperaturen innerhalb der Schichten plötzlich stark ansteigen. Solange Feuchtigkeit in den Bekleidungsschichten vorhanden war, stieg die Temperatur nie höher als die Temperaturen die in gleichen trockenen Mustern gemessen wurden. Erst nachdem alle Feuchtigkeit verdampft ist, näherten sich die Temperaturen den Werten der trockenen Vergleichsmessungen an.

Man nimmt an, dass Dampfverbrennungen bei Feuerwehreinsätzen vor allem bei niederen Strahlungsintensiäten entstehen. Da jedoch während der Verdampfung keine höheren Hitzeflüsse gemessen wurden als bei den trockenen Vergleichsmessungen, liegt der Schluss nahe, dass die Dampfverbrennungen durch die zusätzliche Energieübertragung durch Kondensation des Dampfes auf der Haut entstehen. In einer weiteren Studie wurde daher der Feuchtigkeitstransfer innerhalb der Bekleidungsschichten mit Röntgenradiographie untersucht. Feuchtigkeit hat sich in den inneren Schichten der Bekleidung (Unterwäsche und Futter der Feuerwehrjacke) angesammelt. Da die dazwischen liegenden Schichten während der Messung mehrheitlich trocken blieben, lässt sich schliessen, dass ein Feuchtigkeitstransfer durch Verdampfung und Kondensation zu den inneren Schichten stattgefunden hat.

NOMENCLATURE

A	Area	$[m^2]$	$\dot{m}$	Mass flux	$[kg/m^2s$ or $kg/m^3s]$
b	Mass transfer coefficient	$[m/s]$	n	Constant depending on whether	
C	Moisture concentration	$[mol/m^3]$		flow is laminar or turbulent	-
D	Diffusion coefficient	$[m^2/s]$	P	Total pressure	$[Pa]$
d	Thickness	$[mm]$	ΔP	Effective pressure gradient	$[Pa]$
E	Evaporation coefficient	-	p	Partial pressure of the	
f	Volume fraction of voids	-		water vapour	$[Pa]$
g	Gravitational acceleration	$[m/s^2]$	Pr	Prandtl number	-
Gr	Grashof number	-	Q	Heat flux	$[W/m^2]$
H	Supplied heating power	$[W]$	R	Universal gas constant	$[J/mol{\cdot}K]$
ΔH	Heat of adsorption per unit mass	$[J/kg]$	r	Capillary radius	$[mm]$
h	Natural convection heat		Ra	Rayleigh Number	-
	transfer coefficient	$[W/m^2K]$	R_{ct}	Thermal resistance	$[m^2K/W]$
h_{max}	Maximal wicking height	$[mm]$	R_{et}	Water vapour resistance	$[m^2Pa/W]$
I	Intensity of the attenuated		Rg	Moisture Regain	-
	X-ray	$[photons/mm^2s]$	RH	Relative humidity	-
I_0	Incident intensity	$[photons/mm^2s]$	R_{H2O}	Specific gas constant	
k	Thermal conductivity	$[W/m{\cdot}K]$		of water vapour	$[J/kg{\cdot}K]$
L	Characteristic length	$[m]$	T	Temperature	$[K]$
l	Length	$[mm]$	t	Time	$[s]$
M	Local moisture content	$[kg/kg]$	V	Volume	$[m^3]$
	respectively moisture content per unit		v	Fluid movement rate	$[m/s]$
	area or per volume	$[g/m^2$ or $g/m^3]$	W	Molecular weight	$[g/mol]$
m	Mass	$[kg]$	X	Volume fraction	-

Greek

α	Thermal diffusivity	$[m^2/s]$
β	Volumetric thermal expansion coefficient	$[1/K]$
γ	Surface tension	$[N/m]$
δ	Diffusion resistance factor	-
ε	Absorption coefficient of the textile surface	-
ε_γ	Volume fraction of the gas phase	-
η	Viscosity of the fluid	$[Pa\cdot s]$

θ	Equilibrium contact angle	$[°]$
λ	Geometric constant	-
μ	Attenuation coefficient	$[1/cm]$
ν	Kinematic viscosity	$[m^2/s]$
ρ	Density	$[kg/m^3]$
σ	Stefan-Boltzmann constant	$[W/m^2K^4]$
τ	Fabric tortuosity	-
Φ	Porosity	-
φ	Latent heat of evaporation	$[J/kg]$
Ω	Damage integral	-

Subscripts

air	Air
amb	Ambient
clim	Conditioned
cond	Conduction
cosa	Condensation
cove	Convection
dr	Dripped off
dry	Dry
eff	Effective
evap	Evaporation
fab	Fabric
fib	Fibres
g	Gas
H_2O	Water
in	Into the system
J	Jacket
lid	Lid of the measurement cell

liqu	Liquid water
max	Maximal
out	Out of the system
p_2, p_3	Phase 2, phase 3
rad	Radiation
sat	Saturation
skin	Skin
sorp	Sorption
SU	Station uniform layer
sup	Supplied
surf	Surface
sys	System
tot	Total
UW	Underwear
vap	Water vapour
w	Water
wet	Wet

PART I: INTRODUCTION

1   BACKGROUND

Although firefighters are often admired as heroes, they are no supermen. They need protection against the hazardous working environments. Dangerous thermal exposures are manifold and reach from a hot environment, high thermal radiation, contact with hot objects, exposure to different kinds of flames up to flashover situations. Working under those conditions is not only hazardous in sight of possible burns, but it also puts great physical demands on the firefighter.

A main problem in firefighting is the very moist environment. Water is used to fight the fire and sweat is produced by the body in order to cool down during intense physical exercise. It is unavoidable that moisture accumulates in the protective clothing. There it strongly affects the heat protection properties of firefighter protective garments. Heat transfer properties in textile layers change severely with additional moisture. The presence of moisture increases both thermal conductivity and heat capacity of the fabric. The effect of moisture in clothing combinations has been studied by different authors [1-6]. Contradictory results have been found for different conditions as either an increase or a decrease of heat protection was reported. The addition of moisture to clothing causes a variety of effects depending on its amount and its location [5, 7].

Altering heat protection properties is not the only problem caused by moisture trapped in clothing layers. When exposed to a sudden temperature rise, moisture in the clothing layers might evaporate, move towards the skin, condense and cause burns. These 'steam burns'

occur due to the evaporation of moisture caught in the clothing layers [2, 4]. This phenomenon seems to emerge especially at low level radiant heat fluxes [8]. However, little is known about the development of steam burns. In order to analyze the evaporation of moisture and the transport to the skin it is important to know the distribution of moisture in textile layers and the temperatures reached in these layers during exposures to heat. This may allow quantification of the amount of moisture that can evaporate and thus has the potential to cause steam burns. The location and amount of moisture in the protective clothing affects the ability of hot steam to arise and also to move through the clothing layers towards the body. Up to now, it is not firmly known which layers contain how much moisture and how this moisture affects the occurrence of steam burns.

Aim of this thesis was to gain a deeper insight into the formation of steam burns. The process of moisture accumulation in protective clothing assemblies and evaporation of the moisture within the clothing system was studied thoroughly. In order to be able to propose new textile or non-textile solutions, fundamental knowledge about the absorption, accumulation and transfer of moisture within the clothing layers had to be gained. Furthermore, it was important to understand the evaporation process of the moisture within the clothing system and the development of burns due to steam.

At first, the distribution of moisture in textile layers was analysed thoroughly. Experiments to determine the distribution and accumulation of moisture in the different layers of the protective clothing depending on time were performed and the amount of delivered moisture was analysed.

In a further study, the heat and mass transfer through wet protective clothing layers was studied. The temperature distribution within clothing layers exposed to low level thermal radiation was analysed. The amount of water that evaporated out of the clothing combinations into the environment and the moisture transfer through textile layers was determined with the aid of x-ray radiography by analysing the differences in x-ray absorption due to the changing moisture content in the textile layer. The conditions and the speed at which moisture evaporates from textile layers into air of different temperatures and relative humidity were investigated.

In a further part of the thesis, a survey about the physical processes was made. Models of the heat and moisture transfer process through textile layers, including diffusion, evaporation,

condensation, wicking, conduction, convection and thermal radiation as well as heat of sorption and heat of evaporation were compared.

Finally, suggestions for new materials, textile combinations or non-textile solutions that reduce the risk of steam burns and also improve the physiological properties of the combinations were proposed.

1.1   Firefighting

1.1.1   Firefighting environment

Firefighting environments are manifold and depend mainly on the kind of fire grounds which are for example residential, manufacturing, wildland, storage or mercantile fires. Although flashover situations in which the firefighter is surrounded by the fire are highly feared, such situations are rather rare. Firefighters normally do not fight the fire from the inside but rather from the outside of the flaming environment [9]. Heat exposure is mostly due to radiation (over 80% [10]) and firefighters are typically exposed to low thermal radiation of 5 to 10 kW/m^2 [11]. Intensities up to 200 kW/m^2 can be reached in emergency situations as for example in industrial fires [12, 13]. Ambient temperatures measured by Rossi [11] in a training situation reached 100-190 °C at 1 m above ground. Lawson [2] reported temperatures over 300 °C on the floor in post flashover situations.

The severity of the thermal exposure depends on air temperature as well as radiative heat flux. Three levels of firefighter exposure conditions were defined by Hoschke [14] based on Abbott et al. [15]:

- In routine conditions air temperatures range up to 70 °C and 1.6 kW/m^2. This corresponds to firefighting with a distance to the fire, which is like being outside on a hot summer day or close to a small open fireplace.
- Ambient temperatures in hazardous conditions range from 70 °C to 300 °C and 1.6 kW/m^2 to 12 kW/m^2. Those conditions arise commonly when fighting a fire outside a burning room or a small burning building. Protective clothing provides protection in order to fight that kind of fire, which lasts normally less than 30 minutes [5].

- Emergency conditions are defined by air temperatures over 300 °C in combination with radiative heat flux over 12 kW/m^2. Such conditions may appear in flashover situations or in aircraft incidents with burning fuel. Protection provided by the protective clothing might be enough to escape the situation.

Even at relatively low air temperatures high thermal radiation may appear [11]. Outside of burning buildings high thermal radiation can be reached even though the environmental temperature is low. In a distance of 6 m from a burning house there may still appear thermal radiation of 50 kW/m^2 [2].

Statistics normally do not provide details about how skin burns occurred [9]. Most of the firefighting assignments are performed at low level thermal radiation. Emergency conditions are quite rare. But long-time exposure to low heat fluxes may also lead to burn injuries. Furthermore, heat strain, fatigue and heat collapse are quite common incidents. In a statistical analysis about firefighter fatalities in the United States 45% of the firefighters deaths were caused by overexertion or stress while only 7% of the firefighters died due to burns [16].

1.1.2 Physiology

Effective physiological performance of a human is only possible if the body core temperature does not rise above 39 °C. If the core temperature rises beyond 39 °C the effectiveness of the person is reduced [2, 11, 17, 18]. Heat stress may cause thermal discomfort, impaired performance, illness and collapse. At a core temperature of 41 °C, thermoregulation may not function anymore and above 43 °C, it may even be fatal [2]. This means that the human body has to keep a balance between heat production and heat dissipation, which in turn means that at high temperatures or high physical activity it constantly has to get rid of metabolic heat. The metabolic rate of an average resting human is about 60 W/m^2. Average metabolic ranges are between 100 W/m^2 for light physical exercise and 250 W/m^2 for very heavy work [19]. As firefighter protective clothing is heavy, stiff and very insulating the metabolic rate increases due to this extra load. The additional equipment like breathing apparatus, belt, helmet and other devices have also to be taken into consideration. This equipment may reach up to 30% of the body weight of a firefighter [18]. All in all, the metabolic rate may reach up to 500 W/m^2 during firefighting or even higher for a short time [19, 20].

As firefighter protective clothing provides a very good insulation against heat coming from the environment, it also insulates the heat produced by the body. The only possibility to release heat in such situations is by evaporation of sweat. During an assignment of 20 to 30 minutes a firefighter looses about 1.2 l/h - 1.8 l/h sweat [2]. The sweat rate may even reach up to 4 l/h for short duration [11]. Per evaporation of 1 l sweat, 672 Wh are taken from the body (at a temperature of 35 °C). The sweat has to evaporate directly from the skin. Otherwise the cooling effect of the body is reduced, as only a part of the sweat is actually cooling the body. Parts of the moisture wick to the protective clothing or drip off. In their study Schopper-Jochum et al. [18] performed wear trials with 4 trained human subjects wearing 5 different firefighter jackets. The trials were performed at 30 °C, 50% RH and a wind speed of 0.2 m/s. The subjects reached average metabolic rates ranging between 350-1242 W. In this study, Schopper-Jochum et al. [18] found that 30% to 44% of the sweated amount of moisture accumulated in the clothing system. This moisture is lost for the body cooling as it will not evaporate directly on the skin.

A more detailed review about the physiology of firefighters working in a hot environment was made by Taylor [21].

1.2 Burns

Even though firefighters are well equipped, burns cannot always be avoided. They appear due to contact with hot objects, exposure to thermal radiation or to hot liquids. The heat imposed on skin causes protein coagulation at the surface or within the skin. Burns are divided into three degrees. This classification is based on the depth of tissue damage [22]:

- First degree burns are superficial burns. The skin is bright red and sensitive to pain, which is a typical inflammation reaction with increased blood circulation.
- In second degree burns, blisters appear due to deep dermal damage. The epidermis is detached and disintegrated. The burned area shows dullness to pain but is still sensitive to touch.
- Third degree burns are full thickness skin burns where the burned area is completely insensitive.

A thorough study about thermal injury has been performed by Moritz et al. [23]. They carried out experiments on pigs and also on human volunteers to find the relation between the skin

temperature and the duration of the thermal exposure to cause pain and irreversible skin injury. They found that at a skin temperature of 44 °C irreversible damage to epidermal cells appeared. At this temperature, it took about 6 hours to cause burns. But for each degree of temperature rise between 44 °C and 51 °C, half of the time was needed until irreversible damage was visible. Above 51 °C the rate of injury decreased and the time-temperature curve approached the temperature axis asymptotically. At skin temperatures above 70 °C less than 1 second is required to cause full thickness burns. From these results they derived an equation to calculate thermal injury depending on skin temperature and duration of the exposure [23-26]. This equation (1.1) is known as damage integral Ω:

$$\Omega = 3.1 \cdot 10^{98} \int_0^t e^{-75000/(T_{skin}+273)} dt \qquad\qquad (1.1)$$

| Ω | Damage Integral | - |
| T_{skin} | Skin temperature | [K] |

At values of Ω less than 0.53, no irreversible epidermal injury is recognisable. Exposures with Ω higher than 1 cause transepidermal necrosis.
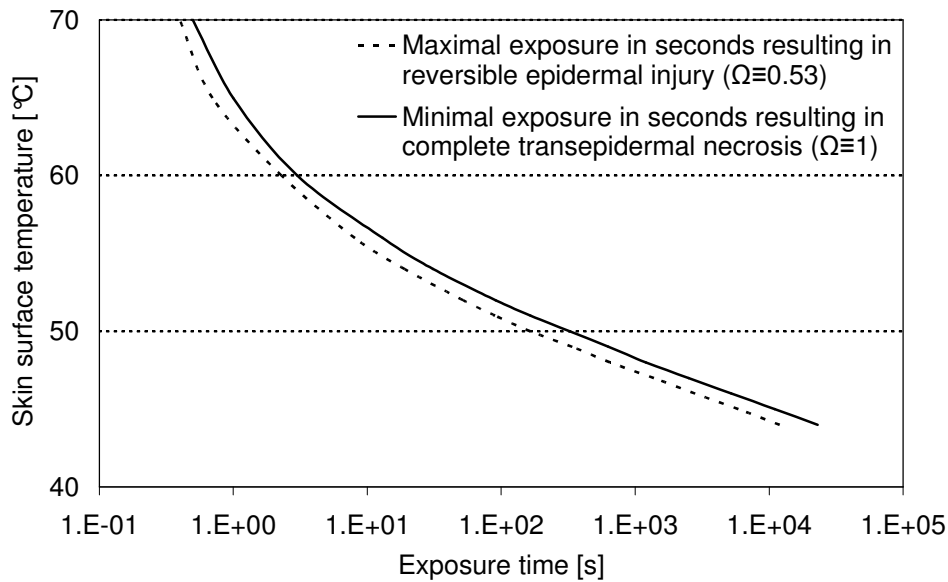
Figure 1.1: Maximal exposure time at different temperatures to cause reversible epidermal injury respectively minimal exposure time resulting in transepidermal necrosis according to Henriques damage integral [24].

In another study, Hardy et al. [27] found, that the immersion of the skin into water with a temperature between 36 °C and 40 °C evoked pain. This pain disappeared after 5 to 6 s. Stoll and Chianta [28] reported a threshold value of 44 °C skin temperature at which pain appeared.

Holcombe [12] related the duration until second degree burn was reached to the energy transfer to unprotected skin. With 1.3 kW/m^2 second degree burn appeared after 167 s while it lasted only 7 s at 12.6 kW/m^2. In firefighting second degree burns are used as threshold value for security norms, as the skin layers are not completely destroyed and no irreversible damage appears [12].

Most of the burns of firefighters appear at the hands, the shoulders, the arms (biceps), knees and also at the head [2]. A lot of burns appear even without being in contact with the fire at temperatures of the clothing lower than 100 °C [2]. The clothing stores a huge amount of energy and burns may appear even after the end of the thermal exposure.

1.2.1 Steam burns

A big problem in firefighting is the moisture in the protective clothing. It is assumed that most of the burns appearing during firefighting are scalds [4]. Scalds are thermal injuries due to hot liquids or steam. Temperatures at scalds are relatively low and proteins are degenerated in the most superficial tissues [22].

Up to now, steam burns are thought to appear due to sudden evaporation of moisture trapped in the clothing layer at thermal exposure. Hot steam moves to the inside, driven by temperature and vapour pressure gradients and condenses on the skin what causes burns.

The probable formation of steam burns is shown in Figure 1.2. Latent heat of evaporation (2257 kJ/kg at 100 °C) is released to the environment during condensation of water vapour. As the skin has a higher heat capacity than the surrounding air, it will absorb a big amount of this energy. This energy will additionally increase the skin temperature and thus contribute to the burn. These burns are thought to be more severe than dry burns as skin may absorb hot steam [29].

During human subject test in a firefighter training house, Rossi [11] reported that one of the firefighters suffered burns at measured skin temperatures of only 42 °C while other

firefighters reached skin temperatures of up to 45.5 °C without any burns. Rossi concluded that this firefighter, who was wearing a PVC coated jacket, suffered burns of his own sweat.
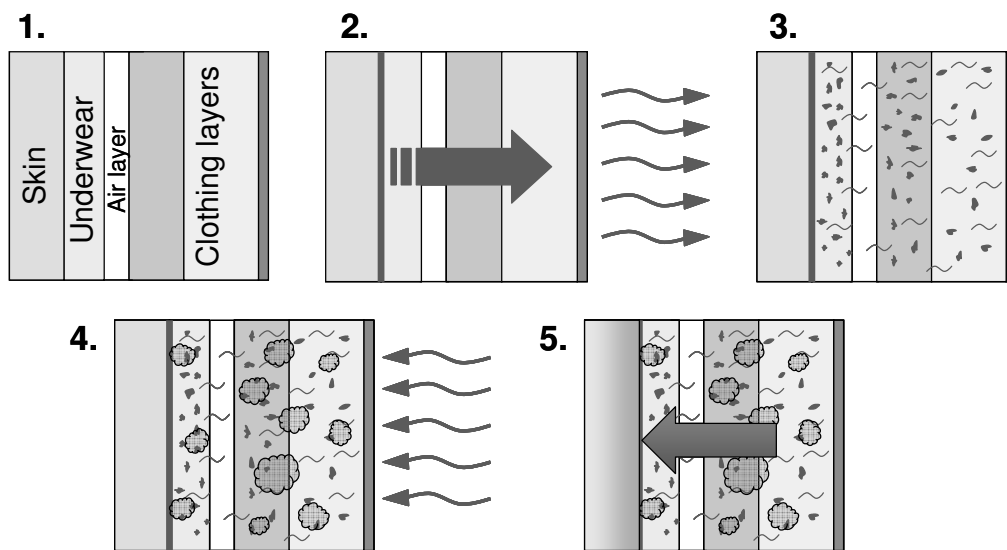
Figure 1.2: Probable formation of steam burns: (1) Clothing combination. (2) The firefighter starts to sweat. Some of the moisture diffuses out of the garment. (3) But some moisture condenses in the clothing layers. (4) The firefighter is exposed to a hot environment and the moisture in the clothing layers starts to evaporate. (5) The hot steam moves towards the skin and causes steam burns.

The severity of scalds is in the beginning mostly underestimated, as only redness of the skin is visible. Only a few days later the epidermis dissolves from the dermis and the whole degree of the burn gets visible. Brans et al. [30] compared scalds with contact burns of pigs. They stated that there is a clear difference in the pathophysiology of scalds and contact burns. Scalds seemed superficial but they healed with pronounced scar formation. In contact burns the epidermis was detached and disintegrated. In scald burns the epidermal layer was intact during the first days after injury, but lost its adherence to the dermis afterwards.

It is almost impossible to find statistical information about scalds of firefighters. A lot of burns are minor burns which do not need medical treatment. The others, which need medical treatment, are not differentiated from dry burns.

Figure 1.3 shows a firefighter approaching an open fire. On the right side the steam escaping the protective clothing is clearly visible. High environmental temperatures do not implicate that immediately burns appear. In a steam bath, temperatures range between 40 °C and 50 °C at a relative humidity of 100%. And in Finnish saunas temperatures of up to 120 °C at about 40% relative humidity are reached. The body does not seem to have any problems with those

conditions. It is able to cool down by the evaporation of sweat on the skin and by changing the blood circulation through the vessels close to the skin [31]. A few sauna-related burns are reported by Morris et al. and Papp [32, 33]. Most of the accidents in saunas happen due to exceeding alcohol consumption. In one case reported by Morris et al. decreased blood pressure resulting in impaired skin circulation was thought to be responsible for the occurrence of burns [32]. A man with a circulatory collapse in a sauna suffered second degree burns on the whole body. Morris et al. concluded that the reduced blood perfusion due to the circulatory collapse resulted in a reduced heat transfer by blood circulation, what finally resulted in burns.

Figure 1.3: A firefighter is approaching the fire. Steam escaping his protective clothing is visible on the right side, which is towards the fire.

Up to now, not much is known about how steam burns happen and what could be done to reduce the risk of steam burns.

1.3   Protective clothing

Firefighter protective clothing is essential for firefighters in order to protect against heat, hot liquids, chemicals and mechanical impacts. The protective clothing enables the firefighter to approach the fire in order to rescue people from the fire and to fight the fire. Many studies have been performed in this area [2, 11, 12, 15, 18, 19, 34-37]. A broad survey about research in the area of protective clothing for firefighters was done by Torvi et al. [38]. Since then, different groups like [5, 19, 34, 39-46] worked in this field and mainly concentrated on physiological aspects of firefighter protective clothing as well as on the influence of moisture on thermal protection.

Firefighter protective clothing has to fulfil a variety of different demands according to the European norm (EN 469) [47]:

- protection against heat from flames and thermal radiation
- protection against hot liquids and other chemicals
- resistance against abrasion and other mechanical loads
- not flammable and not fusible
- no shrinking
- easy to wash
- light and comfortable
- breathable

Some of those demands are even contradictory, as for example the protection against heat from flames and thermal radiation decreases the comfort of the clothing. Firefighter protective clothing has improved continuously for the last few decades. Former clothing systems consisted of leather with woollen nonwoven as lining. Leather is quite heavy and it is shrinking strongly when exposed to heat. Wool on the other hand is hygroscopic and absorbs a big amount of moisture which reduces the wear comfort of firefighting protective clothing.

Later, PVC (polyvinylchloride) coated jackets appeared on the market. Most of them were still in combination with woollen nonwoven liner. The problem of PVC was its water vapour impermeability. Moisture was not able to escape the clothing. Water vapour pressure within the clothing increased until it reached the saturation pressure [19]. Little evaporative cooling could take place and heat collapses were quite common with those clothing systems [11, 18, 37]. Studies comparing PVC coated jackets with jackets including a breathable membrane

showed that core temperature [37] and also sweating rate [18] were bigger for subjects wearing PVC jackets.

The occurrence of burns due to the evaporation of moisture trapped in the clothing layers was also increased with water vapour impermeable clothing systems [4, 11].

Following these results, multilayer protective clothing containing a water vapour permeable membrane (as for example PTFE (polytetrafluorethylene)) became widely accepted. Holcombe [12] showed that multilayer protective clothing assemblies provide a better protection than single layer protective clothing, as air layers within the clothing system provide the best insulation [2]. The heat transfer properties are about the same for most of the fibres. The thermal properties of a textile are mostly independent of the kind of fibres. They depend rather on the textile construction and the amount of air trapped between the fibres [12].

State-of-the-art firefighter protective clothing is a multilayer high tech product, consisting mainly of four layers:

- **Outer layer:** protects against all kind of thermal hazards and mechanical impacts
- **Water barrier:** breathable membrane, which protects against water and other fluids
- **Thermal barrier:** insulating layer, which protects against heat
- **Inner layer:** eudermic lining, which protects the thermal barrier against abrasion
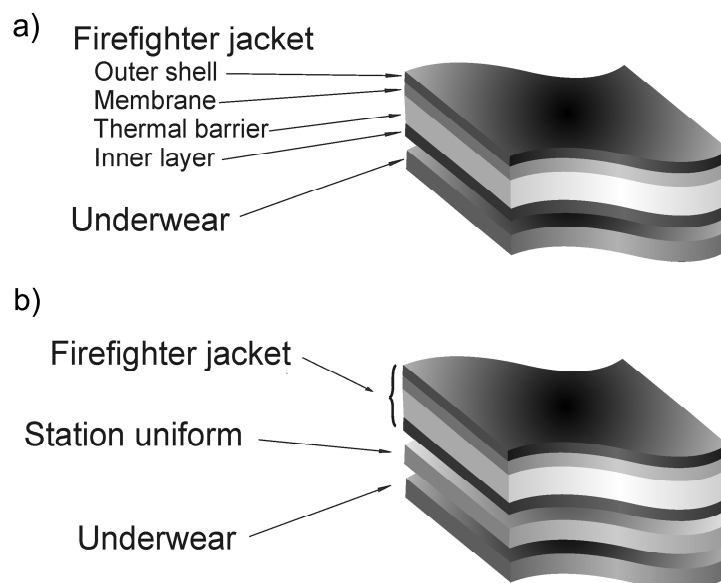
Figure 1.4: Typical layers of a firefighter protective clothing system. a) Firefighter jacket and underwear, b) occasionally, an additional station uniform is worn between the underwear and the firefighter jacket.

Firefighters wear occasionally an additional station uniform between the underwear and the firefighter protective clothing.

Heat and moisture transfer properties of clothing assemblies are not the sum of the properties of the single layers [48]. For example different outer layers may have a big influence on the performance of the underwear. At short term thermal exposure mainly the outer layer of the assembly protects against the heat. At longer term exposure also the thermal barrier gets involved into the heat protection as well [5].

Problems of state-of-the-art firefighting protective clothing systems are caused by the too good thermal insulation of the clothing. Firefighters used to feel the heat on their earlap. The earlap was not protected by any protective clothing layer. If pain appeared on the earlap, they knew that they were too close to the fire and could escape the situation. As state-of-the-art firefighter protective clothing is very well insulated, firefighters do not feel when they are too close to the fire. There is no alarm system. Energy is stored in the protective clothing system. As soon as the firefighter starts to feel pain and withdraws from the fire, it might already be too late. Heat stored by the clothing system (mostly in the outer layer) is transferred to the inside, increases the temperature within the clothing and might cause burns (reported by members of a professional fire brigade, 2007).

1.3.1 Moisture and firefighting

Properties of firefighter protective clothing are strongly influenced by the presence of moisture. It affects heat transfer as it alters thermal properties such as heat capacity or thermal conductivity of the protective clothing system. Both, the heat capacity and the thermal conductivity increase due to the presence of moisture [49]. The influence of moisture in clothing systems on heat transfer has been studied extensively [50, 51]. In most of these studies, the clothing systems were analysed or simulated at ambient temperatures or in cold climates. Only a few studies were performed on heat and mass transfer in protective clothing systems under thermal radiation [1-3, 8] or under flash fire exposure [40].

Lee et al. [3] found that the effect of moisture on thermal insulation depends on the intensity of the thermal radiation. At 20 kW/m^2 moisture improved the thermal protection but at 84 kW/m^2, it had a negative impact on the thermal protection. Contrary to this, Barker et al. [1] found in their study that already at low level thermal radiation of 6.3 kW/m^2 high moisture

contents in the clothing system decreased the time until second degree burns arose. A minimal burn time was reached at about 15% moisture content. Rossi et al. [52] also found that at low level radiant heat flux moisture present in the inner layers of the protective clothing decreased the protective performance.

Those contradictory results are not surprising as a variety of different factors influence the heat transfer in protective clothing. The most important factors are the kind of heat transfer, the amount and the location of the moisture, the type and conditioning of the materials and the duration and intensity of thermal exposure [7]. For most studies time to second degree burns or alarm time were used. Due to its high heat capacity, the water within the protective clothing stores a big part of the supplied energy and reduces initially the energy transferred to the skin [3]. But as the amount of stored energy within the clothing increases [41, 53], energy may still be released after the thermal exposure.

From his findings Lawson [2] proposed ideas for the improvement of firefighter protective clothing:

- **reduce the amount and control the location of the moisture**
- **reduce the thermal conductivity of the fabrics**
- **reduce the heat capacity of the fabrics**

Those are first ideas of how to improve firefighter protective clothing. However, a physical understanding of the effects of moisture in protective clothing will help to find better solutions for the moisture management in firefighter protective clothing.

1.4 Physical background

The physical processes involved in a firefighting environment mainly consist of heat and mass transfer (Figure 1.5). The main processes of heat transfer are conduction, convection and thermal radiation [54, 55]. Mass transfer is driven for liquid water by capillary processes and for water vapour by diffusion [56]. Heat and mass transfer processes are coupled by evaporation and condensation.

The physical model consists of three different parts, which are connected by heat and mass exchange:

- The human body producing heat (metabolic heat) and water (sweat) with its own temperature regulation system (blood perfusion and evaporation of sweat) in order to keep a constant core temperature of 37° +/-2 °C.
- Heat flux from high temperature source (e.g. conduction, convection and radiation)
- Multilayer protection system storing surplus of water and absorbing thermal energy in order to avoid temperature increase at the body surface.
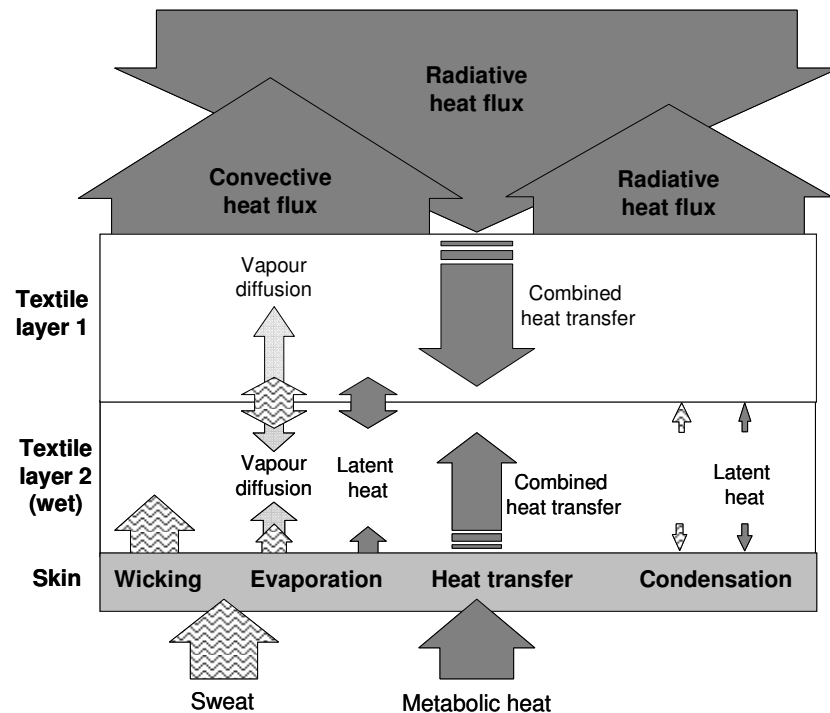
Figure 1.5: Processes involved in heat and mass transfer of wet firefighter protective clothing.

1.4.1 Heat transfer

Heat is transferred due to the temperature gradient between the skin and the firefighting environment. Metabolic heat is released by the skin (up to 500 W/m^2 [19]). Energy transfer from outside to the skin depends on the kind and intensity of thermal exposure.

Conduction

Conductive heat transfer happens as soon as the skin gets into contact with the protective clothing. For example if the firefighter is touching a hot object or is kneeling on the ground. Conductive heat transfer is defined by:

$$Q_{cond} = \frac{k}{d} \cdot (T_{skin} - T_{surf})$$ (1.2)

Q_{cond}	Heat transfer by conduction	[W/m^2]
k	Thermal conductivity	[W/m·K]
d	Thickness of the compressed clothing	[mm]
T_{surf}	Temperature of the hot surface	[K]
T_{skin}	Skin temperature	[K]

The thermal conductivity of air (k_{air} = 0.024 W/m·K @ 20 °C - 0.032 W/m·K @ 100 °C) is small compared to the one of the fabric (k_{fab} = 0.04 W/m·K) or of water (k_{liqu} = 0.6 W/m·K). Therefore, air is a very efficient insulator. Energy transferred to the skin decreases with increasing air layer up to 7 mm [45]. Conductive heat transfer gets more harmful if the protective clothing is pressed against the skin. Worst situation would be if the protective clothing is sucked with water and then pressed against a hot object.

Convection

Convective heat transfer is the exchange of heat of an object with the surrounding air and is caused by wind movement, for example by external ventilation or by body movement (forced convection) or it appears due to flows caused by density differences due to temperature gradients (natural convection):

$$Q_{cove} = h \cdot (T_{surf} - T_{amb})$$ (1.3)

Q_{cove}	Convective heat transfer	[W/m^2]
h	Natural convection heat transfer coefficient	[W/m^{2}K]
T_{surf}	Surface temperature	[K]
T_{amb}	Ambient temperature	[K]

Natural convection can be neglected within air spaces smaller than 8 mm [45]. Therefore air layers within protective clothing of 7-8 mm provide the best thermal insulation.

Thermal radiation

Thermal radiation heat transfer is caused by the temperature difference between two facing surfaces, for example the surface of the protective clothing and the surrounding surfaces:

$$Q_{rad-out} = \varepsilon\sigma\left(T_{surf}^{\;4} - T_{amb}^{\;4}\right)$$

(1.4)

$Q_{rad-out}$	Thermal radiation outward heat flow	[W/m^2]
ε	Absorption coefficient of the textile surface	-
σ	Stefan-Boltzmann constant	[W/m^{2}K^4]
T_{surf}	Surface temperature	[K]
T_{amb}	Temperature of the surrounding surfaces	[K]

Textiles have a quite high absorptivity (absorption coefficient of 0.95-0.98) [11]. Therefore, they absorb high amounts of the radiative energy. Protective clothing systems with a lower absorptivity would not heat up that fast. Such clothing, for example aluminised, exists on the market. Polished aluminium has a low absorptivity (absorption coefficient of ~0.1) and most of the impinging thermal radiation is reflected. However, during firefighting the protective clothing gets dirty and wet, which increases the absorptivity and decreases the radiant heat protection.

1.4.2   Mass transfer

Diffusion

Vapour transfer through a porous material is described by the diffusion equation (1.5) [56]:

$$\frac{\partial C}{\partial t} = \frac{\partial}{\partial x}\left(D_{eff}\frac{\partial C}{\partial x}\right)$$

(1.5)

C	Moisture concentration	[mol/m^3]
D_{eff}	Effective diffusion coefficient of water vapour through a textile	[m^2/s]

Diffusion is driven by a vapour pressure gradient [57]. The effective diffusion coefficient in a textile layer differs from the diffusion coefficient into air and is given by Chitrphiromsri et al. [40]:

$$D_{eff} = \frac{D\varepsilon_\gamma}{\tau}$$

(1.6)

ε_γ	Volume fraction of the gas phase	-
τ	Fabric tortuosity	-

Liquid moisture transfer

Liquid moisture transfer is a process depending on hydrophilic properties of the material (fibres), the yarn, the fabrication process of the fabric as well as the finish and combination of different layers. Extensive research has been performed in this area [58-63].

A differentiation between wetting and wicking can be made. Wetting describes the replacement of a solid-air interface with a solid-liquid interface. Wicking is defined as the transport of a liquid into a textile by capillary action [64]. Capillary forces are caused by spontaneous wetting.

The wicking kinetics is described by Poiseuille's equation (1.7) [65-67]:

$$v = \frac{r^2 \Delta P}{32 \eta l} \tag{1.7}$$

v	Fluid movement rate	[m/s]
l	Distance travelled within the capillary	[mm]
η	Viscosity of the fluid	[Pa·s]
r	Capillary radius	[mm]
ΔP	Effective pressure gradient	[Pa]

Whereof the maximal wicking height of a capillary with radius r can be derived:

$$h_{max} = \frac{2 \gamma \cos \theta}{r \rho_{liqu} g} \tag{1.8}$$

h_{max}	Maximal wicking height	[mm]
γ	Surface tension	[N/m]
θ	Equilibrium contact angle	[°]
ρ_{liqu}	Density of liquid water	[kg/m³]
g	Gravitational acceleration	[m/s²]

Hydrophilicity of a textile is very important for the wickability, as it dominates the equilibrium contact angle [64]. But also porosity and the size of the pores influence the wicking [66]. The effect of pore size distribution has been studied thoroughly by Zhu et al. [68] and the capillary flow in complex geometries was analysed in more details by Rajagopalan et al. [69].

The liquid moisture transfer gets more complex as soon as different textile layers are combined to a clothing system. Layer to layer wicking is only possible if in one layer a threshold amount of moisture is reached [31, 60, 70]. This amount depends on the kind of fabrics and starts at about 30% above regain [70].

Evaporation / Condensation

Evaporation from a liquid surface takes place as long as the water vapour partial pressure is smaller than the saturation pressure at the same temperature. As soon as the partial pressure reaches the saturation pressure, condensation starts.

The saturation pressure depends on the temperature and is defined by the Clausius-Clapeyron equation (1.9):

$$p_{sat} = 1.333 \cdot 10^{\left(-\frac{2919.611}{T} - 4.79518 \cdot \log_{10} T + 23.03733 \right)}$$
(1.9)

p_{sat}	Saturation pressure of water vapour	[mbar]
T	Temperature	[K]

Although often assumed for the sake of simplicity, evaporation and condensation coefficients are not equal. The condensation coefficient exceeds the evaporation coefficient [71].

Evaporation from a completely wetted textile into air is assumed to equal the evaporation of a liquid surface with the same area into air [72] and is defined by the Hertz-Knudsen equation (1.10) [73]:

$$\dot{m}_{evap} = E \sqrt{\frac{W_{H_2O}}{2\pi R}} \left[\frac{p_{sat}(T_{surf})}{\sqrt{T_{surf}}} - \frac{p_{amb}}{\sqrt{T_{amb}}} \right]$$
(1.10)

$\dot{m}_{evap}$	Evaporative mass flux	[kg/m^{2}s]
T_{surf}	Temperature at the liquid surface	[K]
T_{amb}	Ambient temperature	[K]
$p_{sat}(T_{surf})$	Saturation pressure at the liquid surface	[mbar]
p_{amb}	Ambient partial pressure of water vapour	[mbar]
R	Universal gas constant	[J/mol·K]
W_{H2O}	Molecular weight of water vapour	[g/mol]
E	Evaporation coefficient	-

The evaporation coefficient depends on the conditions at which evaporation takes place. It spreads in a range of over two decades [71].

Krischer [72] expressed the evaporation equation (1.12) by using a mass transfer coefficient b which is related with the convective heat transfer coefficient α. From this follows:

$$\dot{m}_{evap} = \frac{b}{R_{H_2O}T}\left(p_{sat}(T_{surf}) - p_v\right)$$ (1.11)

R_{H2O}	Specific gas constant of water vapour	[J/kg·K]
b	Mass transfer coefficient	[m/s]

He derived the evaporation rate within a porous material where the evaporating surface is at a distance d from the outer surface of the material:

$$\dot{m}_{evap} = \frac{1}{R_{H_2O}T}\frac{1}{\dfrac{1}{b}+\dfrac{\delta d}{D}}\left(p_{sat}(T_{surf}) - p_v\right)$$ (1.12)

d	Thickness of the textile layers above the evaporation surface	[m]
δ	Diffusion resistance factor	-
D	Diffusion coefficient	[m^2/s]

Heat of evaporation / condensation

Heat and mass transfer are linked by the heat released during evaporation, which is given by:

$$\Delta Q_{evap} = \varphi_{evap}\,\dot{m}_{evap}$$ (1.13)

ΔQ_{evap}	Heat released during evaporation	[W/m^2]
φ_{evap}	Latent heat of evaporation	[J/kg]

Heat of sorption

Adsorption is defined as the adhesion of molecules of a gas or liquid, to the surface of a solid or liquid. In our case it defines as the process of fibres taking up water vapour. Adsorption of water vapour is only happening in hygroscopic fibres and it can be described by means of a diffusion equation (1.14) into the material [74]:

$$\dot{m}_{sorp} = (1 - \Phi)\frac{\partial M_{fib}}{\partial t} \qquad\qquad (1.14)$$

$\dot{m}_{sorp}$	Rate of adsorption	$[kg/s \cdot m^3]$
Φ	Porosity of the fabric	-
M_{fib}	Moisture content of the fibres	$[kg/m^3]$

Whereof the heat of sorption can be calculated (Equation (1.15)):

$$\Delta Q_{sorp} = \varphi_{sorp} \cdot \dot{m}_{sorp} \qquad\qquad (1.15)$$

ΔQ_{sorp}	Heat of sorption	$[J/mol]$
φ_{sorp}	Latent heat of sorption	$[J/kg]$

Latent heat of sorption is in the same range as heat of condensation. But especially at non-hygroscopic materials the amount of moisture adsorbed by the fibres is small. Therefore, heat of sorption was neglected in the physical model.

1.4.3 The effect of salt on heat and mass transfer

Sweat consists to 99% of water and to 1% of sodium chloride and a couple of further substances such as urea, uric acid, fatty acids, amino acids, ammonia, saccharide, lactic acid, ascorbic acid and cholesterol. The density of sweat ranges from 1001-1006 kg/m^3, which is a bit higher than the density of water (1000-958 kg/m^3 at 0 °C-100 °C) [75]. The specific heat decreases minimally with increasing salt concentration [76]. If sweat evaporates from the skin or the clothing layers, the salt is left behind what further increases the salt concentration on the skin or in the clothing. Salt in the sweat decreases the surface tension of the water and the skin is wetted more readily. But it also reduces the local water vapour pressure. The decrease in water vapour pressure negatively impacts the evaporation rate. Surplus of sweat, on the other hand, drips off and washes up excess of salt. An equilibrium concentration of salt at the skin surface was reported to be about 5% [77]. This salt concentration has little impact on the vapour pressure and also heats of vaporisation are stated to be equal to that of water at temperature ranges of 20-60 °C [77].

2 MEASUREMENT TECHNIQUES, DEVICES AND MANIKINS

Tests on human subjects help to research the influence of clothing on human physiology in different environmental conditions. However, the behaviour of humans spreads strongly and it is time consuming and very costly to get significant results. Moreover, in hazardous environments, human subject tests would be too dangerous and are thus not possible. Therefore simpler tests to measure material characteristics, comfort properties and safety qualities are necessary. There exist various different standard tests in clothing science as well as in firefighting protective clothing: water vapour resistance, thermal resistance, thermal protective performance test (TPP) and many more. But also more complex devices and manikins such as sweating cylinder [11], sweating torso [78], sweating agile manikin (SAM) [79] or thermal manikins [80] were developed in order to study physiological and thermal incidences. Holmer gives a broad survey about different thermal manikins [81].

2.1 Comfort tests

2.1.1 Sweating guarded hot plate

The sweating guarded hot plate consists of a heatable sintered metal plate which is located in a climate chamber. In order to avoid thermal losses to the sides, the plate is surrounded by a guard with the same temperature as the plate. The temperature of the plate is kept constant at 35 +/-0.2 °C which corresponds to the average human skin temperature. The temperature of

the plate is controlled by a PT-100 temperature sensor. An air stream with a velocity of 1 +/-0.02 m/s overflows the guarded hot plate in order to remove still air layers.

Using the guarded hot plate, the thermal resistance R_{ct} [m^{2}K/W] and the water vapour resistance R_{et} [m^{2}Pa/W] of a single textile layer or a textile combination can be determined. Thermal resistance and water vapour resistance according to EN 31092 [82] are standard values in order to describe comfort properties of textiles or textile combinations.

Thermal resistance R_{ct}

The thermal resistance (R_{ct}) is defined as the temperature difference between the two outer surfaces of the sample divided by the heat flux per surface area resulting along the temperature gradient [82]:

$$R_{ct} = \frac{(T_{surf} - T_{amb}) \cdot A}{H}$$
(2.1)

A	Area of the hot plate	[m^2]
H	Supplied heating power	[W]
T_{surf}	Temperature of the hot plate	[K]
T_{amb}	Ambient temperature	[K]

In order to measure the thermal resistance, the sample is placed flat onto the guarded hot plate. As soon as the system reaches steady-state, the supplied heating power is measured, whereof the thermal resistance can be calculated. From this value, the thermal resistance of the bare hot plate has to be subtracted.

Water vapour resistance R_{et}

The water vapour resistance (R_{et}) is defined by the difference of the water vapour partial pressure between the two outer surfaces of the sample divided by the evaporative heat flux per unit area along the partial pressure gradient [82]:

$$R_{et} = \frac{(p_{surf} - p_{amb}) \cdot A}{H}$$
(2.2)

A	Area of the hot plate	[m^2]
H	Supplied heating power	[W]

p_{surf} Water vapour partial pressure at the surface   [Pa]

of the hot plate

p_{amb} Water vapour partial pressure in the ambient air   [Pa]

The sintered metal plate is soaked with distilled water and covered by a vapour permeable but liquid impermeable membrane (e.g. cellophane foil). The samples are placed flat on the membrane. In order to avoid condensation effects within the sample, the measurement is made at isothermal conditions, meaning that the environment has the same temperature as the hot plate (35 °C). At steady-state conditions, the heating power required to keep the temperature of the hot plate constant, is measured. The water vapour resistance is then calculated according to (2.2). From this value, the water vapour resistance of the plate only covered by the membrane has to be subtracted.

There exist a couple of other methods in order to measure water vapour permeability, e.g. the upright cup method, the inverted cup method or the desiccant inverted cup method. A comparison of those methods can be found in McCullough et al. [83].

2.1.2 Sweating torso

The sweating torso consists of a cylinder with the dimensions of an adult human torso (Figure 2.1) which corresponds from its surface to a quarter of the whole body. The torso is composed of different layers (Teflon, polyethylene and aluminium), which mimic the different layers of the human skin (epidermis, dermis and subcutaneous layer) as they have similar thermal properties such as heat capacity and thermal conductivity.

The torso is operated either with constant surface temperature or with constant heating power. As it is heated electrically by heating slides, either the surface temperature of the torso or the heating power can be controlled. Furthermore, it is equipped with 54 individually controllable sweating outlets allowing variable sweat rates.

Tests on the torso can be run with different predefined sequences of phases to simulate different human activities. The average surface temperature of the torso is recorded during the measurement using two nickel wires as resistance temperature detectors (RTD). Additionally PT-100 temperature sensors are distributed within the different layers of the torso.

In order to avoid thermal losses on both ends of the torso, it is equipped with two heatable guards. The weight of the torso is measured throughout the measurement (accuracy of the scale 0.1 g). Further details of this measuring device can be found in [78].

The torso is located in a climate chamber and the measurements on the sweating torso are usually performed at standard climatic conditions of 20 +/-2 °C and 65 +/-5% relative humidity.
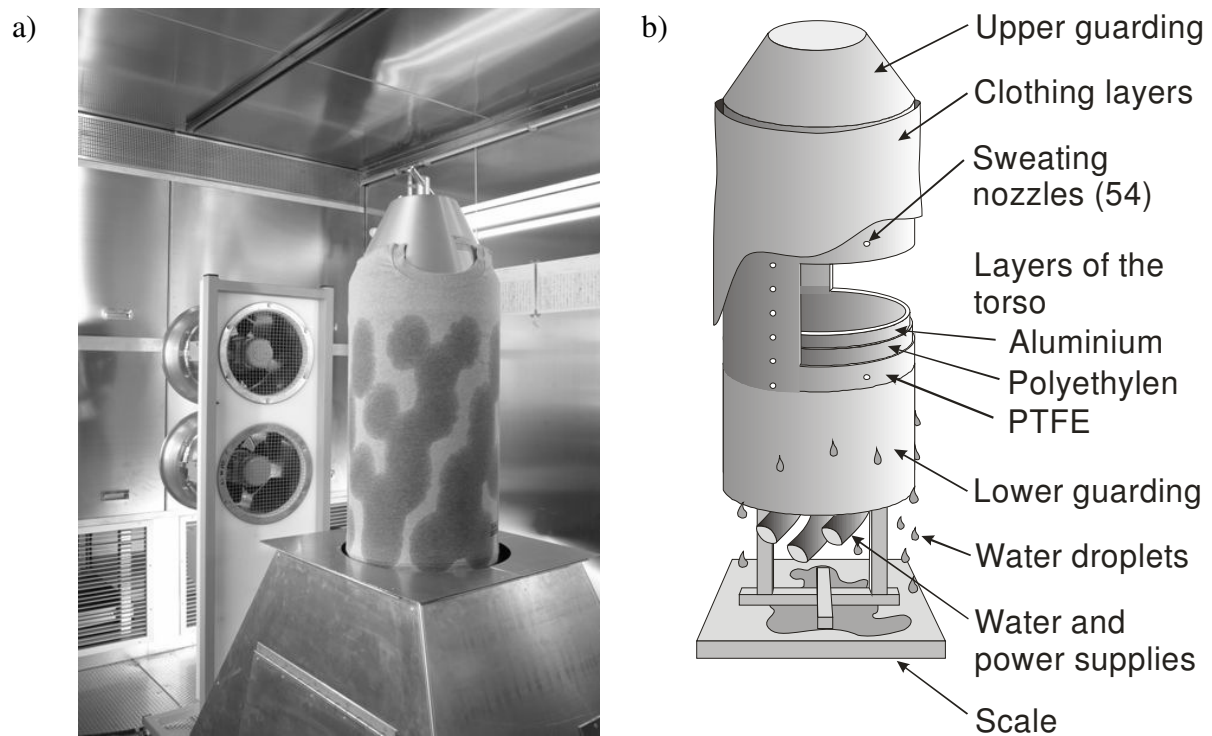
Figure 2.1: a) Sweating torso, b) sketch of the sweating torso, illustrating the major components [78].

Normally three phases are run during a torso measurement. The first phase is an acclimatization phase without sweating during which the surface temperature of the torso is kept constant at 35 °C. During the second phase each desired physical activity of the human body can be simulated. The third phase mimics the reduced activity after the exercise in order to determine the cooling of the body due to sweat still located in the clothing (post exercise chill). The number and setups of the different phases can be defined individually for the particular intention.

If the weight of each layer of the sample is determined directly before and after the measurement, the amount of moisture accumulated in that particular clothing layer during the measurement can be determined. Dripped-off water is also collected and weighed. Therefore

the evaporated amount of moisture is equal to the difference between the amount of water released during the test and the sum of water accumulated in the textile and dripped-off water.

2.1.3   Sweating cylinder

The sweating cylinder is the smaller equivalent of the sweating torso. It has the dimensions of a human upper arm. Similarly to the sweating torso, it can be run with either constant heating power or with constant surface temperature as well as with the possibility of sweating.

The sweating cylinder has two independent controllable sweating levels. Each one is equipped with 6 sweating outlets. The cylinder is heated electrically by four heating elements. Four PT-100 temperature sensors are distributed within the cylinder. During the measurement, both surface temperature and weight of the cylinder are recorded continuously. Two guards on both sides of the cylinder avoid thermal losses across the borders.

The sweating cylinder stands on a scale and the weight of the cylinder is continuously recorded.

Figure 2.2: Sweating cylinder standing on the scale.

The sweating cylinder is located in a climate chamber and the measurements are usually performed at standard climatic conditions of 20 +/-2 °C and 65 +/-5% relative humidity.

Like for the sweating torso, different phases of human exercises can be defined. The standard measuring procedure is similar to the torso measurement. For the sweating cylinder arbitrary conditions and cycles can be defined as well.

2.2   Tests of hydrophilic properties

There exist several tests to determine the hydrophilic properties of a material DIN 53814, DIN 53923, DIN 53924 [84-87]. Thereof, the method of determining the rising height in order to determine the velocity of soaking water of textile fabrics is a very common one (DIN 53924 [86]). Hereby, textile stripes (250 mm x 50 mm) are dipped into water at their lower end. After 10 s, 30 s, 60 s, and 300 s the rising height of the water inside the textile stripes is measured. This is made in both directions (weft and warp).

Another important parameter for the moisture management properties of textiles is the moisture regain. It is defined as the moisture content within a textile in relation to its dry mass. In order to determine the regain of a textile, it is weighed at standard conditions (m_{clim}). Afterwards it is dried in an oven at 110 °C until it reaches a constant weight (m_{dry}) [88].

$$Rg = \frac{m_{clim} - m_{dry}}{m_{dry}} \tag{2.3}$$

Rg	Moisture Regain	-
m_{clim}	Mass of the conditioned sample	[g]
m_{dry}	Mass of the dry sample	[g]

There exists a characteristic hysteresis curve between the regain and the relative humidity, which means that the value of the regain depends on whether it is approached from higher or lower relative humidity.

2.3   Thermal protection tests and standards

The performance requirements for thermal protective clothing are defined in EN 469 [47]. Requirements for firefighter protective clothing are for example limited flame spread, convective heat transfer (flame), thermal radiation heat transfer, dimensional changes, tensile strength, penetration by liquid chemicals, surface wetting, tear strength, waterproofness as

well as physiological parameters as described in Chapter 1.1.1. Materials used for firefighter protective clothing must not burn and melt.

For thermal protection tests, two values are very important:

- TI_{12} [s]: time at which the temperature inside the protective clothing increases by 12 +/-1 °C. This time is a rough measure for the time until pain appears.
- TI_{24} [s]: time at which the temperature inside the protective clothing increases by 24 +/-2 °C. This time is a rough measure for the time until second-degree burns appear.

The difference between TI_{12} and TI_{24} is defined as the alarm time. It gives a measure how long a firefighter has time to escape from a dangerous situation as soon as he feels pain. For different thermal exposures and types of clothing, different limits for TI_{12} and TI_{24} exist.

2.3.1 Protection against radiant heat

The measurement of the protection against radiant heat is defined in ISO 6942 [89]. The test sample is put over a copper calorimeter and exposed to 40 kW/m^2 thermal radiation. The thermal radiation is generated by six silicon carbide (SiC) heating rods. After warming up, these rods reach a temperature of about 1100 °C. By calibrating the distance between the surface of the sample and the heating rods, thermal radiation of 5 kW/m^2 to 80 kW/m^2 can be reached. According to EN 469, TI_{12} and TI_{24} are measured at 40 kW/m^2. For thermal radiation, TI_{12} is called $RHTI_{12}$ and TI_{24} analogously $RHTI_{24}$. Two different protection levels are defined in EN 469. The minimal values in order to achieve the requirements of those protection levels are listed in Table 2.1.

	Protection level 1	Protection level 2
$RHTI_{24}$	≥ 10.0 s	≥ 18.0 s
$RHTI_{24}$-$RHTI_{12}$	≥ 3.0 s	≥ 4.0 s

Table 2.1: Minimal values for second degree burn ($RHTI_{24}$) and alarm time ($RHTI_{24}$-$RHTI_{12}$) for radiant heat transfer for two different protection levels.

2.3.2   Protection against flames

EN 469 defines the protection against convective heat (flames). The sample is put horizontally on the sample holder and is covered by a copper calorimeter. It is exposed to a gas flame below the sample. The incident heat flux is calibrated to 80 kW/m^2. For convective heat transfer TI_{12} is called HTI_{12} and TI_{24} analogous HTI_{24}. The minimal values for HTI_{12} and HTI_{24} according to EN 469 are listed in Table 2.2.

	Protection level 1	Protection level 2
HTI_{24}	≥ 9.0 s	≥ 13.0 s
HTI_{24}-HTI_{12}	≥ 3.0 s	≥ 4.0 s

Table 2.2: Minimal values for second degree burn (HTI_{24}) and alarm time (HTI_{24}-HTI_{12}) at convective heat transfer for two different protection levels.

2.3.3   Thermal manikin: Henry

Henry (Figure 2.3) is a life-size manikin equipped with 122 temperature sensors which was built especially for testing ready-made garments under flash fire conditions. The surface of the manikin consists of epoxy resin to make the manikin temperature resistant and to give it thermal properties close to human skin.
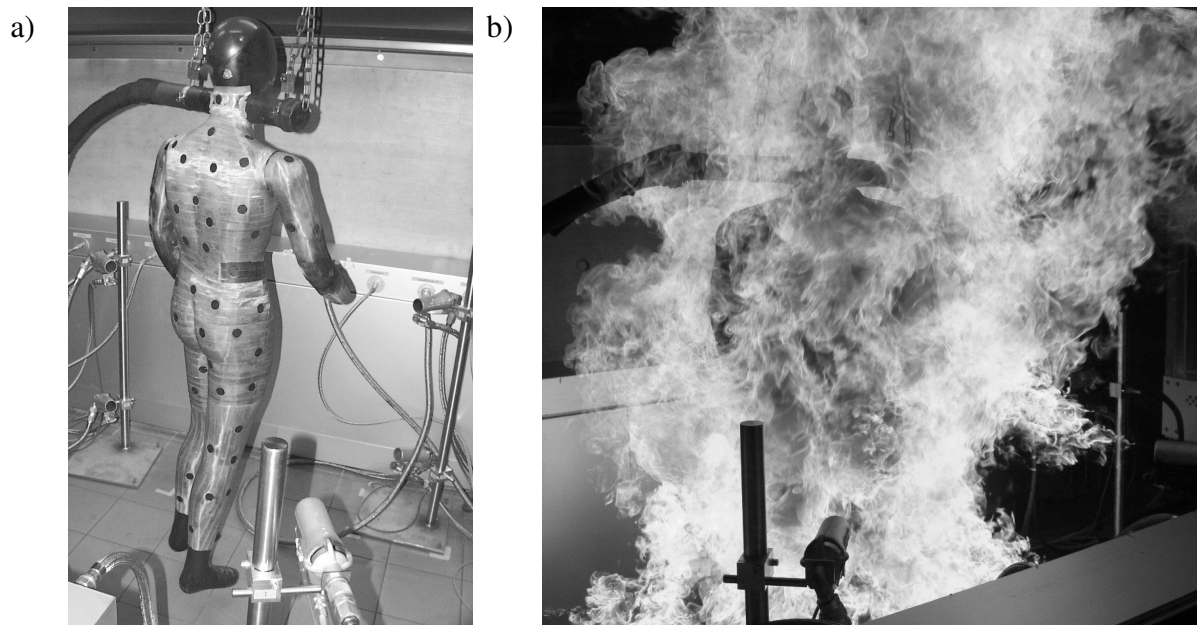
Figure 2.3: The thermal manikin Henry (a) exposed to a flashover (b).

T-type thermocouples encapsulated in epoxy resin are used to measure the temperature. The manikin can be exposed either to different levels of thermal radiation or to a flash fire.

The thermal radiation heat source consists of 6 silicon carbide (SiC) rods, which can reach temperatures up to 1100 °C. By calibrating the distance between the SiC rods and the manikin, thermal radiation from 5 kW/m^2 to 40 kW/m^2 can be regulated.

Flash fire situations are simulated with a gas burner system according to ISO/DIS 13506.3 [90]. The system consists of 12 gas burners, running with propane gas, arranged in two circles of 6 burners surrounding the manikin on hip level and just above the floor. The flash fire is calibrated to an average heat flux to the manikin of 80 +/-4 kW/m^2.

From the temperatures measured on Henry, times to reach first, second, and third degree burns are calculated according to the Henriques damage integral [24]. The areas suffering burns are shown in a map of the body for different times of the measurement (Figure 2.4).
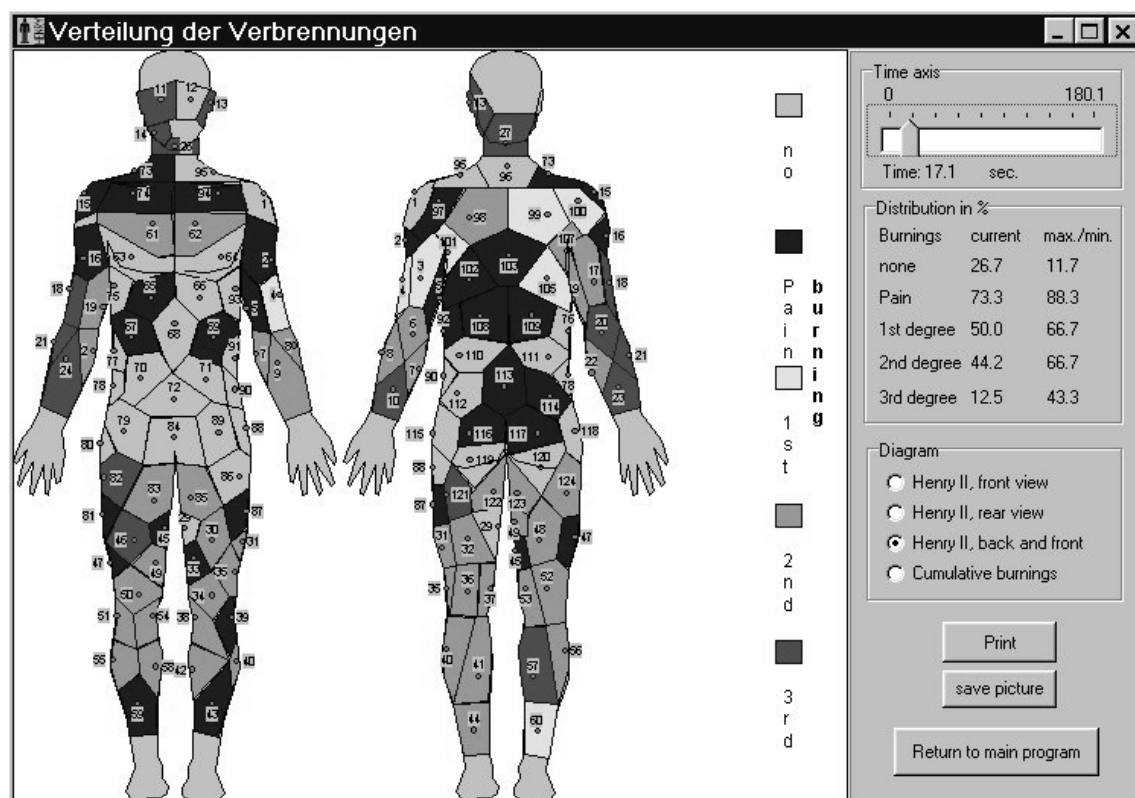
Figure 2.4: Example of a body map showing the distribution of pain and first to third degree burns after flash fire exposure.

Furthermore, temperature curves of each sensor can be printed out and energy fluxes through the skin are calculated according to Crown et al. [91].

2.4   Temperature measurement

Temperature measurement is essential for many industrial applications to control for example production, quality or security. It belongs to the basic tasks of the measurement technology and there exist a diversity of measurement principles [92, 93]. Only the basics of the sensors used for this thesis will be described in this paragraph.

Resistance temperature detectors (RTD)

The electric resistance of conductive materials changes with temperature. This dependence is linear for a wide range of temperature for different metals, e.g. copper, nickel, platinum and wolfram. Temperature sensors based on this principle are called resistance temperature detectors (RTD). This effect was used for the sensors of the sweating torso, where two nickel wires were wound around the torso. For high precision measurements, reliable platinum sensors are used (e.g. PT-100). Resistance temperature detectors have a high accuracy which ranges around 0.1 °C depending on the temperature range and the material. Due to their high mass and their high heat capacity, RTDs have relatively long response times depending on the material and mass of the sensor.

Thermocouples

If two different metals are connected to a circuit, a temperature gradient between the junctions of the circuit will induce a DC voltage. This effect was discovered by Seebeck in 1821 and is thus called Seebeck effect or also thermoelectric effect.

$$V \sim (\vartheta_1 - \vartheta_2)$$

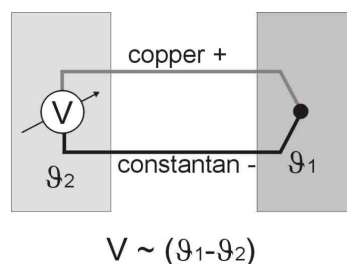Figure 2.5: Sketch of a T-type thermocouple

Thermocouples are based on this effect. They consist of the junction formed from two different metals (e.g. copper and constantan for T-type thermocouples) whereof one junction is kept at a reference temperature (e.g. 0 °C) while the other is used for temperature measurement. By measuring the voltage of the circuit, temperature at the junction can be

determined. Thermocouples are widely used for temperature measurement because they are inexpensive, rugged and reliable. They can also be used over a wide temperature range. Depending on the type of the thermocouple, they can measure temperatures over a large temperature range from -200 °C to 1600 °C. Due to the low mass of the junctions, the response time of thermocouples is fast. But the accuracy of thermocouples is worse than of RTD (up to 1 °C).

Copper calorimeter

The copper calorimeter of the radiant heat test differs from the calorimeter of the flame test. For the radiant heat test it consists of a copper rectangle of 50 mm x 50.3 mm which is 1.6 mm thick. This copper plate has a weight of 36 g and is bent with a radius of 130 mm. Temperature is measured by means of a copper constantan thermocouple which is mounted on the back of the copper plate. The copper plate is embedded in a block of thermal insulating material. In order to avoid thermal reflection, the copper plate is coated with a thin film of an optically black paint having an absorption coefficient exceeding 0.9. The copper calorimeter of the flame test differs from the calorimeter of the radiant heat test only in the form of the copper plate. It consists of a circular copper plate with radius 40 mm and thickness 1.6 mm. Thermocouple, insulating block and black paint are the same as for the radiant heat test calorimeter.

2.5   Humidity measurement

Exact and reliable measurement of humidity is most difficult [92, 93]. There exist different variables to measure humidity of a gas which can be classified in three groups [94]:

- absolute moisture content:
  - water vapour partial pressure [mbar]
  - absolute humidity (vapour density) [g/m^3]
  - dew point temperature [°C]
- relation to the dry amount of gas
  - mixing ratio [g/kg]
  - vapour content (volume fraction) [Vol %, ppm, ppb]
- relation to the saturation condition
  - relative humidity[%]

There exist different measurement principles for humidity. Some of them use the change of a physical parameter of a material, e.g. change of geometrical dimension, dielectric constant, conductivity or resonance frequency of a piezoelectric oscillator. Other methods measure the change of the equilibrium temperature e.g. over an aqueous LiCl-solution, the cooling threshold temperature of a thermal insulated water reservoir or the dew point temperature of a cooled surface. Moisture can also be measured gravimetrically by the difference of weight of a drying agent before and after absorption [92, 93].

The measurement of humidity at high temperatures (>100 °C), which is essential for the study of moisture transfer processes in firefighter protective clothing, is challenging [95]. At temperatures above 100 °C the partial pressure exceeds 1014 mbar. For measurements at environmental pressure close to the saturation pressure, air is completely displaced by water vapour and the relative humidity looses its original meaning [92, 93]. Therefore, it is only possible to measure humidity by methods relying on the physical properties of the water molecules, e.g. condensation, heat content, elasticity and structural moments of the water molecules [95].

Further restrictions in the measurement of moisture within protective clothing layers are caused by the limited space. The size of the sensor has to be small if used for measurements between the textile layers. Capacitive humidity sensors meet these requirements as they are small (~5 x 10 mm). An electrode structure of two meshing combs is mounted on a carrier substance. These electrodes are covered with a moisture absorbing polymer layer. The dielectric constant of the polymer and thus the capacity of the capacitor changes with the moisture content.

The main exclusion criterion for measuring humidity within protective clothing layers by means of humidity sensors is the fast change of temperature and humidity. Humidity is strongly dependent on the temperature. Therefore, the temperature of the sensor has to be the same as the ambient temperature. Due to its relatively large dimensions, temperature changes of the sensor are slow compared to the temperature changes of the environment.

In order to determine the behaviour of humidity sensors at sudden temperature and humidity changes we performed an exploratory study. Figure 2.6 shows the signal of a capacitive humidity sensor (Sensirion, SHT15) put into operation at 20 +/-3 °C and 20 +/-5% RH immersed into a constant climate of 35 +/-2 °C and 60 +/-5% RH. The overamplifying in the

beginning is clearly visible as humidity peak in the curve. Such peaks were also noticed in measurements of the humidity within clothing layers exposed to thermal radiation in preliminary tests. It took more than 20 minutes until a constant relative humidity was measured.
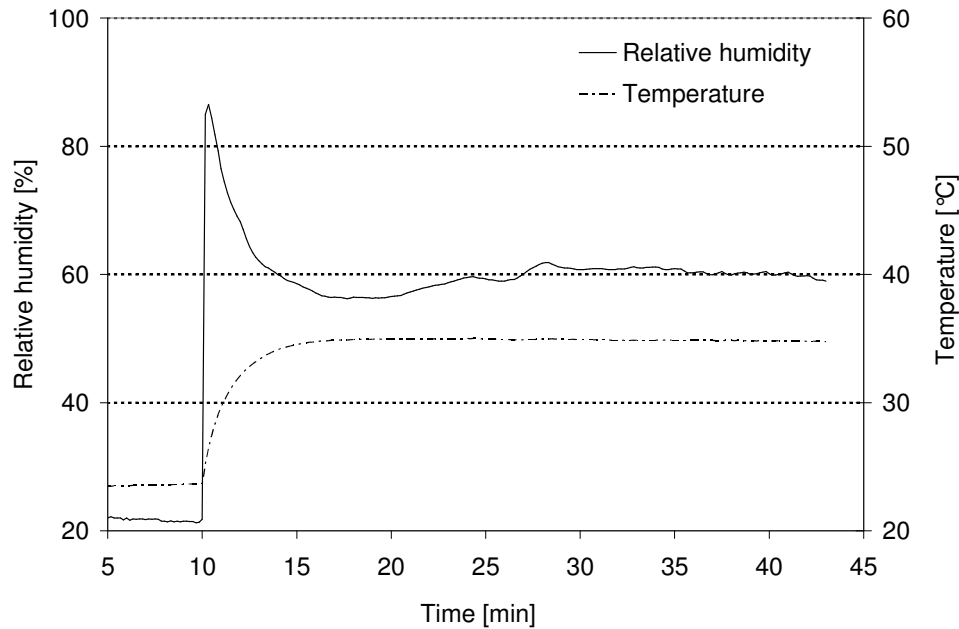
Figure 2.6: Overamplifying of the humidity of a humidity sensor suddenly immersed into a climate with 35 +/-2 °C and 60 +/-5% RH.

Considering all those demands, no state-of-the-art humidity sensor fulfilled the requirements in order to measure moisture transfer within protective clothing layers at high temperatures.

2.6   X-ray radiography

X-ray radiography is not only known in medicine, it is also a common method used for non-destructive testing. X-rays are produced by high-voltage electron streams striking against an electrode in a vacuum tube. They are a kind of electromagnetic radiation with wavelengths of around 0.01-10 nanometers. Different targets are used for different applications of X-ray radiography, which are mostly tungsten, molybdenum or copper.

The attenuation of X-rays depends on the density of the penetrated materials. The effects resulting in the attenuation of X-rays are photoelectronic absorption, Compton scattering, pair production, Rayleigh scattering and photo disintegration. By analysing the amount of radiation that penetrates an object an X-ray pattern of the inside of the object ca be gained.

3   MATERIALS

Materials used for firefighter protective clothing have to satisfy rigorous demands according to EN 469 [47]. They have to provide protection against flames, thermal radiation, liquid chemicals and mechanical impacts while keeping their mechanical strength. They are supposed not to shrink or melt. Furthermore, physiological and comfort requirements have to be fulfilled as well. The materials should be light, ductile and breathable. Only few materials satisfy those requirements.

3.1   Aramid

A frequently used material for firefighter protective clothing is aramid, an aromatic polyamide. Aramid fibres are long-chain synthetic polyamides of which two different forms exist; meta-aramid which is poly(meta-phenyleneisophthalamide) and para-aramid which is poly(para-phenyleneterephthalamide). The two forms differ in the connection of the monomers (Figure 3.1).
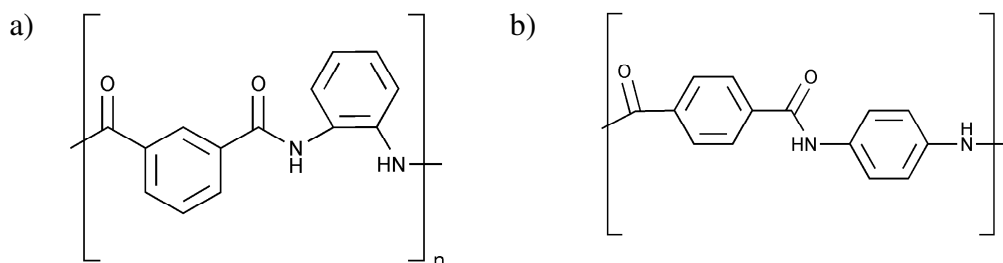
Figure 3.1: Monomer bonding of a) meta-aramid and b) para-aramid. [96]

Aramides have a high strength, temperature resistance and light weight. They are fireproof and decompose prior to melting. The decomposition temperature is 370 °C for meta-aramid and 550 °C for para-aramid.

Properties	Meta-aramid	Para-aramid
Density [g/cm^3]	1.38	1.44
Melting point [°C]	---	---
Decomposition point [°C]	370	550
Moisture regain at 20 °C, 65% RH [%]	~ 5	~ 5

Table 3.1: Physical properties of meta- and para-aramid fibres. [97, 98]

As meta-aramid is less stiff and has the more textile-like behaviour than para-aramid, it is more often used for clothing application. It is used in different forms for different layers of the protective clothing: as dense weave for the outer layer, as spunlace for thermal barriers, knitted for underwear and as blend with viscose for the liner of the firefighter jacket and trousers.

3.2   Viscose

Viscose fibres consist of cellulose and are chemically similar to cotton fibres. Viscose is easily flammable. Therefore, it has to be treated with flame retardant finishes (FR-viscose) and it is mostly used in blends with aramid. It is supposed to improve the comfort properties of the aramid fabrics as it increases their hydrophilicity. Viscose/aramid blends are mostly used as liner of firefighter jackets and trousers.

Properties	Viscose
Density [g/cm^3]	1.52
Melting point [°C]	---
Decomposition temperature range [°C]	250-397
Moisture regain at 20 °C, 65% RH [%]	13.5

Table 3.2: Physical properties of FR-viscose fibres. [99]

3.3 Teflon (PTFE)

Polytetrafluoroethylene (PTFE) is a synthetic fluoropolymer, which is better known as Teflon. It can be expanded to a thin porous membrane with about 1.4 billion pores per cm^2. This membrane is impermeable for liquid water but permeable for water vapour. By using such a breathable membrane, the physiological properties of the clothing are improved. Water vapour is able to escape the clothing, which increases the ability of sweat to evaporate on the skin, while the inner clothing layers are protected against liquid water coming from outside. In firefighter protective clothing, the Teflon membrane is used as a water barrier. As Teflon starts to deteriorate at 260 °C and to significantly decompose at about 350°, it is laminated on aramid spunlace and placed within the protective clothing assembly in order to be protected from thermal impacts.

Properties	Teflon
Density [g/cm^3]	2.1-2.3
Melting point [°C]	327
Decomposition temperature range [°C]	350-400
Moisture regain at 20 °C, 65% RH [%]	0.01

Table 3.3: Physical properties of Teflon.

3.4 Cotton

Cotton is a natural cellulose fibre, commonly used for clothing. For physiological reasons, cotton is not appropriate for firefighter protective clothing. As cotton is very hygroscopic, it absorbs and stores large amounts of sweat. This sweat is kept close to the skin, but it is not used for evaporative cooling of the body [100]. Additionally, cotton is inherently flammable. It has to be treated with flame retardant finishes in order to fulfil European standards.

Nevertheless, especially in auxiliary fire brigades, firefighters often wear cotton underwear or even cotton station uniforms under their protective clothing. Therefore, cotton is considered as well in the following studies concerning the appearance of steam burns.

Properties	Cotton
Density [g/cm^3]	1.55
Melting point [°C]	---
Decomposition temperature range [°C]	250-397
Moisture regain at 20 °C, 65% RH [%]	8

Table 3.4: Physical properties of cotton fibres. [99]

3.5   Superabsorbers

Superabsorbers are defined as substances able to absorb large amounts of liquid corresponding to at least 20 times of their own weight. Usually, superabsorbers are superabsorbing polymers (SAP) made from partially neutralised, lightly cross-linked poly(acrylic acid) [101]. Due to the moisture absorption, superabsorbing polymers are swelling strongly. They can reach a multiple of their dry volume. Moisture is either absorbed between the gel particles as well as in clefts by capillary forces [102].

Superabsorbing polymers were mainly used in sanitary products. Different other areas adopted SAPs for different applications where moisture has to be stored. In firefighting, SAPs are used as cooling system in the protective clothing. For example as superabsorbing vests, they are saturated with water, which evaporates gradually. Due to the heat of evaporation taken from the vest, it cools down and produces a cooler microclimate within the protective clothing. Such superabsorbing polymers could also be used to store surplus amount of sweat during the firefighting assignment.

3.6   Materials used for the studies

The setups of the protective clothing combinations used in this thesis are shown in Figure 1.4. Cotton and aramid underwear were used together with two different state-of-the-art firefighter jackets and three different station uniform garment materials (Table 3.5).

Material	Weight [g/m²]	Thickness [mm]	R_{et} (SD) [m²Pa/W]	$R_{ct} \cdot 10^{-3}$ (SD) [m²K/W]
Underwear				
UCo — Cotton underwear rip knit *100% Cotton*	175	1.2	3.7 (0.1)	18.9 (1.1)
UAm — Aramid underwear jersey knit *Meta-/para-aramid blend*	140	1.4	4.5 (0.1)	38.3 (1.1)
Station Uniform Garment				
SCo — Flame retardant cotton twill *100% Cotton*	320	0.8	5.0 (0.1)	16.6 (0.8)
SAmVi — Aramid/Viscose twill with hydrophobic treatment *50% FR-Viscose* *50% Meta-/para-aramid blend*	250	0.7	4.8 (0.1)	18.6 (0.5)
SAm — Aramid twill *Meta-/para-aramid blend*	220	0.7	4.2 (0.1)	21.5 (4.3)
Firefighter Jackets				
Jacket 1	**600**		**31.7 (0.5)**	**205.1 (12.0)**
J1-In/Tb — **Inner layer and thermal barrier:** Aramid/Viscose plane weave quilted to aramid needlefelt *In: 50% FR-Viscose* *50% Meta-/para-aramid blend* *Tb: Meta-/para-aramid blend*	120 + 150	4.7	12.4 (0.4)	155.9 (13.6)
J1-Mb — **Membrane:** PTFE membrane laminated on aramid spunlace *PTFE membrane* *Meta-/para-aramid blend*	135	1.3	13.0 (0.4)	45.3 (3.5)
J1-Ou — **Outer shell:** Aramid twill *Meta-/para-aramid blend*	195	0.7	4.3 (0.2)	24.4 (3.6)
Jacket 2	**535**		**24.8 (0.4)**	**146.0 (12.4)**
J2-In — **Inner layer:** Aramid jacquard weave *Meta-/para-aramid blend*	115	0.4	3.0 (0.1)	18.2 (2.3)
J2-Tb — **Thermal barrier:** Aramid spunlace *Meta-/para-aramid blend*	50	1.0	2.8 (0.1)	29.7 (5.4)
J2-Mb — **Membrane:** PTFE membrane laminated on aramid spunlace *PTFE membrane* *Meta-/para-aramid blend*	135	1.3	13.0 (0.4)	45.3 (3.5)
J2-Ou — **Outer shell:** Aramid special weave *Meta-/para-aramid blend*	185	0.6	3.6 (0.1)	20.0 (0.8)

Table 3.5: Materials of the separate layers used in the combinations with their weight, thickness, water vapour resistances (R_{et}) and thermal resistances (R_{ct}) measured according to EN 31092, 1994, with standard deviation (SD) values given in brackets.

Cotton and aramid are customary materials used in firefighting, which have differing hydrophobic properties. Cotton is hygroscopic and is able to absorb a big amount of moisture. Aramid in contrast is hydrophobic. Those materials were chosen to analyse the influence of hydrophobic properties of the underwear on the moisture distribution and the evaporation.

The materials used for the three station uniform garments were flame retardant cotton, aramid/viscose and aramid. Materials differing in hydrophobic properties have been used for the station uniform as well, which were cotton as hygroscopic material on one hand and the hydrophobic aramid on the other. The station uniform made of aramid/viscose was treated with a hydrophobic finish in order to avoid excessive water uptake.

The firefighter jackets consisted of four layers: a heat resistant outer shell, a water vapour permeable membrane, a thermal barrier and an inner layer. They differed mainly by the inner layer and the thermal barriers. Two different material compositions (aramid or aramid/viscose blend) were used for the liner of the firefighter jackets. Aramid is a hydrophobic material and the addition of viscose usually increases the hydrophilic properties of the fabric. Both firefighter jackets contained an aramid non-woven as thermal barrier with different thicknesses for the two jackets. The thermal barrier and the inner layer of firefighter jacket 1 (J1-In/Tb) were quilted. The same PTFE membrane laminated on a heat resistant aramid non-woven was used for both jackets. The outer layers of the jackets were aramid weaves.

All samples were washed once at 40 °C according to ISO 6330:2000 procedure 5A/40 °C in order to remove residues of surface coatings. They were conditioned for at least 24 hours at standard climatic conditions of 20 +/-2 °C and 65 +/-5% relative humidity prior to the measurements.

Weight, thickness, R_{et} and R_{ct} of all samples are listed in Table 3.5. In order to determine the hydrophilic properties of the materials, we performed the test of determining the rising height (DIN 53924 [86]). The measurements were performed in both directions (i.e. weft and warp) of the textile. The results are shown in Figure 3.2. If the textile was hydrophobic, no rising of the water took place, as for example in the aramid/viscose station uniform (SAmVi), both outer layers of the jacket (J1-Ou and J2-Ou), the membrane (J1-Mb and J2-Mb) and the thermal barrier of jacket J1 (J1-Tb).
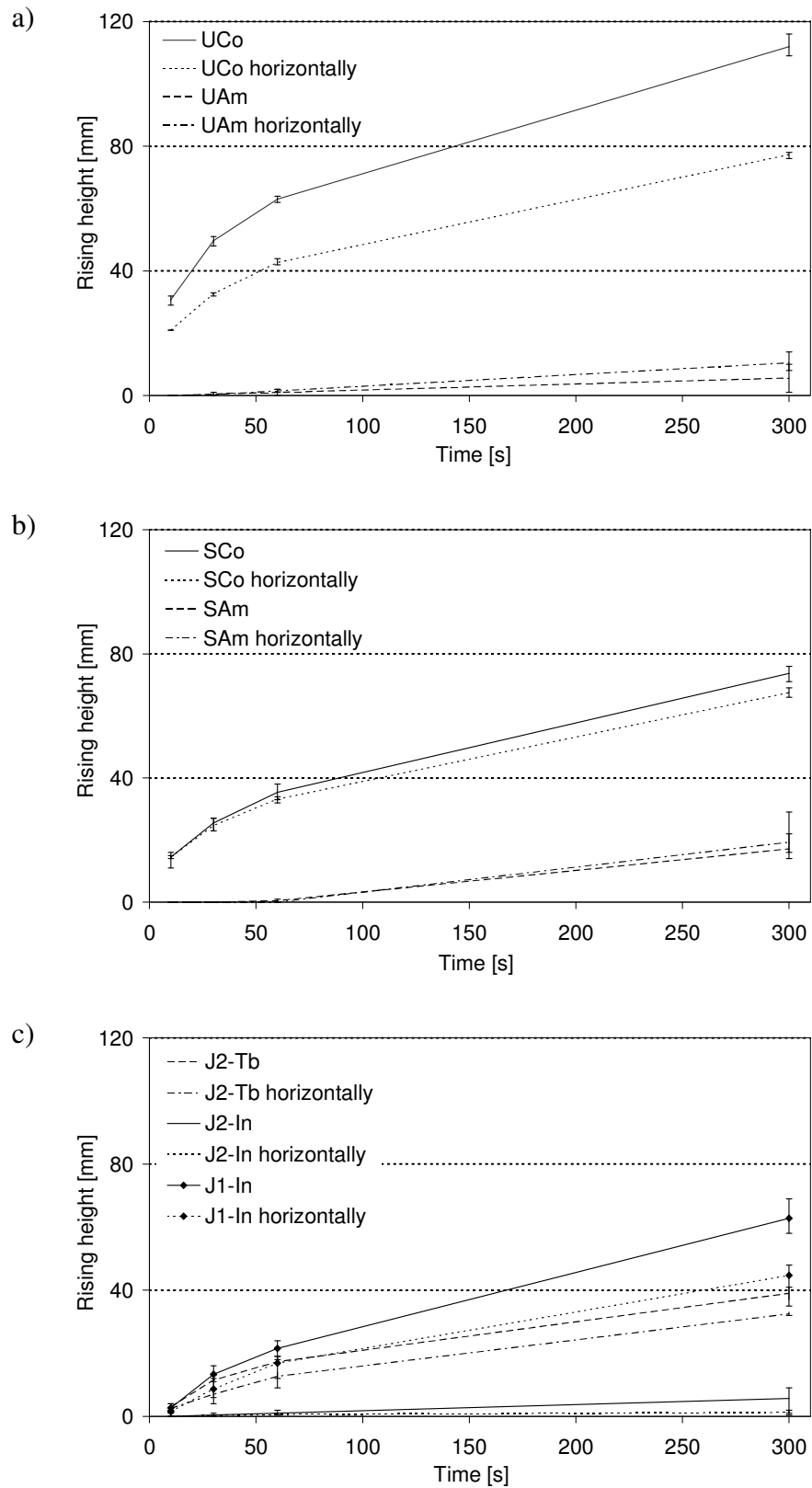
Figure 3.2: Rising height (DIN 53924 [86]) of the different not completely hydrophobic layers in lengthwise (weft) and cross (warp) direction for a) the underwear b) station uniform layers and c) layers of the jackets.

As expected, the rising height of the hygroscopic cotton layers (i.e. cotton underwear and cotton station uniform layer) was the highest (Figure 3.2 a), whereof the lengthwise direction of the cotton rip knit (UCo) reached 112 +/-2 mm after 300 s. The cross direction of the cotton rip knit (UCo) as well as the weft and warp direction of the cotton station uniform layer (SCo) weave reached still 68-77 +/-2 mm after 300 s. The rising height of the two liners of the jackets (J1-In and J2-In) ranged around 33-63 +/-6 mm after 300 s whereof the liner of jacket J1 (J1-In) was more hydrophilic. This is plausible as this layer consisted of an aramid-viscose blend. The rising heights of the aramid layers did not reach more than 20 mm after 300 s.

The drying rates of the surface water of different layers are shown in Figure 3.3. The samples were drying freely hanging on a hook of a scale. Crow et al. [60] stated in their study, that the drying rate is constant, independent of the kind of textile. Our measurements confirmed those findings as can be seen in Figure 3.3. Crow et al. measured a drying rate of 61 g/m^2h at standard conditions (20 °C and 65% RH). We received drying rates ranging around 51 +/-6 g/m^2h at the same standard environmental conditions.

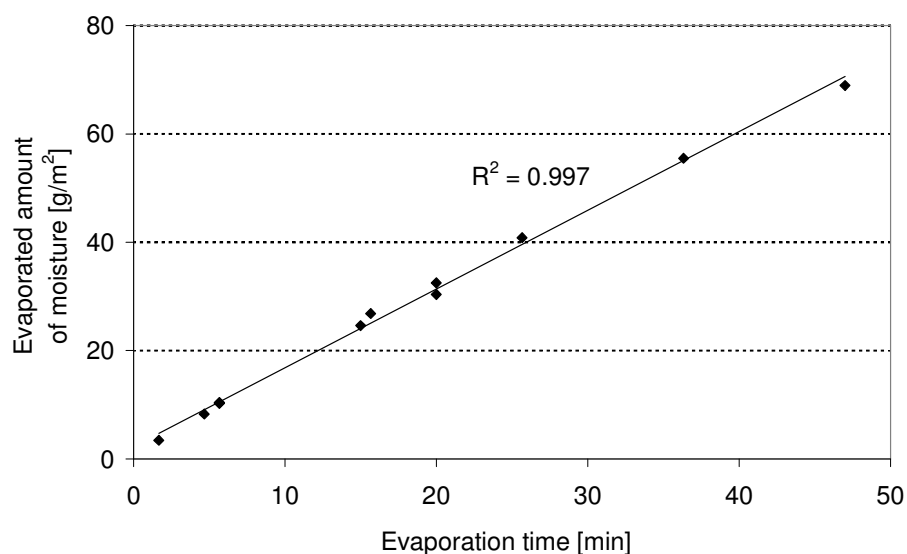Figure 3.3: Correlation between water content and drying time of the surface water of the different textile layers.

Combining the different single layers either with or without station uniform, resulted in 16 different combinations listed in Table 3.6. All these combinations are typical for the use in the daily work of firefighters as the protective clothing may be worn with or without station uniform.

The resistances R_{et} and R_{ct} of all combinations are listed in Table 3.6. All combinations with firefighter jacket J1 have higher R_{et} and R_{ct} values than the combinations with jacket J2. The thermal barrier of firefighter jacket J1 is over twice as thick as two layers of the thermal barrier of jacket J2. As the insulation properties depend, among others, on the thickness of the layer, the thermal barrier of J1 has the higher insulating properties. Though the R_{et} and R_{ct} values of a textile combination are not equal to the sum of the R_{et} and R_{ct} values of its single layers [11], the influence of the insulating thermal barrier dominates the properties of the combinations.

Combination	Layers			R_{et} [m²Pa/W] (SD)		$R_{ct} \cdot 10^{-3}$ [m²K/W] (SD)	
1	UCo		J1	36.2	(0.2)	228.9	(5.4)
2	UCo		J2	30.0	(0.8)	162.4	(8.4)
3	UAm		J1	37.7	(0.8)	232.8	(4.9)
4	UAm		J2	31.0	(1.1)	168.8	(11.6)
5	UCo	SCo	J1	40.0	(0.3)	235.1	(8.1)
6	UCo	SAmVi	J1	41.4	(0.2)	229.0	(9.6)
7	UCo	SAm	J1	40.2	(0.4)	237.9	(2.6)
8	UCo	SCo	J2	35.3	(1.2)	183.8	(2.0)
9	UCo	SAmVi	J2	34.6	(0.6)	181.1	(9.1)
10	UCo	SAm	J2	34.6	(1.8)	189.0	(1.7)
11	UAm	SCo	J1	41.6	(0.8)	240.4	(8.7)
12	UAm	SAmVi	J1	41.5	(0.6)	250.1	(5.8)
13	UAm	SAm	J1	41.5	(1.0)	248.6	(14.7)
14	UAm	SCo	J2	35.2	(0.9)	195.5	(1.5)
15	UAm	SAmVi	J2	35.4	(0.6)	187.9	(10.3)
16	UAm	SAm	J2	34.8	(0.9)	201.3	(1.0)

Table 3.6: Composition of the combinations in the measurement and their water vapour resistances (R_{et}) and thermal resistances (R_{ct}) measured according to EN31092, 1994, with standard deviation (SD) values given in brackets.

By comparing the influence of the different underwear on the R_{ct} values of each combination no significant difference could be observed. The differences between the combinations with and without station uniform layer for each jacket were not significant, either.

For the water vapour resistance (R_{et}) no significant difference between the different station uniform layers or between the different underwear was found.

PART II: EXPERIMENTAL

4   THE DISTRIBUTION OF MOISTURE WITHIN FIREFIGHTER PROTECTIVE CLOTHING

The investigation of moisture distribution in firefighter protective clothing layers is very important in terms of the occurrence of steam burns. The location and amount of moisture in the protective clothing affects the ability of hot steam to arise and also to move through the clothing layers towards the body. Up to now, it is not firmly known which layers contain how much moisture and how this moisture affects the occurrence of steam burns. In the following chapter the moisture distribution within firefighter protective clothing systems is analysed thoroughly. The interaction between the different layers as well as the influence of the way moisture is supplied to the system is considered. This knowledge will contribute to understand the development of steam burns and help developing new fabric combinations in order to minimize steam burns by adequately combining hydrophilic and hydrophobic properties of the layers.

4.1   Moisture accumulation in firefighter protective clothing at high metabolic rates

A sweating torso was used in order to simulate high metabolic rate and sweating of a firefighter during an assignment. The accumulation of moisture in the different layers of the clothing combination was determined by weighing the single layers before and after the measurement.

The distribution of moisture in textile layers has been analyzed primarily in experiments performed in cold environments so far. In their study, Weder et al. [103] analyzed the distribution of moisture in different multilayered (4 layers) clothing structures using X-ray tomography. For the measurements they constructed a heatable sample holder to which moisture was supplied from the bottom. They analyzed the effect of the combination of hydrophilic and hydrophobic textile layers on the distribution of moisture. In their study, it was observed that most of the moisture was accumulated in the two layers near the skin, which are for example the underwear and the inner liner of a garment. Rossi [48] obtained similar results when comparing the moisture distribution in clothing layers with different underwear. Mäkinen et al. [4] also noted only a small amount of moisture in the outer garment layer.

4.1.1 Methods

The setup of the protective clothing combinations used in this study was described in Chapter 3.6. Cotton and aramid underwear were used together with two different material combinations typically used in firefighter jackets and three different station uniform garment materials (Figure 4.1).
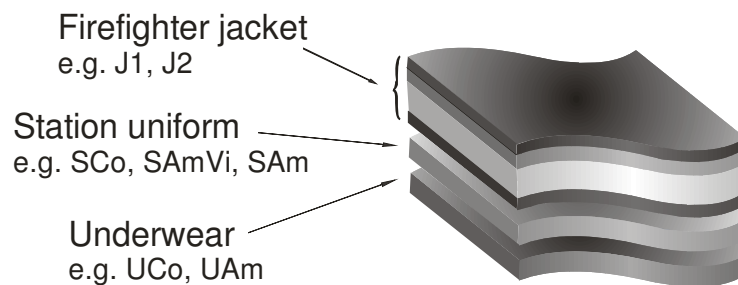
Figure 4.1: Setup of the material combinations used: underwear (e.g. UCo or UAm), station uniform (e.g. SCo, SAmVi or SAm) and firefighter jacket (e.g. J1 or J2).

We studied 16 different combinations of the clothing layers listed in Table 3.6 either with or without station uniform. All samples have been washed once at 40 °C according to ISO 6330:2000 procedure 5A/40 °C to remove residues of surface coatings. Afterwards, all combinations were conditioned for at least 24 hours at standard climatic conditions of 20 +/-2 °C and 65 +/-5% relative humidity.

Measurements on the sweating torso

Firefighters usually put on their protective clothing before they approach the fire. They have to get ready and carry around additional equipment they need for their assignment before arriving on the fire ground. They sweat during those preparations. Therefore the measurements on the sweating torso were performed at standard climatic conditions of 20 +/-2 °C and 65 +/-5% relative humidity. For the measurements on the torso, the single textile layers were wrapped around the upright standing torso without air gaps between the layers. Each measurement was repeated three times. Three different phases of 60 min each were run (Figure 4.2). The first phase was for acclimatization in which the surface temperature of the torso was kept constant at 35 °C during one hour. During the second phase, the torso ran with a constant power of 125 W and a sweating rate of 250 g/h. This corresponds to a physical activity of a human of 500 W and 1 l/hour sweating which is an average sweating rate during exercise [104]. Then, sweating was stopped for the third phase and the power was kept constant at 25 W (equivalent to 100 W for a human) during another hour.
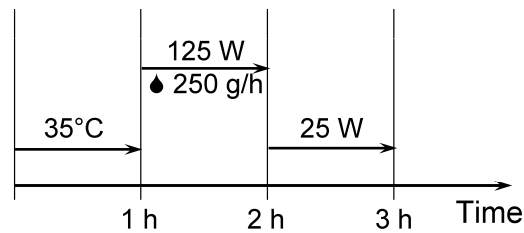
Figure 4.2: Definition of the three phases which have been run on the sweating torso.

During all three phases the surface temperature, the power and the weight of the torso were recorded. Directly before and after each measurement the weight of each clothing layer was measured and also water that dripped off was collected and weighed. The difference in weight between the wet and dry samples corresponds to the amount of moisture accumulated within the clothing layers. Therefore, the evaporated amount of moisture is equal to the difference between the amount of water excreted during the test and the sum of moisture accumulated in the textile and water which dripped off. The water that dripped off was collected on the scale. Some water was also evaporating from the dripped off water.

Measurements on the sweating cylinder

To get deeper insight into the distribution of moisture, additional measurements on a smaller sweating cylinder were performed. This sweating cylinder has the dimensions of a human upper arm and similarly to the sweating torso it can be run with either constant heating power or with constant surface temperature with the possibility of sweating. During the measurement both surface temperature and weight of the cylinder were recorded.

For the tests using the sweating cylinder, the moisture distribution during the sweating phase was investigated without a subsequent drying phase. Therefore only two phases were run. The first phase was for acclimatization and lasted one hour as for the sweating torso. Afterwards the sweating phase with 25 W power and 50 g sweat per hour (equivalent to 500 W and 1 l/h sweating for a human) started and lasted 30 minutes. The layers were separated and weighed immediately after the sweating phase in order to determine the moisture content of each layer.

4.1.2   Results

A statistical analysis of the results was performed using multivariate analysis of variables (ANOVA) combined with Tukey post hoc test [105]. The significance level of 0.05 was used throughout this analysis. The ANOVA model was validated and verified by checking normal distribution and variance homogeneity of the residuals.

The measurements on the sweating torso gave insight into the distribution of moisture in textile layers and also into the evaporation behaviour of the different combinations.

During the first 5 minutes of the sweating phase almost no moisture was evaporating from the clothing layers (Figure 4.3). The water was not evenly distributed in the underwear at the beginning of the measurement. There were wet spot around the sweating glands, which just started to spread. The evaporating surface was therefore small at the beginning and increased during the first minutes of the measurement. After that time evaporation reached its final rate and the evaporation rates of all combinations started to spread. On average 35 +/-4% of the supplied amount of moisture evaporated from the clothing system at the end of the sweating phase. Most of the moisture evaporated from combinations 2 (UCo-J2, 42%) and 4 (UAm-J2, 43%) and least evaporated from combinations 5 (UCo-SCo-J1, 31%) and 11 (UAm-SCo-J1, 30%). As expected from the relatively low vapour resistance of jacket 2 (J2), the most moisture evaporated in the combinations with this jacket.
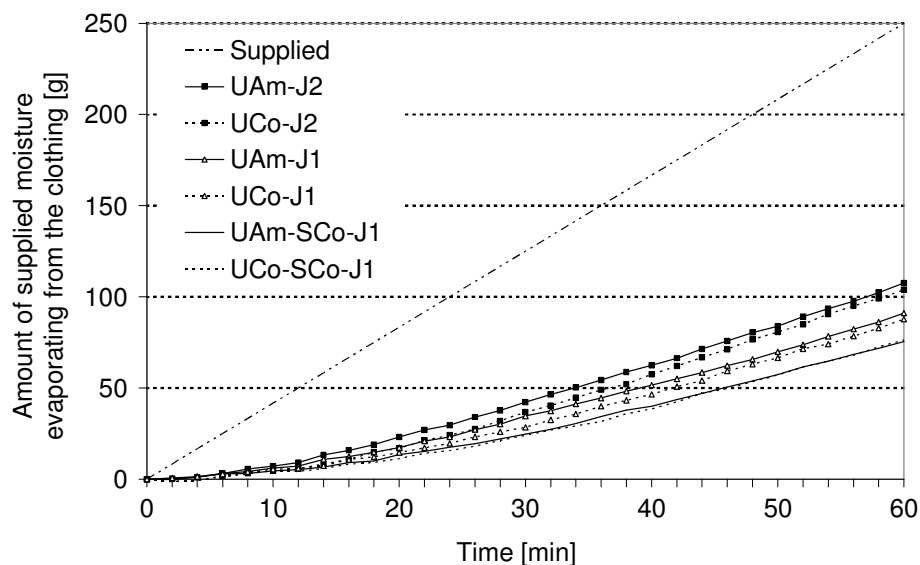
Figure 4.3: Moisture evaporated from the clothing layers compared with the total amount of moisture supplied during the sweating phase.

Figure 4.3 shows the evaporation of moisture out of combinations with cotton underwear (1: UCo-J1 and 2: UCo-J2), aramid underwear (3: UAm-J1and 4: UAm-J2) and cotton station uniform layer (5: UCo-SCo-J1 and 11: UAm-SCo-J1). At the end of the sweating phase 57% (4: UAm-J2) to 70% (14: UAm-SCo-J1) of the supplied moisture either remained in the clothing layers or had dripped off.
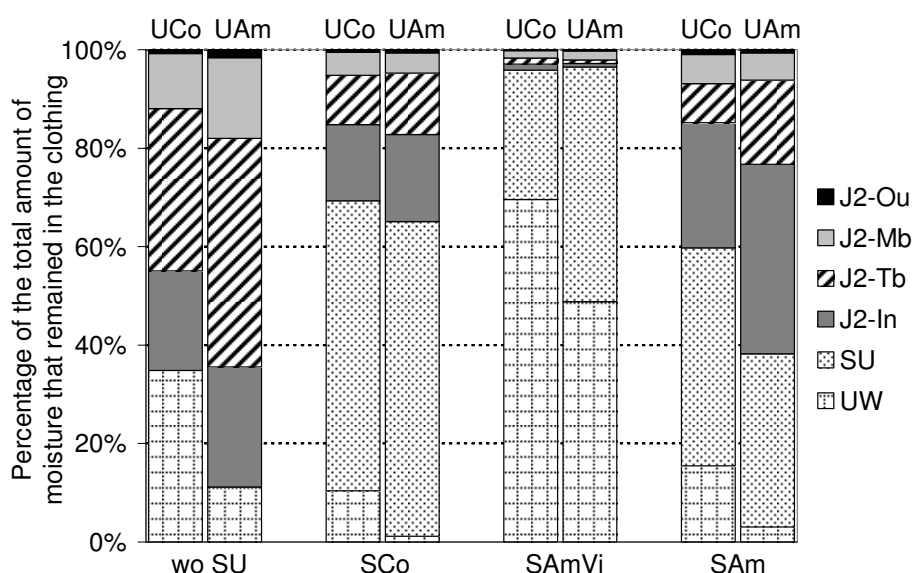
Figure 4.4: Distribution of the moisture remaining in the clothing after one hour of drying; comparison between cotton and aramid underwear combined with different station uniform layers (SCo, SAmVi and SAm) respectively without station uniform (wo SU) and with firefighter jacket 2 (J2).

Figure 4.4 shows the distribution of the moisture in the combinations with jacket 2 (J2) combined with different underwear and station uniform layers. Over 75% of the moisture that remained in the material layers was located in the innermost three layers, which were the underwear, the station uniform layer and the inner layer of the firefighter jacket. As the weights of the individual layers were remeasured only after the drying phase, a large part of moisture was found to have already evaporated from the combinations. Only 10% - 20% of the supplied moisture remained in the layers after the drying phase.
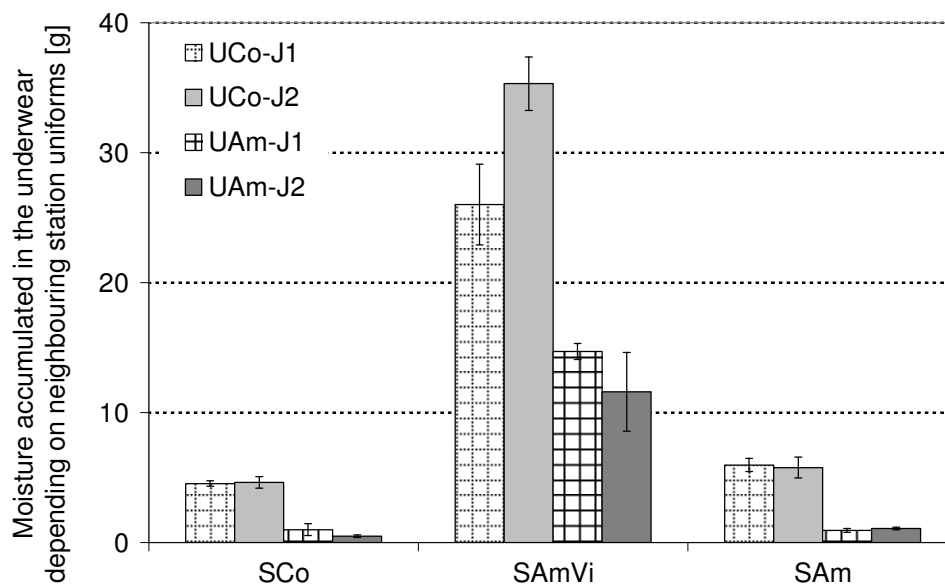
Figure 4.5: Moisture accumulated in the underwear depending on the different neighbouring station uniform layers.

Comparing all the combinations, we found that in samples with cotton underwear generally more moisture was accumulated in the underwear than in the respective samples with aramid underwear (Figure 4.5). The amount of moisture stored in the underwear strongly depended on the type of the neighbouring station uniform layer. If for example the hydrophobic treated station uniform layer SAmVi was next to the underwear, on average 30.7 +/-6.6 g moisture accumulated in UCo and 13.2 +/-2.2 g in UAm. But if station uniform layer SCo or SAm was next to the underwear, on average only 5.2 +/-0.8 g moisture accumulated in UCo and 0.9 +/-0.3 g in UAm.

Several combinations with aramid underwear (3: UAm-J1, 4: UAm-J2, 12: UAm-SAmVi-J1 and 15: UAm-SAmVi-J2) but only one combination with cotton underwear

(6: UCo-SAmVi-J1) were not able to absorb the whole amount of moisture and thus water dripped off (Table 4.1).

Moisture which dripped off [g] (SD)		
Layers	**UCo**	**UAm**
J1	---	4.5 (3.8)
J2	---	9.5 (1.0)
SCo-J1	---	---
SAmVi-J1	1.2 (0.2)	34.6 (2.6)
SAm-J1	---	---
SCo-J2	---	---
SAmVi-J2	---	39.9 (5.3)
SAm-J2	---	---

Table 4.1: Moisture which dripped off.

Comparing the absorbed amounts of water of the separate layers in different combinations showed that some of the layers, for example the underwear or the inner layer of the firefighter jacket, would have been able to absorb more moisture than they actually did, as they absorbed more moisture when imbedded in other assemblies. In spite of this fact water did drip off from some of those combinations. In the two combinations with aramid underwear and aramid/viscose station uniform layer (12: UAm-SAmVi-J1 and 15: UAm-SAmVi-J2), more moisture dripped off than the total amount of moisture absorbed by all layers. The outer layers would also have been able to absorb more moisture than they actually did.

Combination 4 (UAm-J2) showed a special behaviour (Table 4.1). 9.5 g water dripped off and only 12.6 g water remained in the clothing combination. All three inner layers would have been able to absorb more moisture than they did. This can be seen for example by combination 12 (UAm-SAmVi-J1) where the aramid underwear itself absorbed 14.7 g water and in combination 16, the J2-Ou layer absorbed 14 g water. This would have been enough to absorb also the amount that has dripped off.

In combinations 1 (UCo-J1) and 3 (UAm-J1) 59% to 63% of the moisture was accumulated in the second layer which was more than in the second layer of the combinations with jacket 2 (J2). But the second layer of those combinations actually consisted of two sublayers, as they were quilted.
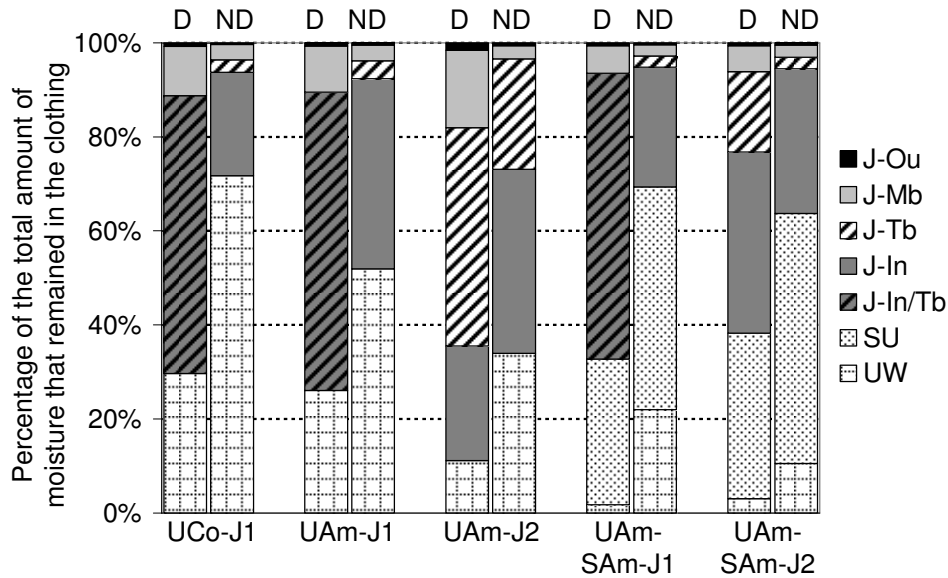
Figure 4.6: Comparison of the moisture content in the underwear (UW), the station uniform (SU) and the different layers of the jacket (J-In/Tb, J-In, J-Tb, J-Mb, J-Ou) of the measurements with drying phase (D - on the sweating torso) and without drying phase (ND - on the sweating cylinder).

As the moisture distribution in the clothing layers still changed during the drying phase, we performed further experiments on a smaller sweating cylinder, in which the measurement was stopped after 30 minutes sweating and the layers were separated immediately for weighing. The results are shown in Figure 4.6. At the end of the measurement on the sweating cylinder 45 +/-5% of the supplied moisture evaporated from the clothing layers. More moisture was accumulated in the underwear and the second layer than it was after the drying phase on the sweating torso. The underwear and the second layer contained 59% to 94% of the accumulated moisture after the sweating phase while after the drying phase 77% to 94% of the moisture was stored in the first three layers. However, measurements on the sweating torso and the sweating cylinder cannot be directly compared as the size of the cylinder is not the same. But the influence of the difference in geometry is assumed to be minor and similar results could be gained.

Comparing the moisture accumulation in the station uniform layer of the different combinations, it can be seen that the amount of moisture accumulated in the station uniform layer did not depend significantly on the neighbouring clothing layers (Figure 4.7). Only the properties of the station uniform itself influenced the amount of moisture absorbed.
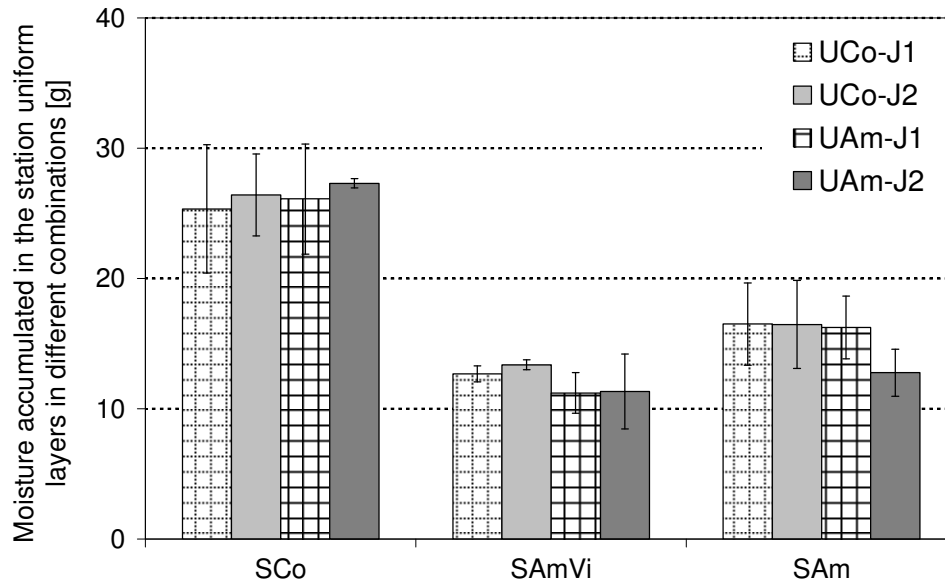
Figure 4.7: Moisture accumulated in the station uniform layers for the different underwear and firefighter jackets.

The impact of the clothing combination on the wear comfort

Analysing the torso surface temperature, conclusions about the comfort of a clothing combination can be drown. Figure 4.8 a) shows the impact of the underwear on the torso surface temperature in measurements with the protective assemblies without the station uniform layer. In the sample using aramid underwear (UAm-J2), the torso surface temperature reached its maximum of 35.2 °C three minutes after the start of the sweating phase. At that point, the evaporative cooling started and the temperature dropped to 33.7 °C at the end of the sweating phase. The temperature of the sample with cotton underwear (UCo-J2) rose to 35.4 °C at five minutes after the beginning of the sweating phase. But after the beginning of the evaporative cooling the decrease of temperature with cotton underwear was larger than with aramid underwear and a temperature of 33.5 °C was reached at the end of the sweating phase.
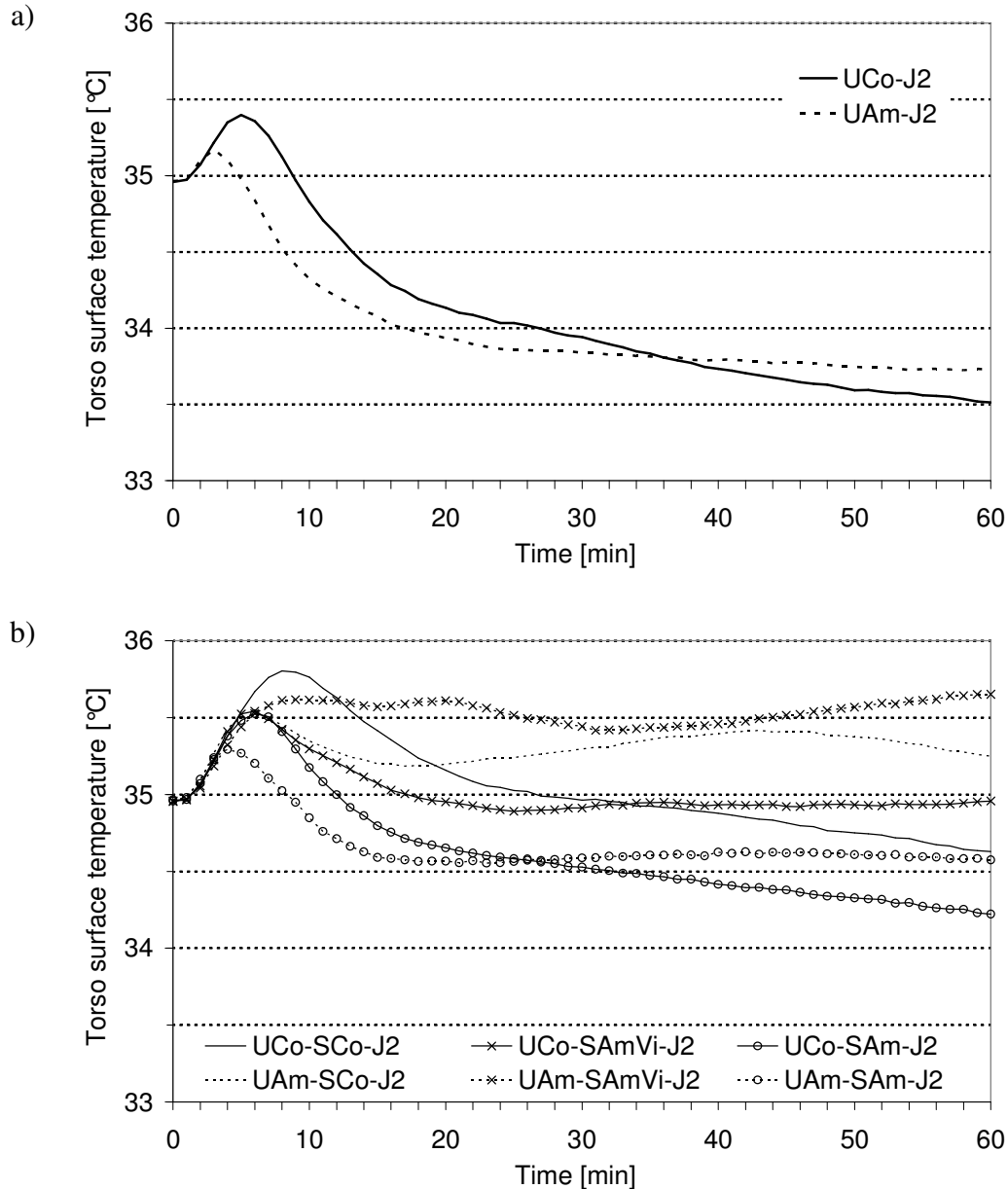
Figure 4.8: Surface temperature of the torso during the sweating phase: a) Comparison of the samples in combination with two different underwear layers and without the station uniform layer. b) Comparison of the samples with different combinations of two different underwear and three different station uniform layers.

Figure 4.8 b) shows the behaviour of the samples consisting of two different underwear and three different station uniform layers combined with the protective clothing fabric. During the first four minutes of the sweating phase, the torso surface temperature of all samples rose at similar rates until sample UAm-SAm-J2 reached its maximal temperature of 35.3 °C. Six minutes after the start of the sweating phase samples UCo-SAmVi-J2, UCo-SAm-J2 and UAm-SCo-J2 reached all the same maximal temperature of 35.5 °C. The temperatures of

samples UCo-SCo-J2 and UAm-SAmVi-J2 continued rising until they reached maximal values of 35.8 °C and 35.6 °C respectively after 8 minutes. In UAm-SAmVi-J2 the torso surface temperature did not drop after reaching its maximum, but remained constant until the end of the sweating phase. Similarly, the temperature of UAm-SCo-J2 dropped only by 0.3 °C between reaching the maximum and the end of the sweating phase.

The samples with the aramid station uniform (UAm-SCo-J2 and UAm-SAm-J2) showed a similar behaviour as the samples without a station uniform (UCo-J2 and UAm-J2). Sample UCo-SCo-J2 also showed a temperature course similar to the other curves for samples with cotton underwear. The only sample with cotton underwear that behaved differently was sample UCo-SAmVi-J2. In this sample the temperature dropped until a steady-state temperature was reached and stayed constant until the end of the sweating phase.

4.1.3 Discussion

By analyzing the moisture distribution in the different combinations it could be observed that more than 75% of the moisture that remained in the clothing layers was located in the innermost three layers, which were the underwear, the station uniform layer, and the inner layer of the firefighter jacket, partly confirming previous results in former studies [4, 48, 103]. Mäkinen et al. [4] performed wear trials with different kinds of underwear combined with firefighter protective clothing at 30°C ambient temperature and 30% relative humidity. They showed that 50% - 80% of the sweat accumulated in the inner two layers. It should be noted that the movement of the human body, additional air layers and pressure on certain parts of the garment were considered in those results. In another study performed on the sweating torso with normal clothing (underwear, outer fabric and rainwear) Rossi [48] found that 80% of the moisture remained in the inner two clothing layers after 10 minutes sweating and still more than 60% after 20 minutes.

In the present study, in the measurements with the sweating torso, the clothing layers were weighed one hour after the end of the sweating phase and about 80% - 90% of the moisture supplied had evaporated to the environment before weighing. A maximum of 25% of the moisture remaining in the clothing moved to the outer layers of the clothing combination. In additional measurements on the sweating cylinder, which were stopped directly after 30 minutes of sweating, over 90% of the moisture remained in the first three layers.

The moisture supplied M_{sup} is equal to the sum of the moisture in the underwear M_{UW}, the moisture in the station uniform layer M_{SU}, the moisture in the jacket M_J, the moisture evaporated M_{evap} and the moisture which has dripped off M_{dr}, thus

$$M_{sup} = M_{UW} + M_{SU} + M_J + M_{evap} + M_{dr} \qquad (4.1)$$

M_{sup}	Moisture supplied	[g/m^2]
M_{UW}	Moisture in the underwear	[g/m^2]
M_{SU}	Moisture in the station uniform layer	[g/m^2]
M_J	Moisture in the jacket	[g/m^2]
M_{evap}	Moisture evaporated	[g/m^2]
M_{dr}	Moisture which has dripped off	[g/m^2]

If all moisture would evaporate out of the underwear, without accumulating in the outer layers and evaporating from there, the evaporated amount of moisture can theoretically be calculated using

$$M_{evap} = \frac{\Delta p \cdot \Delta t}{R_{et} \cdot \varphi} \qquad (4.2)$$

Δp	Difference of the partial pressure of the water vapour	[Pa]
Δt	Time	[s]
φ	Latent heat of evaporation	[J/g]
R_{et}	Water vapour resistance of the whole clothing combination	[m^{2}Pa/W]

We calculated the evaporated moisture according to equation (4.2) and compared it with the experimentally determined amount of evaporated moisture equation (4.1). The amount determined according to equation (4.1) was always higher (7% - 28%) than the calculated value (4.2). This may be explained by the fact that it not only evaporates from the underwear but some moisture also drips off or accumulates in the outer layers and evaporates from there. Therefore M_{evap} also strongly depends on the amount of moisture which is accumulated in the station uniform layer and the jacket.

Many different aspects, such as the wettability, the structure of the textile or the pressure supplied to the textile layers contribute to the distribution of moisture in textile layers. In former studies mostly wettability was mentioned as the criterion for the distribution of

moisture [103, 106, 107]. Weder et al. [103] compared different combinations of hydrophilic and hydrophobic layers and showed that, if the second layer was hydrophobic, all the moisture remained in the first layer. If the second layer was hydrophilic, it also absorbed a part of the moisture. In the present study the second layer proved to be of high importance for the distribution of moisture in the clothing system. There were no significant differences in moisture accumulation in the station uniform layers depending on the underwear (Figure 4.7). Thus MSU appears to be similar for a given station uniform layer. In contrast the station uniform had a significant impact on the amount of moisture stored in the underwear. This result confirms the result of Adler and Walsh [70] that the water content of a single layer depends not only on its own material properties but also on the neighbouring layers.

In Figure 4.5 it can be seen that the underwear behaved completely differently depending on the kind of station uniform layer that followed. In protection combinations containing the station uniform material made of aramid/viscose blend SAmVi and aramid underwear UAm an average of 13.2 +/-2.2 g of moisture was accumulated in the underwear and with cotton underwear UCo 30.7 +/-6.6 g. In combinations with other station uniform layers the underwear only stored 0.9 +/-0.3 g (UAm) respectively 5.2 +/-0.8 g (UCo). A similar behaviour could be found comparing the moisture accumulated in the layers following the station uniform (inner layer of the firefighter jackets J1-In/Tb and J2-In). In combinations with the hydrophobic station uniform layer SAmVi only 2.9 +/-0.1 g (J1) and 0.4 +/-0.3 g (J2) was transferred to the inner layer of the firefighter jacket while with the other two station uniforms 23.9 +/-5.6 g (J1) and 9.5 +/-3.2 g (J2) was accumulated on average in the inner layer of the firefighter jacket. Therefore not only the wettability of the textile is of importance but also the transfer of water between layers, which has been referred to as demand wetting [64]. It could be shown that both effects, the moisture absorption of a layer and the wicking properties of the neighbouring layer are interacting.

In their study Crow et al. [60] showed that there must be a threshold amount of water in a wet layer before water starts to wick to the following initially dry layer. If a layer is not able to absorb the amount of water required to be able to wick water to the next layer, it will act as a water barrier. This happened with the station uniform layer SAmVi which was treated with a hydrophobic finish. This layer was not able to transfer the moisture to the following layers efficiently and therefore much less moisture spread to the outer layers than in combinations

containing other station uniform layers (Figure 4.4). As SAmVi itself had a limited absorbing capacity, the moisture was stored in the underwear or dripped off.

	Moisture in the Underwear [g] (SD)		Ratio (SD)
Layers	UCo	UAm	UCo/UAm
J1	13.7 (0.7)	11.5 (3.7)	1.2 (0.4)
SAmVi-J1	26.0 (3.1)	14.7 (0.6)	1.8 (0.2)
SAmVi-J2	35.3 (2.1)	11.6 (3.0)	3.0 (1.0)
SCo-J1	4.5 (0.2)	1.0 (0.5)	4.5 (2.1)
SAm-J2	5.8 (0.8)	1.1 (0.1)	5.3 (1.2)
J2	7.5 (1.3)	1.4 (0.1)	5.3 (0.7)
SAm-J1	6.0 (0.5)	0.9 (0.2)	6.4 (1.4)
SCo-J2	4.6 (0.5)	0.5 (0.1)	9.3 (2.8)

Table 4.2: Ratio of moisture accumulated in the different underwear in dependence of the different outer layers.

The moisture accumulated in the underwear depends on the material of the underwear, the interaction with the neighbouring layer, the ability of the water to evaporate and thus on the R_{et} of the whole combination. For all combinations, more moisture accumulated in the cotton underwear than in the aramid underwear (Table 4.2). The ratio between the amounts of moisture accumulated in the different underwear materials seemed to depend on the quantity of moisture in the underwear. When more moisture was stored in the underwear, a tendency to smaller differences in moisture content between the cotton and aramid underwear could be observed, as shown in Table 4.2. This might be explained by the fact that the aramid underwear UAm tended to transfer most of the liquid moisture to the next layer if the neighbouring layer could absorb it, whereas the cotton underwear UCo absorbed part of the moisture due to its hygroscopicity. The three samples with the most moisture absorbed in the underwear UAm (combinations with J1, SAmVi-J1 and SAmVi-J2) also showed large amounts of dripped-off water (Table 4.1) and therefore, it can be assumed that the aramid underwear thus was near to its moisture saturation.

As could be intuitively expected, the samples without a station uniform layer accumulated the least moisture and the torso surface temperature dropped the most until the end of the sweating phase (Figure 4.8). In the beginning of the sweating phase, the temperature of the sample with cotton underwear rose more than the temperature of the sample with aramid underwear. This phenomenon is due to the hygroscopic properties of cotton. Heat of sorption was released during absorption of the moisture by the fibres and the temperature therefore rose higher than with aramid underwear. In combination 2 (UCo-J2), water dripped off. Therefore not all of the moisture could be used for the evaporative cooling of the torso and the temperature did not drop as much as with cotton underwear. The same phenomenon could be observed in combination 7 (UCo-SAm-J1), from which more water dripped off than remained in the clothing. As this moisture could not be used for evaporative cooling, the surface temperature of the torso at the end of the sweating phase was 0.8 °C higher than during the acclimatization.

The fact that more moisture was accumulated in the cotton underwear corresponds with the findings of the better cooling abilities of samples including cotton underwear (Figure 4.8). As more moisture was accumulated in the underwear than in the external layers, it is likely that more moisture evaporated near the skin, where the energy used for the evaporation is taken directly from the skin. If the moisture evaporated in an outer layer, the energy used for the evaporation is taken from the neighbouring layers and the cooling of the body is not that efficient. However, this higher amount of moisture in the underwear might also contribute to an increased risk of steam burns.

4.1.4 Conclusions

The moisture content of a single layer is not only dependent on the material properties of that particular layer but mainly on properties of the neighbouring layers and even of the whole combination. Effects of the moisture absorption ability of the underwear and wicking properties of the neighbouring layer are superimposed. These results suggest that non-hygroscopic underwear materials, such as aramid, do not absorb moisture until the limit of their capacity if they may transfer it to the next layers. Therefore, in combination with other layers, the moisture is led to the more hydrophilic neighbouring materials. Only if the next layer does not absorb any further moisture will aramid underwear absorb similar amounts of water as cotton underwear or drip off excessive moisture.

The second layer of the combination proved to be of high importance for the moisture distribution. If there is a direct contact between the layers, a hydrophilic station uniform layer absorbs moisture and leads it to the outer layers while a hydrophobic station uniform layer only takes up little moisture. If this amount of water is too small in order to be able to be led to the next layer, the second layer will act as a liquid water barrier and the moisture will either be stored in the underwear or drip off.

The material of the underwear largely influenced the torso surface temperature course. With aramid underwear, the temperature decreased faster than with cotton underwear but with cotton underwear, the temperature drop was larger than with aramid underwear.

4.2   Localisation of the dripped off moisture

During the torso measurements, moisture was dripping off in various combinations. In order to find out in which layers this moisture dripped off, we performed additional measurements on the sweating cylinder.

We stuck plastic bags containing stripes of blotting paper at the lower edge of each layer in order to collect the dripped-off moisture from this particular layer. Additionally we stuck stripes of blotting paper directly onto the sweating cylinder and between the plastic bags in order to detect moisture that dripped off between two layers.

We ran a sweating phase of 30 minutes on the sweating cylinder at constant power of 25 W which corresponds to 500 W for the human body. We chose the maximal sweating rate (about 110-120 g/h) in order to maximize the dripped-off water.

Figure 4.9 shows the percentage distribution of the dripped-off moisture from the different layers. Moisture only dripped off from the inner layers - the underwear (UCo and UAm) and the cotton station uniform (SCo), as well as the liner of the jacket (J1-In and J2-In) if there was no station uniform or a cotton station uniform (SCo). Only in the combination with aramid underwear (UAm) and jacket 2 (J2) without station uniform, moisture also dripped off from the thermal barrier.

Moisture dripped off if the particular layer reached the limit of its absorption capacity. As moisture was mainly stored in the inner layers, only the inner layers reached saturation level. The more hydrophilic a layer was, the higher the percentage of dripped-off moisture. For

example without station uniform layer, over 50% of the moisture dripped off from the cotton underwear (UCo) while with the aramid underwear (UAm), less than 10% dripped off. The largest part of dripped-off moisture in the latter combinations (UAm and J1 respectively J2) came from the liner of the jacket (J1) or even from the thermal barrier of jacket 2 (J2-Tb). In the combinations including a cotton station uniform layer (SCo), around 50% of the moisture dripped off from the station uniform layer, while in the same combination including the hydrophobic aramid/viscose station uniform layer (SAmVi), no moisture dripped off from the station uniform.
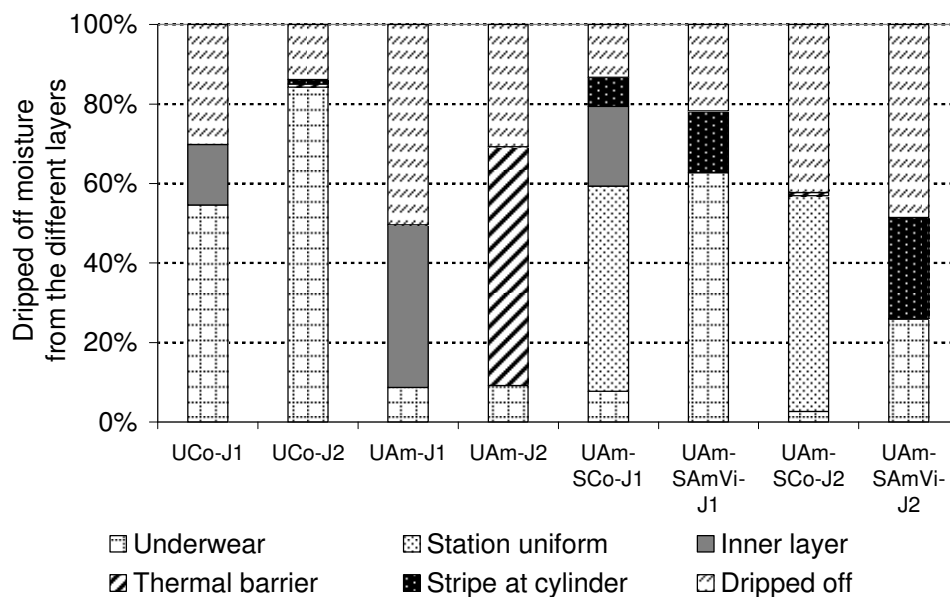
Figure 4.9: Dripped off moisture from the different layers in measurements on the sweating cylinder at maximal sweating rate.

Although the limit of the absorption capacity of the hydrophobic layers was much smaller than of the hydrophilic layers, moisture mainly dripped off from the combinations with the hydrophilic layers. Hydrophobic layers transported the moisture to the more hydrophilic layers instead of storing it up to the limit of their absorption capacity.

4.3   Moisture distribution within soaked combinations passed through rolls

We showed that the amount of moisture remaining in the different clothing layers is dependent on the particular layer but also on the combination of the different layers (see

Chapter 0). In these experiments, moisture was supplied from the inside to the underwear and evaporation was taking place. In the following chapter we show how moisture is distributed in the textile layers if the whole combination is uniformly immersed into water and therefore is not depending on the direction of moisture supply.

4.3.1 Methods

For these experiments, we used the same textile combinations as described in Chapter 3.6 (see Table 3.5). We weighed all single layers prior to the experiment. Then, we immersed the textile combinations into distilled water for one minute. After the removal from the water bath, we let them pass through two rolls pressing the samples with a pressure of 1 bar and a speed of 0.5 m/s (Figure 4.10). We then separated the combinations and weighed again all layers separately. The difference between the wet and the dry weight gave the amount of moisture remaining in the different layers.
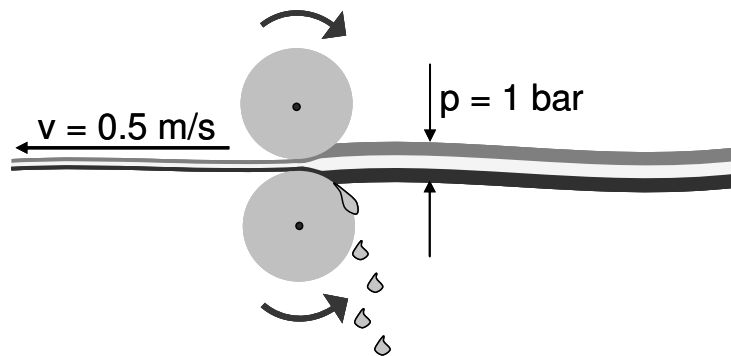
Figure 4.10: Setup of the experiment. The soaked combinations pass two rolls pressing with a pressure of 1 bar and a velocity of 0.5 m/s.

4.3.2 Results

The results are shown in Figure 4.11 and Figure 4.12. The thermal barrier of both jackets (J1-Tb and J2-Tb) stored more water if it was in combination with aramid underwear (UAm) than in combination with cotton underwear (UCo) in combinations without station uniform (Figure 4.11). For jacket 1 (J1) this effect was also visible if there was additionally an aramid respectively cotton station uniform layer (SAm or SCo). In combinations with jacket 2 (J2) this significance disappeared by addition of a station uniform layer.
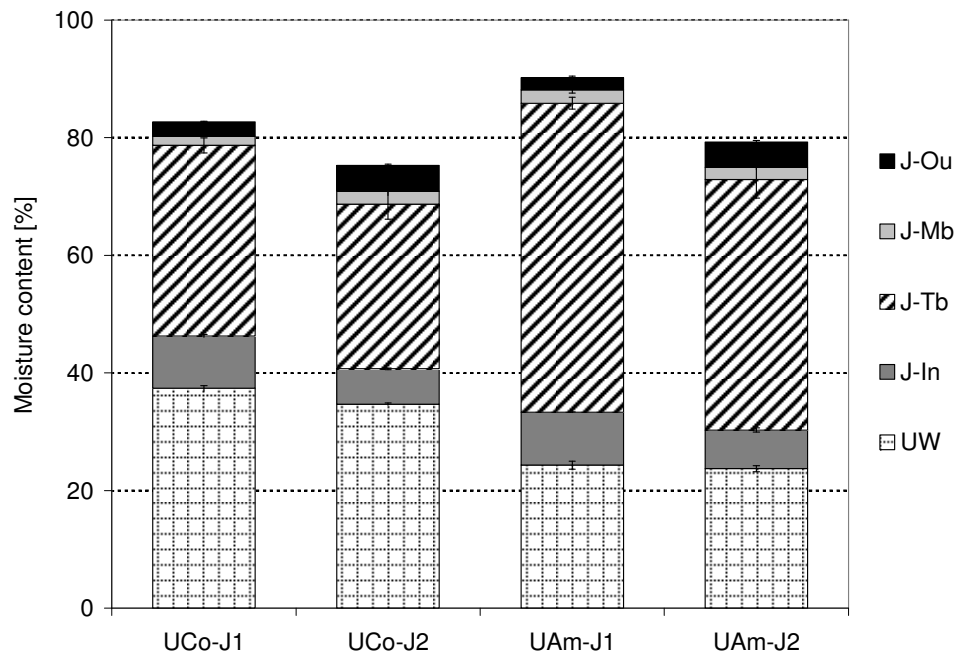
Figure 4.11: Results of the measurement of the moisture accumulation within textile layers.

The moisture contents in the cotton underwear (UCo) in combination with the hydrophobic aramid/viscose station uniform (SAmVi) were significantly lower than in the combinations with the other station uniforms or without station uniform. On the contrary, the moisture content of the aramid underwear (UAm) in combination with SAmVi was significantly higher than in the other combinations.

Comparison between the experiments with initially soaked samples and the results of the torso measurements

If we compare the results of the torso measurements (Chapter 4.1.2) with the results of the study where the initially soaked combinations were passed through rolls (Figure 4.12), we see that the initially soaked combinations store more than double of the amount of water than the combinations measured on the sweating torso. Especially the thermal barriers (J1-Tb and J2-Tb) and the outer layers of the combinations (J1-Ou and J2-Ou) stored more moisture after the roller experiment but also the underwear. The only exception was the cotton underwear (UCo) in combination with the hydrophobic aramid/viscose station uniform (SAmVi). In this case, the underwear of the torso measurement stored more moisture than the underwear which was passed through the rolls.

The station uniform layer retained more moisture in the torso measurements than after passing through the rolls. The only exception for this was combination 16 (UAm/SAmVi/J2) where in the torso measurement 12.8 +/-1.8 g was stored in the station uniform while after passing through the rolls 13.1 +/-0.2 g was stored in the station uniform layer. This difference was particularly big for the aramid/viscose station uniform (SAmVi) which stored 2.2 +/-0.2 g moisture after being passed through the rolls while storing 12.1 +/-0.9 g moisture in the torso test.
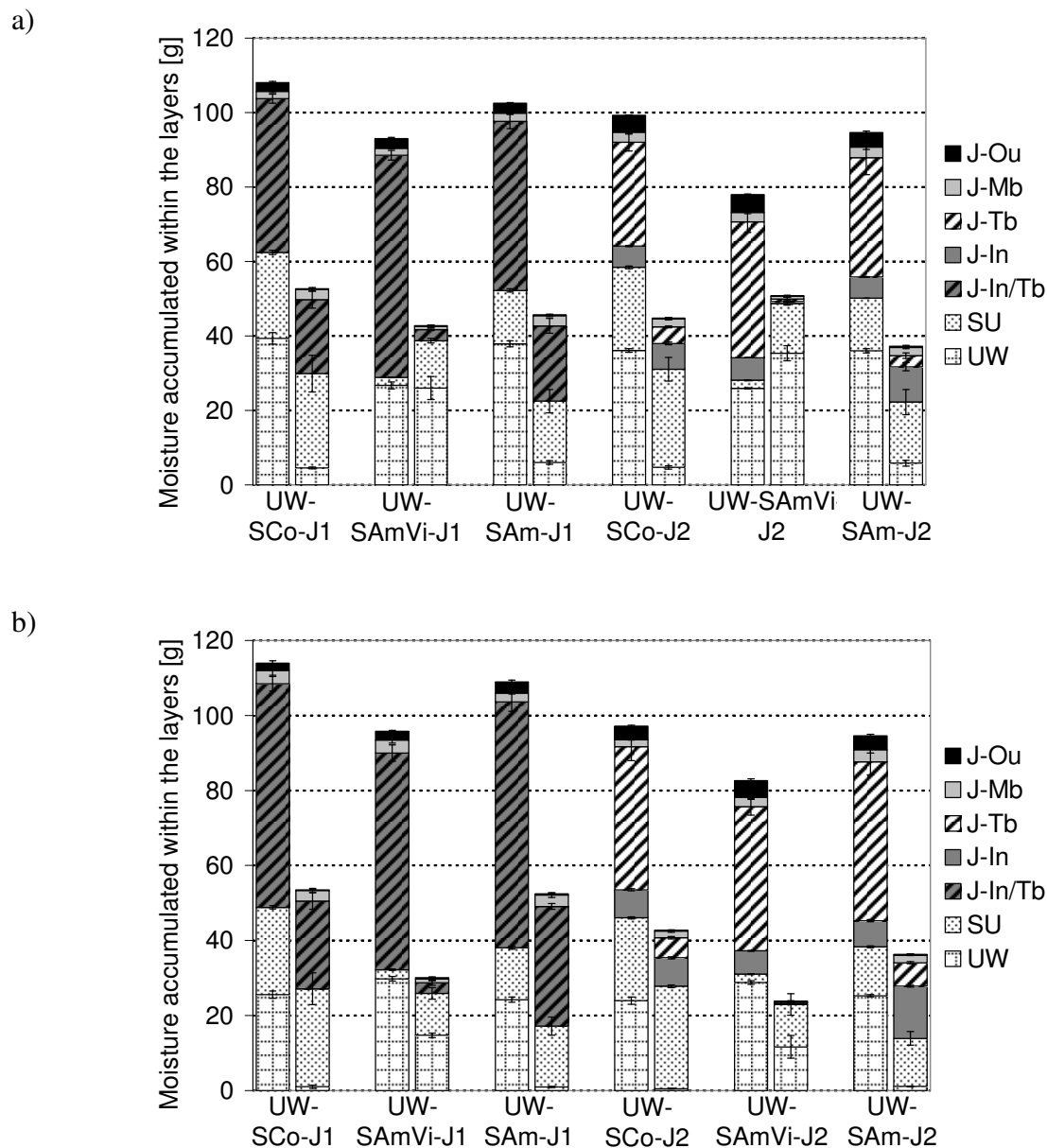
a)

b)

Figure 4.12: Comparison between the results of the moisture content in initially soaked combinations (left) and moisture contents after torso measurements (right) for a) cotton underwear (UCo) and b) aramid underwear (UAm).

4.3.3 Discussion

As the whole combination was initially soaked with water in the measurement with the rolls, more moisture was supplied to these combinations and therefore, they contained more moisture than in the torso measurement. Especially the thermal barriers (i.e. J1-Tb and J2-Tb) and the outer layers (i.e. J1-Ou and J2-Ou) stored more water than in the torso measurement. During the torso measurement, the moisture was supplied continuously to the underwear, where it started to distribute and evaporate. It was absorbed by the underwear and the other more hydrophilic layers. Only very little moisture was transported to the outer layers. Therefore, it is straightforward that more moisture was found in the outer layers if they were initially soaked.

The pressure of the rolls squeezed moisture out of the layers. Due to this additional pressure the station uniform layers (i.e. SCo, SAmVi and SAm) could get rid of surplus water, which either was absorbed by the neighbouring layers or dripped off.

The cotton underwear (UCo) absorbed less moisture in combination with the hydrophobic aramid/viscose station uniform layer (SAmVi) when passed through the rolls than in the torso measurement. During the torso measurement, the moisture was dammed up at the hydrophobic station uniform. Therefore, the underwear had to absorb this moisture up to saturation. However, if an external pressure had been applied, part of this stored water would probably have dripped-off. By passing through the rolls, this pressure was applied to the combination and the surplus of water dripped off, explaining the lower amount of moisture when compared with the torso measurements.

The combination of the cotton underwear (UCo) with hydrophilic station uniform layers (i.e. SCo and SAm) increased the absorption capacity of the underwear as more moisture was accumulated in the cotton underwear when it was combined with the cotton respectively aramid station uniform. Certain combinations of textile layers are able to store moisture in the space between the layers. As the station uniform layer SAmVi is very hydrophobic, water was repelled at its surface. Therefore no moisture could be stored between the layers. The other station uniform layers (SCo and SAm) are more hydrophilic and therefore, moisture was stored between the layers, which divided to the adjacent layers, when they were separated for weighing.

4.3.4   Conclusions

The moisture content in the different layers strongly depended on the way how moisture was supplied. If the whole combination was initially soaked with water, the outer layers contained more water than after the torso measurement. If the water was supplied from inside to the underwear, it was retained at the hydrophobic layers, which suppressed wicking to the outer layers.

Less water was found in the underwear after passing through the rolls than after the torso measurements. Due to the additional pressure applied by the rolls, the water was squeezed out of the oversaturated layers, which were for example the underwear.

5 EVAPORATION OF MOISTURE FROM FIREFIGHTER PROTECTIVE CLOTHING

In order to investigate the occurrence of steam burns, it is essential to know how fast and at which temperatures water located in protective clothing combinations can evaporate. We studied the evaporation process of water out of multilayer protective clothing assemblies containing a wet layer, exposed to low level thermal radiation. In the first part of this chapter the temperatures within the clothing combination is analysed thoroughly. By aid of the temperature patterns, conclusions about the evaporation rates could be drawn. In the second part X-ray radiography was used to visualise the evaporation process of moisture out of protective clothing combinations.

5.1 Temperature analysis for the prediction of steam formation

State of the art humidity sensors are not convenient to analyse the evaporation of moisture and the transfer of hot steam in protective clothing at high temperatures experimentally because they are (a) too slow to record fast humidity changes during evaporation, and (b) too big to be located between the different textile layers. Especially at high humidity, the moisture which condenses on the sensor surface falsifies the results. Therefore the problem of determining steam flow through the layers of the protective clothing has to be approached in a more systematic way integrating the interaction between heat and mass transfer and heat of phase changes.

Temperature and moisture content within the multilayer clothing system are closely related. As the temperature during phase change of a substance stays constant, the evaporation phase can be determined by considering the temperature curves. The goal of this study was therefore to analyse the evaporation process and speed within the clothing layers with the aid of detailed further analysis of internal temperatures measured.

5.1.1   Methods

The setup shown in Figure 5.1 consisted of an upright standing PEEK tube, a support for the textile samples inside the tube and a lamp which emitted uniform infrared radiation.
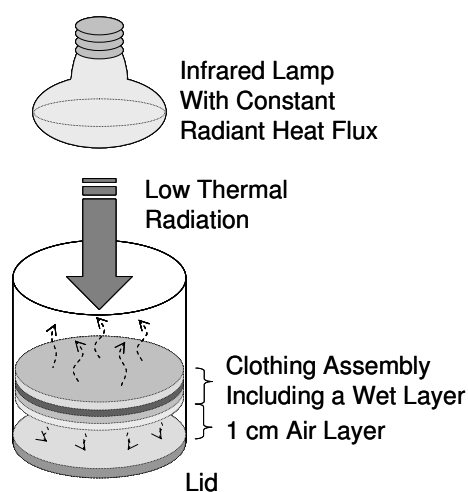
Figure 5.1: Setup of the experiment.

The surface of the uppermost sample inside the tube was 4 cm below the upper edge of the tube. This surface will be referred to as the outer surface. This arrangement ensured that moisture evaporating in the clothing layers was not able to flow sideways. Thus convective heat transfer effects were minimised. As support for the samples, a horizontal net of aramid wire was fixed inside the tube, which served as a support for the textile samples. A second net was placed on top of the samples. This net was weighed down with a lead ring of 100 g in order to impose uniform pressure upon the samples. The thermal radiation source was placed above the textile samples. The distance between the infrared lamp and the outer surface was defined in order to supply a constant radiant heat flux of 5 kW/m² at the surface of the sample. T-type thermocouples with a tolerance of +/-1.7 °C were placed between each of the layers (Figure 5.2) to measure the temperature distribution through the textile assembly during the experiment.
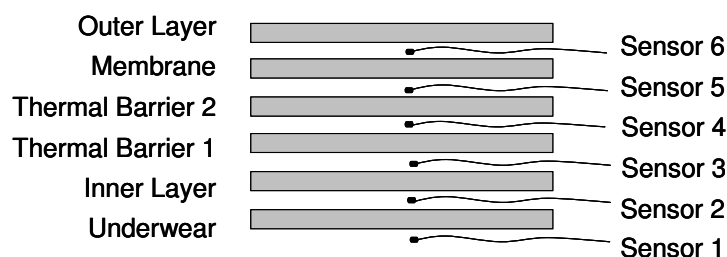
Figure 5.2: Order of the assembly and the thermocouples between the different layers.

At the beginning of the measurement, one specific layer, i.e. the underwear or the thermal barrier respectively, was wetted with a defined amount of distilled water (0.6 g, 1 g or 1.5 g). This corresponds to the moisture contents shown in Table 5.1.

Initial moisture content: absolute amount of supplied moisture		**0.6 g**	**1 g**	**1.5 g**
Underwear	Name of the condition	UW 0.6	UW 1.0	UW 1.5
	Initial moisture content ($M_{moisture}/M_{sample}$)		117% (+/-2%)	
Thermal Barrier	Name of the condition	TB 0.6	TB 1.0	TB 1.5
	Initial moisture content ($M_{moisture}/M_{sample}$)		464% (+/-49%)	

Table 5.1: Initial moisture content of the wetted layers of the assembly, absolute value and percentage of the dry weight of the materials at 20 °C and 65% RH.

The name of the condition refers to the experimental conditions described in the following chapters whereas UW respectively TB indicates the layer which was initially wetted and the additional number indicates the amount of moisture initially supplied.

The assembly including the wet layer was placed inside the tube and irradiated at 5 kW/m^2 during 10 minutes. Temperatures between the layers were recorded continuously throughout each measurement.

5.1.2 Results

A statistical analysis of the results was performed using multivariate analysis of variables (ANOVA) combined with Tukey post hoc test [105]. The significance level of 0.05 was used throughout this analysis. The ANOVA model was validated and verified by checking normal distribution and variance homogeneity of the residuals.

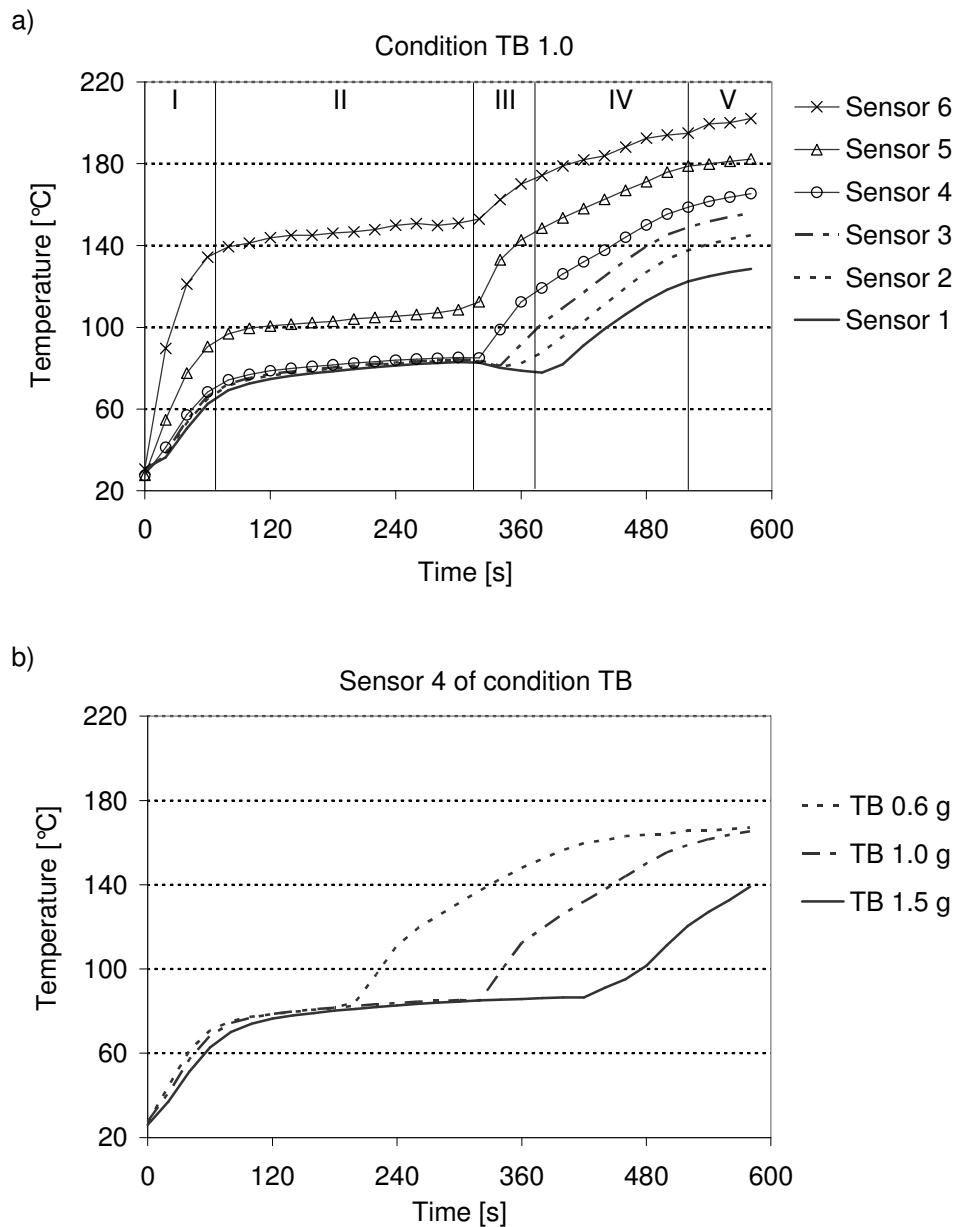Figure 5.3: a) Temperatures between the layers during the measurements with 1 g water located in the thermal barrier. The temperature patterns can be divided into five different phases. b) Temperatures of sensor 4 of the measurement with 0.6 g, 1 g and 1.5 g water in the thermal barrier. All those measurements have been carried out with an air gap between the innermost layer and the cap of the measurement cell.

The curves of the temperatures between the different clothing layers can generally be divided in five different phases (Figure 5.3); I) an initial rising phase, II) a stagnation phase, III) a temperature drop in the inner layers for the TB conditions and a slight initial rise in temperature of the inner layers of the UW conditions, IV) a final rising phase and V) a second stagnation phase. Not all of those phases are visible in each of the conditions. For the statistical evaluation the change of the phases was determined by the point where the change of the gradient was bigger than 1 °C per 6 s.

Phase I: Initial temperature rise

At the beginning of the measurement, immediately after turning on the radiation heat source, the temperatures started to rise strongly in all sensors. As expected, the temperature increase was higher for the outer than for the inner layers. The temperatures of the sensors on the inner side of the wet layer, which were sensors 1-4 of TB conditions and sensor 1 of UW conditions, all rose with the same gradient of 1 +/-0.1 °C/s. In the outer layers, sensors 5 and 6 for moisture in the thermal barrier the gradients reached up to 1 +/-0.1 °C/s and in sensors 2-6 the gradients even reached up to 2 +/-0.1 °C/s when the moisture was located in the underwear. Following this initial increase, temperature curves were flattening off and temperatures stayed constant.

Phase II: Stagnation of the temperature rise

At the first inflexion point, the temperature of sensor 1 was 5 +/-2 °C higher in conditions with wet thermal barrier than on the moist underwear (Figure 5.4). There was no significant difference between the temperatures of sensor 2 of condition UW 0.6 and of condition TB 0.6 while the temperature of sensor 2 of the other conditions was still 5 +/-2 °C higher in TB than in UW.

The temperature gradient between the wet layer and the outermost sensor was higher than 40 °C in TB conditions and even reached up to 95 °C for UW conditions. When 1 g or 1.5 g moisture was located in the underwear (conditions UW 1.0 and UW 1.5), the temperatures measured at the end of phase I using sensors 1 and 2 were approximately the same (Figure 5.4). The first temperature gradient was found between sensors 2 and 3. When only 0.6 g moisture was located in the underwear (UW 0.6), a temperature gradient was already found between sensors 1 and 2. In the combinations with wet thermal barriers, the temperatures in

sensors 1, 2, 3, and 4 remained more or less constant. The first temperature gradient was measured between sensors 4 and 5. The rate of temperature increase between the sensors 4 and 6 was similar for all combinations (62 +/-4°C) and therefore, the end temperature reached in sensor 6 was logically higher in the combinations with wet underwear. However, the temperature gradient over the layer inside the outermost layer for the samples with moisture accumulated in the thermal barrier was twice as high as for the one with moisture in the underwear (Figure 5.4).
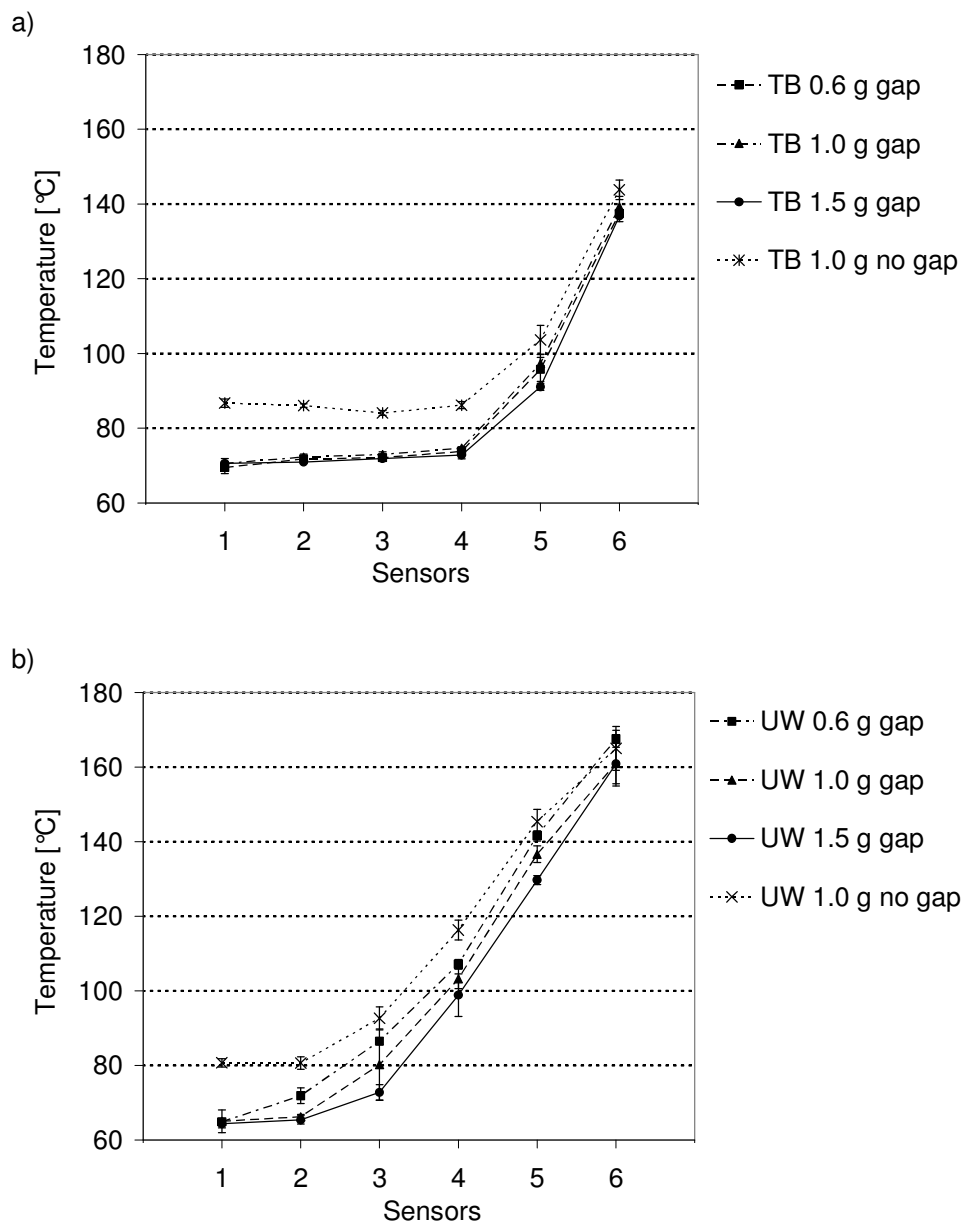

Figure 5.4: Temperatures within the different layers for the different amounts of moisture and the different locations at the time when the temperature gradient is flattening and the temperatures stay constant (end of phase I). a) UW conditions with and without an air gap. b) TB conditions with and without an air gap.

The temperature gradients throughout the textile layers spread significantly for samples with different amounts of moisture located in the underwear. When less moisture was applied initially, higher temperatures were reached within the two outermost layers of the textile combination. For the samples with moisture located in the thermal barrier there was no significant difference in temperature gradients over the layers between the different initial amounts of moisture.

Temperatures on the inner side of the fabrics at the end of the initial rise of the measurements without an air gap were 16 +/-4 °C higher than the corresponding measurements with an air gap (Figure 5.4). But the temperature gradient through the textile layers was smaller and thus there was no significant difference in temperature in the outermost two sensors.

The first inflexion point of the temperature on the inner side of the layers (sensor 1) of TB conditions was reached earlier (after 73 +/-3 s, 84 +/-3 s and 96 +/-3 s for 0.6 g, 1 g and 1.5 g initial moisture) than if the moisture was located in the underwear (respectively after 91 +/-3 s, 94 +/-7 s and 104 +/-9 s). And it was reached earlier when less moisture was applied initially (Figure 5.5). In TB conditions there was no significant difference between the different sensors. The time until the first inflexion point was reached only depended on the amount of initial moisture. In UW conditions the times spread strongly. No significant relationship between the sensors, amounts of moisture and times until first inflexion points were observable.

In the measurements without an air gap, the second phase started after 107 +/-2 s when the moisture was initially located in the thermal barrier and 127 +/-4 s for moisture in the underwear (Figure 5.5) which was later than in the measurements with an air gap.

Throughout the second phase the temperatures rose linearly. Temperature gradients during this phase were 5 +/-1 °C per 100 s in all of the sensors and for all measurements with an air gap. There was no significant difference in the temperature rise during phase II between the samples with moisture located in the underwear and the samples with moisture located in the thermal barrier. The sensor temperatures during this phase depended on the location of the moisture. The amount of moisture had only a significant influence on the measured temperatures of the combination when the moisture was located in the underwear. In this case, the temperature in the outer layers of the assembly was higher at the beginning of phase II when less moisture was supplied initially, although the differences between conditions UW

1.0 and UW 1.5 were small. If the moisture was located in the thermal barrier, there was no significant difference between the temperatures inside the clothing layers for different amounts of moisture.

a)

b)
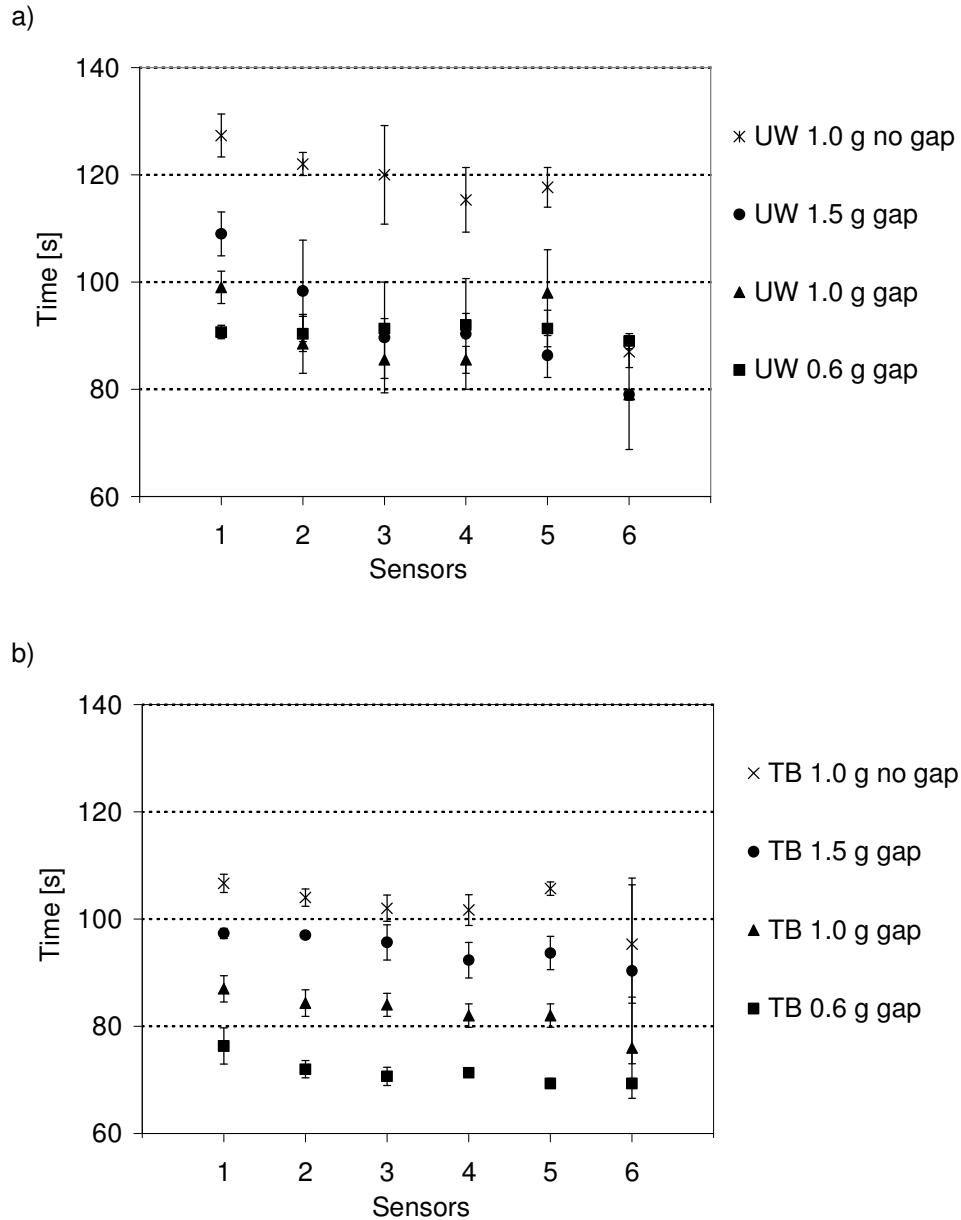
Figure 5.5: Time at which the first inflexion point was reached (end of phase I) for the different amounts of water located in (a) the underwear (UW) and (b) the thermal barrier (TB).

The end of the second phase of the UW conditions was given by a slight temperature rise which was noticeable in sensors 2 and 3. In the measurements where the initial moisture was located in the thermal barrier, the end of the second phase was defined by a sudden

temperature drop of the sensors on the inner side of the wet layer (sensors 1, 2 and 3). For the other sensors there was a recognisable temperature rise (Figure 5.3).

Phase III (TB): Temperature drop in the inner layers of samples with moisture located in the thermal barrier

In the samples with TB conditions, the temperature of the sensors on the inner side of the wet layer (sensors 1, 2 and 3) started to drop at the end of the second phase. The time from the beginning of the measurement until the temperature started to drop was linearly dependent on the initial amount of moisture applied to the thermal barrier as shown in Figure 5.6. We assume that this should be the time when all moisture had evaporated from the layers. In the outer layers the temperature did not drop but started to rise strongly at the same time as the temperature drop started in the inner layers (Figure 5.3).
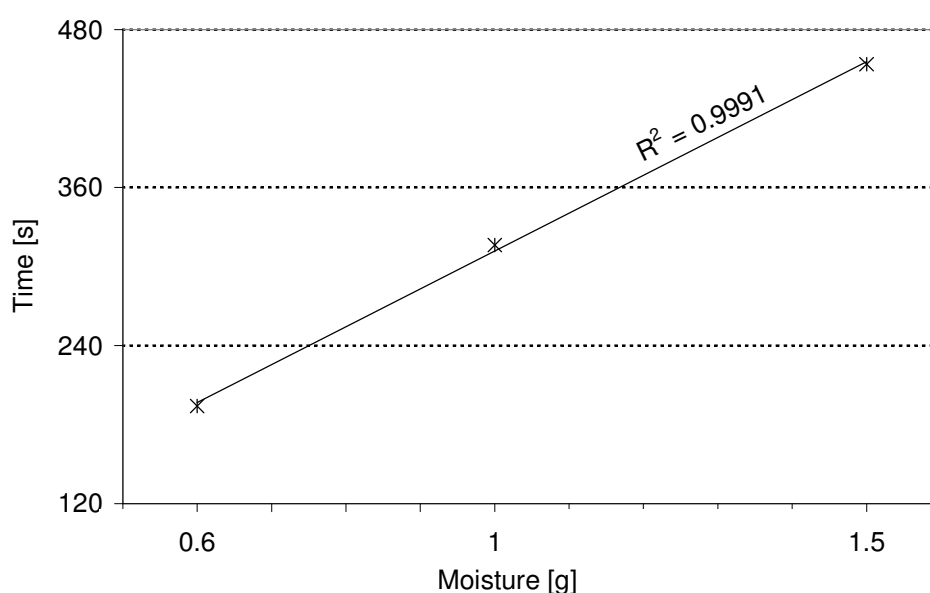
Figure 5.6: Linear correlation of the amount of moisture located in the thermal barrier and the time at the end of phase II.

Comparing the samples with 1 g moisture initially located in the thermal barrier with and without an air gap, we see that the point of the temperature drop was about 16 +/-10 s later in the measurement without an air gap than in the measurement with an air gap (Figure 5.7).

As the temperature of sensors 1, 2 and 3 of the TB conditions dropped initially, it started to rise later than in the outer layers without a temperature drop. The temperature increase of those sensors started one after another, in the order of sensor 4, 3, 2, 1. The same phenomenon

was noticeable in the sample without an air gap but about 20 s (23.6 +/-22.5 s) later than the corresponding sample with an air gap. In this sample, the only exception was the innermost sensor, where the temperature started to rise more than 100 s (112 +/-67.6 s) later than in the corresponding sensor of the measurement with an air gap.
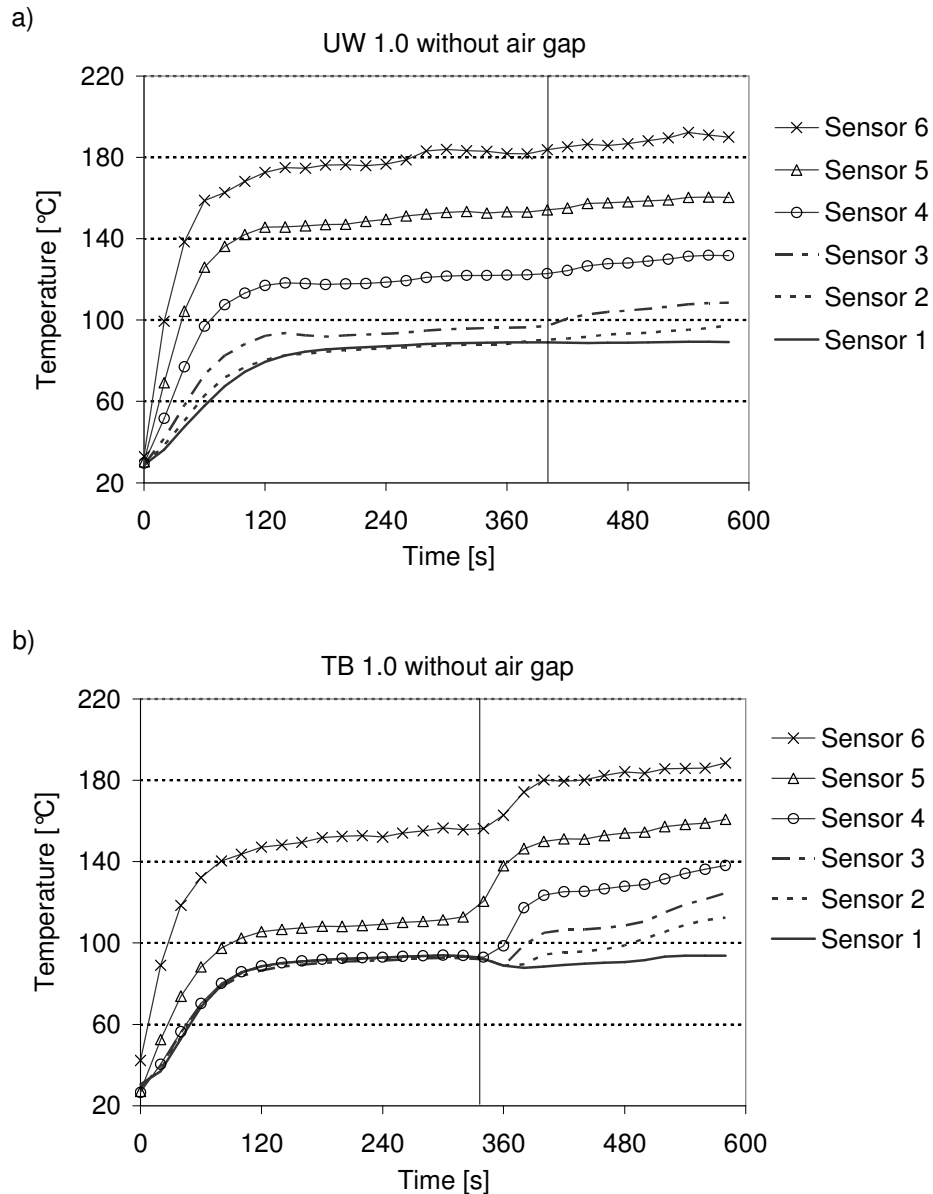
Figure 5.7: Temperatures between the layers of the measurement with 1 g moisture within (a) the underwear and (b) the thermal barrier without an air gap between the innermost layer of the assembly and the cap of the measurement cell.

Due to a slight rise in temperature of 6 +/-2 °C per g initial moisture during evaporation, the temperatures at the end of evaporation were higher in the combinations with more initial moisture than in the combinations with less initial moisture.

Phase III (UW): First temperature rise in samples with moisture located in the underwear

Samples with the initial moisture applied to the underwear showed a different behaviour than the samples with moisture in the thermal barrier, as no temperature drop was noticeable in this case. The first clear change during the second phase was a slight temperature rise after 353 +/-53 s for 1 g initial moisture (condition UW 1.0) and after 564 +/-26 s for 1.5 g initial moisture (UW 1.5). In the case of 0.6 g initial moisture (UW 0.6) there was no such slight initial temperature rise recognisable. The temperatures of the two sensors neighbouring the wet layer (sensors 1 and 2) differed from the beginning of the second phase by 7 +/-0.3 °C. For the other samples, the temperatures of these two sensors did not differ significantly. Thus one might assume that this initial temperature rise was already included in the initial rising phase.

The first slight temperature rise in the sample for condition UW 1.0 and without an air gap was not clearly visible in all of the single measurements. At this point, the temperature of the innermost sensor was 88 +/-0.1 °C, hence about 9 °C higher than in the samples with an air gap.

The linear correlation between the durations of the second phase and the amounts of moisture applied initially shown in the TB conditions can also be assumed in the samples of UW conditions. However, the corresponding point of the measurement with 0.6 g initial moisture is missing as we limited the measuring time to 600 s and thus this assumption cannot be verified.

The temperatures between the layers at the time where the first slight temperature rise took place did not differ significantly between UW 1.0 and UW 1.5. Temperatures of 81 +/-1 °C were reached at the sensors 1 and 2 on the wet layer. Up to 180 °C was reached under the outermost layer of the textile combination.

Phases IV & V: Final rising phase and stagnation

Like in the samples with the initial moisture located in the thermal barrier, a final temperature rise also took place in the samples with initial moisture located in the underwear. The starting point of the increase of temperature was about 100 s - 140 s later for UW moisture conditions

than for TB conditions. It was also dependent on the amount of moisture applied initially. The more initial moisture applied, the later this final temperature rise took place.

a)

b)
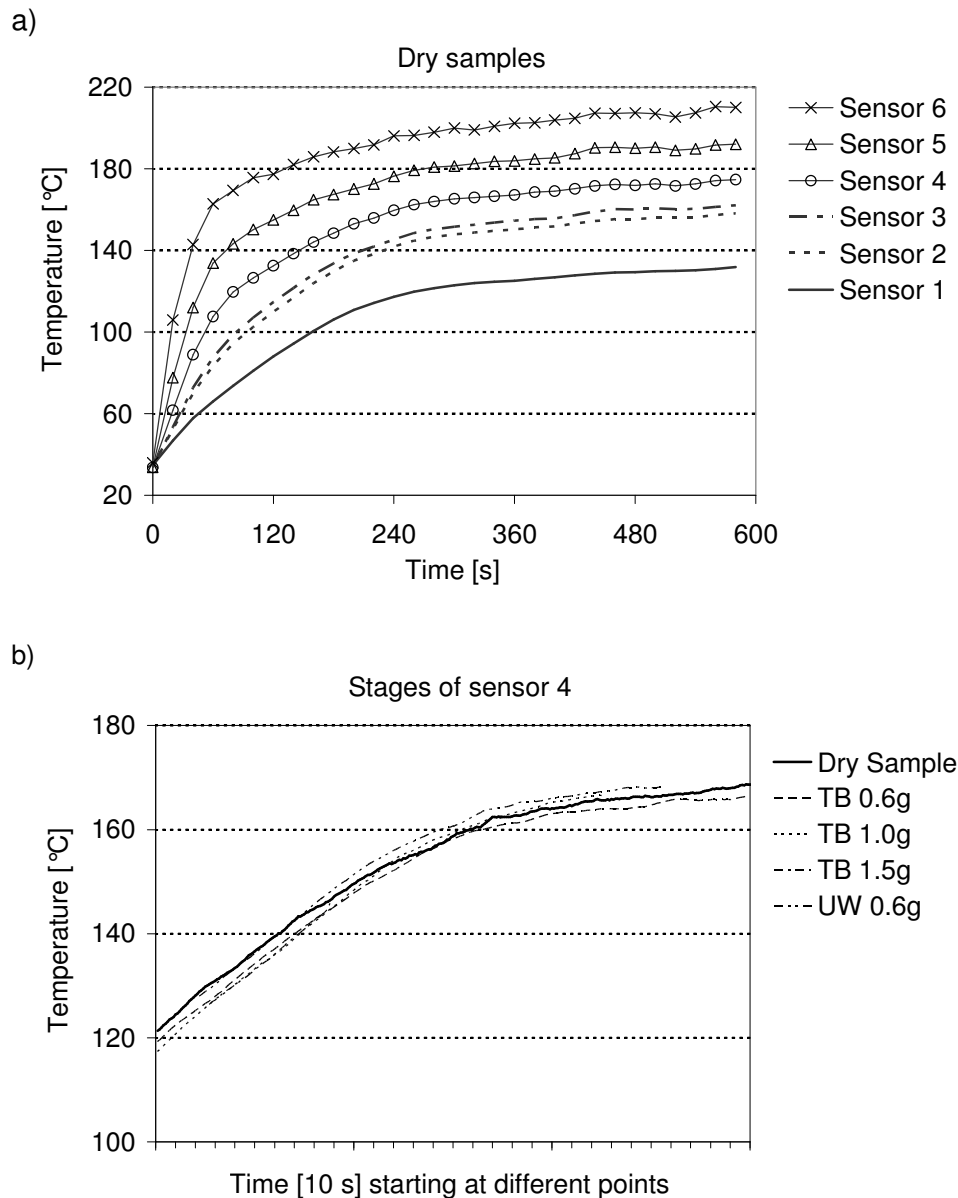
Figure 5.8: a) Temperatures between the layers of the measurement with a dry textile assembly. b) Temperature of sensor 4 of the measurement with dry samples in comparison with the final rising phases of the measurements with different amounts of moisture located in the thermal barrier respectively 0.6 g moisture located in the underwear with an air gap between the innermost layer and the cap of the measurement cell.

This final steep temperature rise which took place in all samples with an air gap until a final inflexion point was reached was similar to the curves from measurements with dry textile combinations (Figure 5.8 a). Figure 5.8 b shows that the temperatures of the measurements

with different amounts of moisture during the final rising phase rose in the same rates as the temperatures of the measurements with dry samples.

The sample without an air gap and with the initial moisture located in the thermal barrier also showed a final temperature rise. But this curve did not show any similarities with the curve of the dry samples. The temperatures rose less than in the dry samples. The temperature of the innermost sensor remained at the lower temperature reached after the temperature drop had occurred.

5.1.3 Discussion

The temperature versus time curves of the measurements can be regarded as consisting of two superimposed curves. First the temperature curve of the textile including a moist layer from which the moisture is evaporating. And second the curve of the heating of the dry textiles after all moisture has evaporated out of the clothing layers. The end of the evaporation is clearly visible as the point at which the temperatures quickly change after a phase with a small temperature rise (phase II). They either drop, mainly in the inner layers, or rise in the outer layers. During the phase change of the water from liquid state, to the vapour state the temperatures within the textile assembly rise with a very small gradient of about 5 +/-1 °C per 100 s. Not all energy applied by thermal radiation was used for phase change during the evaporation, as a part of the energy was also used for heating up the samples. Temperature would only stay constant at the evaporating surface. The textile layers covering the wet layer were still heated up during the evaporation phase. However, the temperature increase of the upper layers was in the same range as the temperature increase at the evaporating surface. This means that the energy absorbed during evaporation was enough to keep the temperature of the whole combination at a almost constant level.

The applied thermal radiation is given as:

$$Q_{rad-in} = \varepsilon Q_{rad} \tag{5.1}$$

$Q_{rad\text{-}in}$	Thermal radiation inward heat flow	[W/m^2]
ε	Absorption coefficient of the textile surface	-
Q_{rad}	Energy emitted from the heat source	[W/m^2]

For textiles, typical ε values range around 0.95-0.98 [11].

The total thermal radiation emitted from the textile surface is defined as:

$$Q_{rad-out} = \varepsilon\sigma(T_{surf}^4 - T_{amb}^4) + \varepsilon\sigma(T_{surf-lid}^4 - T_{amb}^4) \qquad (5.2)$$

$Q_{rad-out}$	Thermal radiation outward heat flow	[W/m^2]
σ	Stefan-Boltzmann constant	[W/m^{2}K^4]
T_{surf}	Temperature at the upper surface of the sample	[K]
$T_{surf-lid}$	Temperature at the outer surface of the lid	[K]
T_{amb}	Ambient temperature	[K]

Thermal radiation within the textile layers is neglected. And no forced convective heat transfer is assumed to take place. Natural convection heat transfer due to the temperature gradient between the hot surface of the sample and the environment is given by:

$$Q_{conv} = h \cdot (T_{surf} - T_{amb}) + h_{lid} \cdot (T_{surf-lid} - T_{amb}) \qquad (5.3)$$

h	Natural convection heat transfer coefficient at the upper surface	[W/m^{2}K]
h_{lid}	Natural convection heat transfer coefficient at the outer surface of the lid of the measurement cell	[W/m^{2}K]

Now we can calculate the energy left for evaporation during the evaporative phase where we assume that the temperature of the system remains constant:

$$\Delta Q_{evap} = Q_{rad-in} - Q_{rad-out} - Q_{conv} \qquad (5.4)$$

The energy used for evaporation follows from:

$$\Delta Q_{evap} = \dot{m}_{evap}\varphi_{evap} \qquad (5.5)$$

$\dot{m}_{evap}$	Evaporative mass flux	[kg/m^{2}s]
φ_{evap}	Latent heat of evaporation	[J/kg]

We get from Equation (5.4) for ΔQ_{evap} 2.1 kW/m^2 and Equation (5.5) gives 1.8 kW/m^2. The energy calculated for the evaporation is lower than the energy from the conservation equation. However, energy losses through walls of the measurement cell were not considered in those calculations.

Constant	Value	Unit
Q_{rad}	5000	$[W/m^2]$
ε	0.95	-
T_{surf}	140	$[°C]$
$T_{surf-lid}$	70	$[°C]$
T_{amb}	20	$[°C]$
h	8	$[W/m^2K]$
h_{lid}	4	$[W/m^2K]$
$\dot{m}_{evap}$	0.00039	$[kg/m^2s]$
φ_{evap}	2257	$[kJ/kg]$

Table 5.2: Constants used for the calculations of the energy balance.

Moisture initially located in the outer layers evaporates faster than moisture located in the underwear. During the second phase (phase II), the temperature of the wet layer is generally higher in the moist thermal barrier (72 °C- 86 °C) than in the moist underwear (66 °C-82 °C).

Only two factors were found to differ between the two locations of moisture and mainly influence the evaporation rate: the temperature of the wet surface which was higher when the moisture was located in the thermal barrier and the diffusion length which was smaller when the moisture was located in the thermal barrier, as there were less textile layers following.

The temperature distribution during the second phase did not depend on the amount of moisture applied to the textile layers. But it strongly depended on the location of the moisture. If the moisture was located in the underwear, the temperature inside the innermost layer was lower than if the moisture was located in the thermal barrier. The temperature distribution also strongly depended on whether there was an air gap present or not. Without an air gap, the temperature of sensor 1 rose up to about 93 °C depending on the location of the moisture.

A linear correlation was observed between the amount of moisture and the time until the moisture had completely evaporated. This correlation could clearly be established when the

moisture was located in the thermal barrier (Figure 5.6). This linear relationship indicates that the evaporation speed is constant for a constant temperature, which was stated before [60].

In TB conditions at the end of phase II temperatures of the inner layers first dropped. We assume that during the evaporation (phase II), part of the moisture was transferred to the inner layers. This could be due to liquid moisture transfer or due to steam which condensed in the inner layers. Liquid moisture was supposed to be present in the inner layers at the end of the evaporation phase, which started to evaporate as soon as all moisture had evaporated from the moist thermal barrier. Due to this evaporation process, the temperatures of sensors 1-3 first dropped until all moisture had evaporated out of the clothing layers, while the temperature of the sensors neighbouring the thermal barrier (4 and 5) started to rise. The fact that this phenomenon was not visible in UW conditions tends to confirm the assumption that moisture was driven from the thermal barrier to the inside and accumulated in the inner layers. Evaporation started in the outermost wet layer first of all and only continued in the next wet layer when the outermost layer had dried out.

Following complete evaporation of the moisture in the textile assembly, the temperatures first rose (phase IV) and then reached an equilibrium (phase V). Similar absolute equilibrium temperatures were reached and temperature courses were followed as measured for the dry samples. Figure 5.8 b gives an example of these temperature courses during phases IV and V for sensor 4. All sensors showed similar curves.

For the measurements without an air gap, the temperatures following evaporation did not reach the same level as in the dry samples. Vapour moved towards the cap of the measurement cell, condensed there and was absorbed by the underwear. At the end of the measurement on average 0.1 g moisture was accumulated in the underwear. This can be seen as a new condition and a new wet temperature pattern is superimposed.

 In the measurements with an air gap, moisture also moved inwards. At the end of the measurement condensed water could be seen on the cap of the measurement cell. The underwear was not in contact with the cell und therefore did not absorb this moisture. Therefore the underwear dried out during the measurement.

To simulate the process of transient heat and water vapour transfer Prasad et al. [8] used an equation system consisting of mass continuity, energy equation and the relation describing the moisture sorption isotherm. They assumed the local moisture content to be in equilibrium at

all times. Capillary action was not considered and volume changes of the fibres due to the changing moisture content were neglected.

Mass continuity:

$$\frac{\rho_{fab}}{f}\frac{\partial M}{\partial t} = -\frac{\rho_g W_{vap}}{P W_{sys}}\frac{\partial p_{vap}}{\partial t} - \frac{\partial}{\partial x}\left[-D\frac{\partial p_{vap}}{\partial x}\right] \tag{5.6}$$

Energy equation:

$$\rho_{tot} C_{tot}\frac{\partial T}{\partial t} = -\frac{\partial}{\partial x}\left(-k_{tot}\frac{\partial T}{\partial x}\right) - \frac{\partial Q_{rad}}{\partial x} - \rho_{fab}\Delta H\frac{\partial M}{\partial t} \tag{5.7}$$

Moisture isotherm:

$$M = funct(T, X) \tag{5.8}$$

C_{tot}	Total heat capacity of the control volume	[J/kg·K]
D	Diffusion coefficient	[m^2/s]
f	Volume fraction of voids in the cloth	-
k_{tot}	Total thermal conductivity	[W/m·K]
M	Local moisture content (moisture regain)	-
p_{vap}	Partial pressure of water vapour	[Pa]
P	Total pressure	[Pa]
Q_{rad}	Thermal radiation heat flux	[W/m^2]
T	Temperature	[K]
W_{sys}	Molecular weight of the system	[g/mol]
W_{vap}	Molecular weight of water vapour	[g/mol]
X	Volume fraction of water vapour	-
ΔH	Heat of adsorption per unit mass	[J/kg]
ρ_{fab}	Density of the dry fabric	[kg/m^3]
ρ_g	Gas density	[kg/m^3]
ρ_{tot}	Density of the whole system	[kg/m^3]

Detailed information about this model can be found in [8].

The temperature curves found experimentally in this study were similar to the curves found by Prasad et al. [8] using this model. They found the temperature at the first inflexion point to be around 50 °C while our first inflexion point was at around 80 °C. And also the dry temperatures were higher than in the present study. However, the superposition of the wet and dry temperature pattern is similar. Prasad et al. [8] used in their study thermal radiation of 2.5 kW/m^2. This would imply that at lower intensities of thermal radiation the evaporation takes place at lower temperatures.
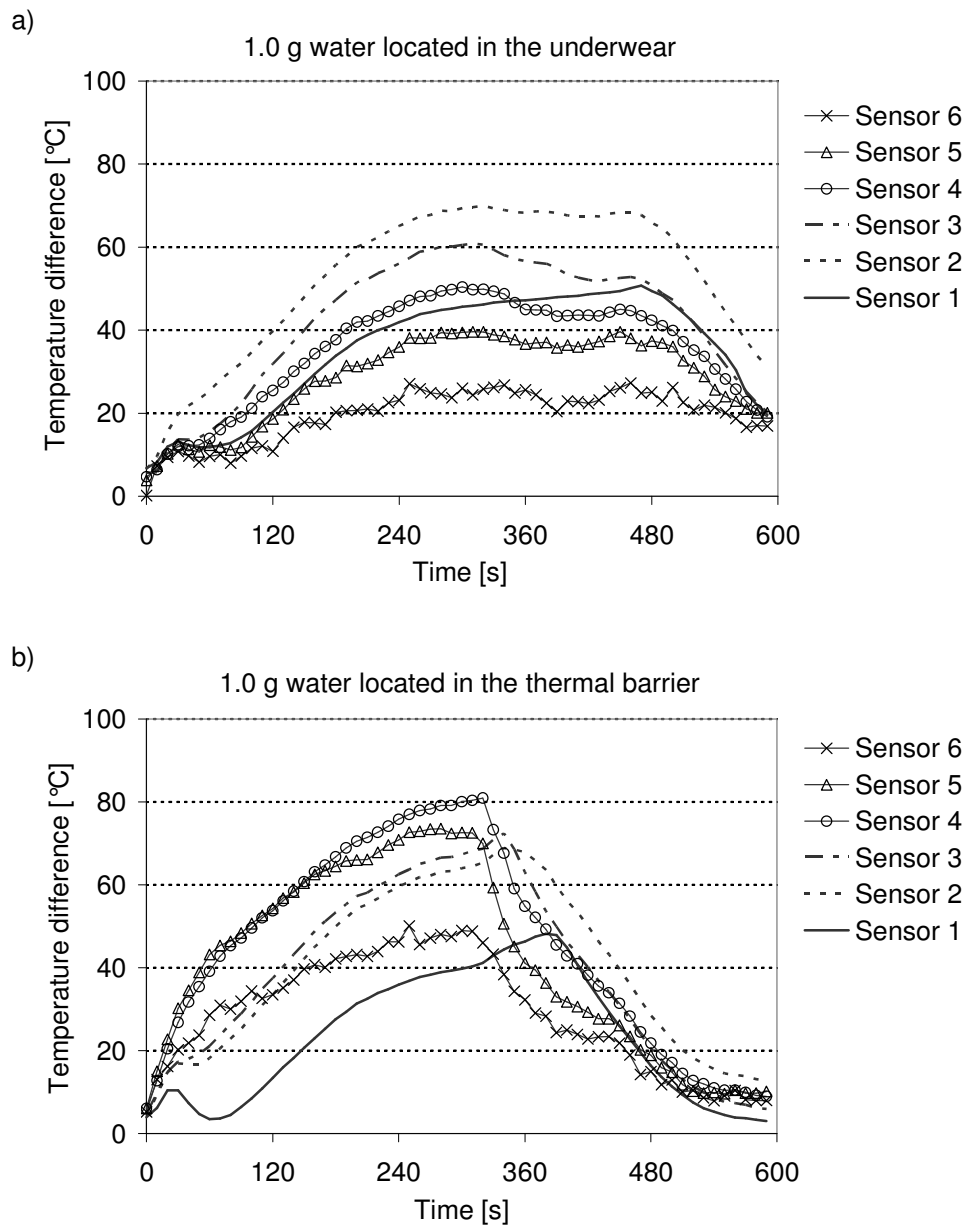
a)

b)

Figure 5.9: Difference between temperatures of the measurement with the dry sample and the temperatures of the measurements for (a) UW 1.0 with an air gap and (b) TB 1.0 with an air gap.

Figure 5.9 shows the difference between the temperatures of the dry sample and the samples with 1 g initial water. The difference between the temperatures in the dry samples and condition UW 1.0 was the highest for sensors 2 and 3 showing that this difference was generally greater for the inner layers than for the outer layers with the exception of the temperature of sensor 1. In the assemblies with condition TB 1.0 the temperature differences were largest for the sensors neighbouring the wet layers (sensors 4 and 5). Hence, the temperatures of the sensors neighbouring the wet layers were influenced the most by the presence of the moisture except for sensor 1 for the UW conditions.

During the evaporation of the moisture, the temperature inside the clothing combination was lower for all sensors than during the measurement of the dry samples. At the end of the evaporation the temperatures of the initially wet samples approached the temperatures of the dry samples but they did not rise higher than the dry samples (Figure 5.9). Thus, moisture is shown to have a positive influence on protection against thermal radiation under the conditions studied here.

Steam burns are assumed to appear during fire fighters assignments. As we did not measure higher heat flux between the different sensors in the wet combinations, it may be assumed that if steam burns occur, they might not be due to a higher heat transfer in wet conditions but more likely due to the condensation of moisture on the skin. Moisture condensed on the cover of the measurement setup during the measurement. This may indicate that steam burns could occur under similar conditions in practice.

5.1.4   Conclusions

During the evaporation of the moisture, a temperature plateau appeared during which temperatures were hardly rising. The energy consumption used for the phase change of moisture located in an assembly dominated the heat transfer process as long as there was moisture present. Moisture located in the outer layers evaporated faster than moisture located in the inner layers and also evaporated at slightly higher temperatures. As soon as all moisture had evaporated, the temperatures approached the temperatures measured for dry samples.

The moisture within the clothing assembly did not lead to increased temperatures compared to the measurements with dry samples. On the contrary, lower temperatures were reached during the evaporation process.

Considering the fact that the second increase in temperature followed exactly the same courses as for measurements with dry samples, one can conclude that at that point, all moisture had evaporated from the clothing assembly. Moisture moved to the inside and condensed on the cap of the measurement cell. This indicated a possible risk for steam burns, although the presence of moisture generally showed a positive effect on the temperature course in the layers of the assembly.

5.2   Determination of the moisture transfer using X-ray radiography

In the following chapter moisture transfer within multilayer protective clothing assemblies at low thermal radiation is analysed using X-ray radiography. X-ray attenuation technique was already shown to work for the analysis of moisture distribution and movement in porous materials. Weder et al. [103] used micro computer tomography to analyse the moisture distribution in multilayer textile assemblies. Roels et al. [108] analysed moisture flow in porous materials using microfocus X-ray radiography. Aim of the study was to quantify moisture movement within protective clothing layers at low thermal radiation by analysing the water content of the layers versus time using X-ray radiography. The radiography/tomography system was located in a large walkable chamber so that the heat flux of the infrared heater could not damage the X-ray system components.

5.2.1   Methods

The same setup as described in the previous chapter (Chapter 5.1) was used for the radiography measurements. The same initial conditions as described in Table 5.1 were used.
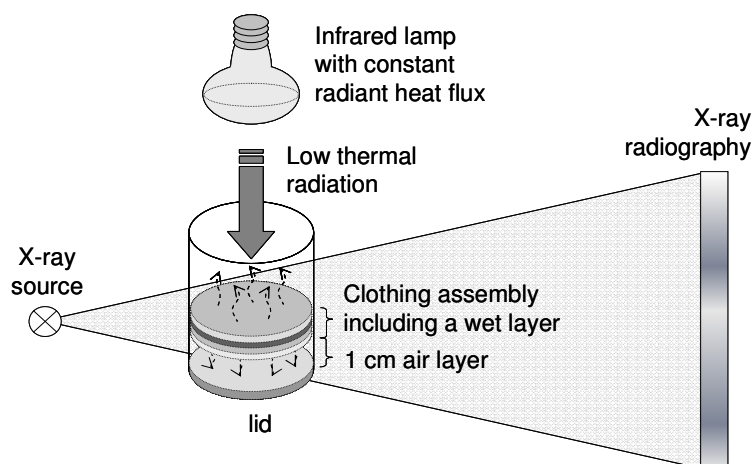

Figure 5.10: Measurement setup including the sample holder, thermal radiation heat source and X-ray source.

X-ray radiography

For the X-ray radiography a directional molybdenum target was used. The window filtering consisted of 0.5 mm beryllium and 0.025 mm silver. This source and the filtering with silver provided a restricted X-ray spectrum around 20 keV thus avoiding beam hardening effects. The X-ray source acceleration energy was 50 keV and the current was set to 0.46 mA. The X-ray spot size was about 100 µm.

The detector was a Hamamatsu 7942 CA-02 flat panel, operated in 4 x 4 binning mode using single non averaged shots of 0.3 sec duration. The front face was carbon fibre reinforced plastic instead of aluminium. One scan per second was done during 10 minutes resulting in 600 pictures. The distance source-detector was 680 mm and the distance source-sample was 180 mm. This resulted in a pixel size referred to sample of 53 µm and a full frame field of view of 30 x 31 mm, based on a full frame of 560 x 592 pixels.

Evaluation

Figure 5.11 shows an X-ray radiography taken with the mentioned setup of condition TB 1.5 (i.e. 1.5 g water initially located in the thermal barrier (TB 2)). In order to determine the moisture content within the different layers, quadrangles were defined in the pictures for each layer. Only the middle part on the side without thermocouples was used for the evaluation.
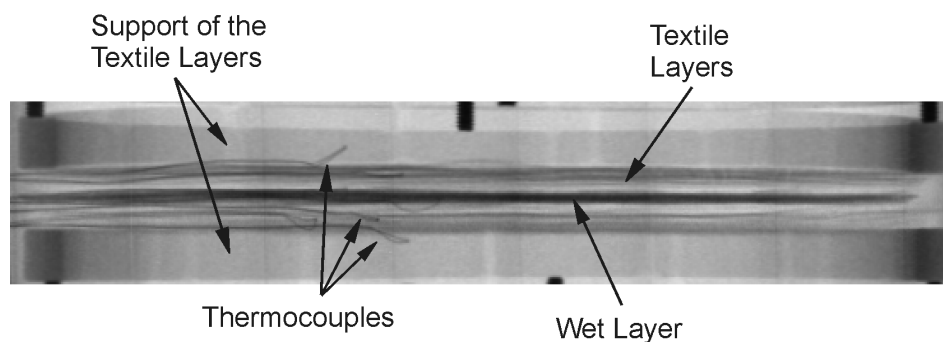

Figure 5.11: X-ray radiography of condition TB 1.5.

According to Beer's law monochromatic radiation with the intensity I is attenuated over a length d with the linear absorption coefficient µ [109]:

$$\ln\left(\frac{I}{I_0}\right) = -\mu d \qquad\qquad (5.9)$$

I_0	Incident intensity	[photons/mm^{2}s]
I	Intensity of the attenuated X-ray	[photons/mm^{2}s]
μ	Attenuation coefficient	[1/cm]
d	Length of the X-ray path through the sample	[cm]

From this equation (5.9) the equation (5.10) to calculate the moisture content within the clothing layers can be derived [108]:

$$M_{fab} = -\frac{\rho_{liqu}}{\mu_w d}\ln\left(\frac{I_{wet}}{I_{dry}}\right) \qquad\qquad (5.10)$$

M_{fab}	Moisture content of the fabric	[kg/m^3]
ρ_{liqu}	Density of liquid water	[kg/m^3]
μ_w	Attenuation coefficient of water	[1/cm]
d	Irradiated length of the sample	[cm]
I_{wet}	Intensity measured for the wet sample	[photons/mm^{2}s]
I_{dry}	Intensity measured for the dry sample	[photons/mm^{2}s]

The absorption coefficient has usually to be determined experimentally. The thickness of the samples and thus the local moisture content within the samples was not the same for all samples. Therefore a calibration for each layer and different moisture contents was performed. In order to calibrate the moisture measurement we supplied the single layers with different amounts of water (0.3 g, 0.6 g, 0.9 g, 1.2 g and 1.5 g). Then X-ray radiographs of each layer with each of the 5 different amounts of water separately without thermal radiation were taken. The calibration curves for the underwear and the thermal barrier (TB 2) are shown in Figure 5.12.

All layers were calibrated separately according to their calibration curves whereof the constant C was determined for each layer:

$$C = \frac{\rho_w}{\mu_w d} \qquad\qquad (5.11)$$

After this calibration the curves still showed a vertical shift. Therefore, the initial moisture contents of the different layers were set arbitrarily to zero. Negative values in the inner layers at the end of the measurement hence implied that water was initially present in those layers.
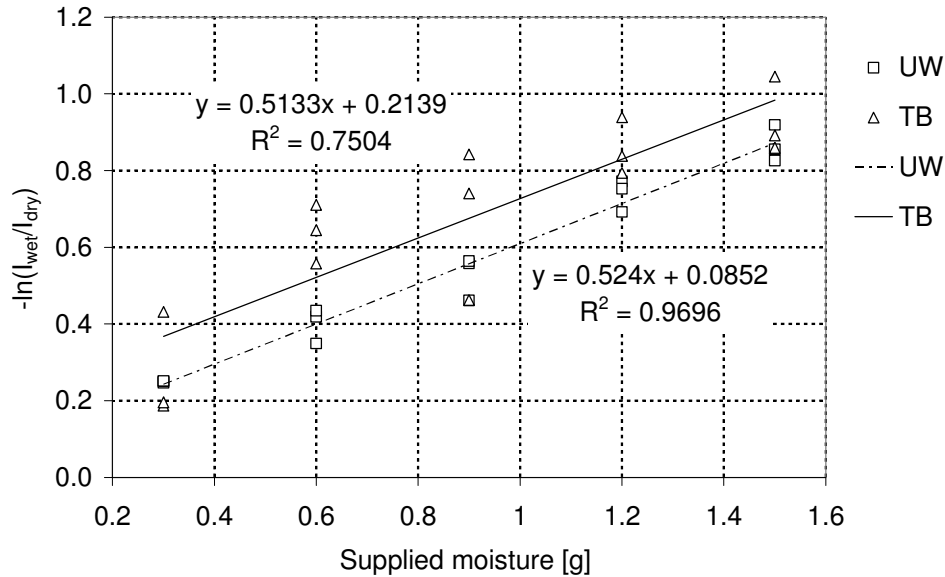
Figure 5.12: Moisture calibration curves presenting the value -ln(Iwet/Idry) as function of the supplied moisture content of the underwear and the thermal barrier.

5.2.2 Results

The results of the X-ray radiography measurements with 1 g water initially located in the underwear (UW 1.0) respectively in the thermal barrier 2 (TB 1.0) are shown in Figure 5.13. The decrease of the moisture in the initial wet layer is visible for both conditions a) in the underwear and b) in the thermal barrier 2. The innermost two layers of the system, which were the underwear and the liner, showed a moisture increase during the evaporation phase when water was initially in the thermal barrier 2. When water was initially in the underwear the inner layer of the jacket (IL) showed an initial increase in moisture content. Thermal barrier 1 without initial moisture of TB conditions reached a negative moisture content at the end of the measurement, which implies that moisture initially must have been present in this layer.

a)

b)
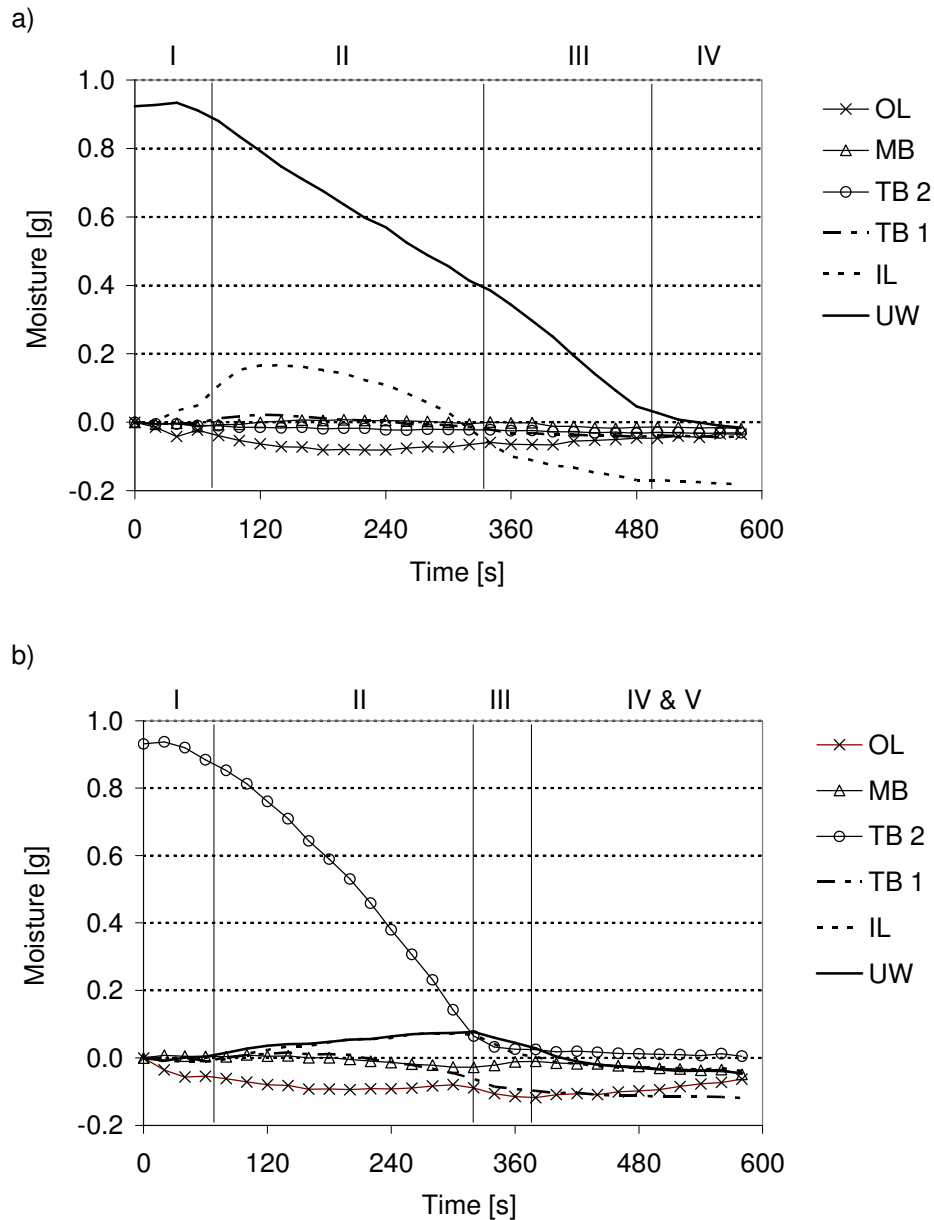
Figure 5.13: Moisture contents in the different layers measured by X-ray radiography a) for 1 g moisture initially located in the underwear (UW 1.0) and b) for 1 g moisture initially located in the thermal barrier 2 (TB 1.0).

The outer layer of the combination showed an initial decrease of moisture and an increase again at the end. The horizontal level of the X-ray source was aligned with the lower surface of the sample. Thus geometrical shifts are assumed to have appeared at the upper surface. Furthermore, the wires of the upper support of the samples stretched and thus the outer layer was flattened during the measurement. Therefore, the apparent moisture changes within this

layer may be caused by geometric errors. In all other layers no significant moisture changes appeared throughout the measurement.
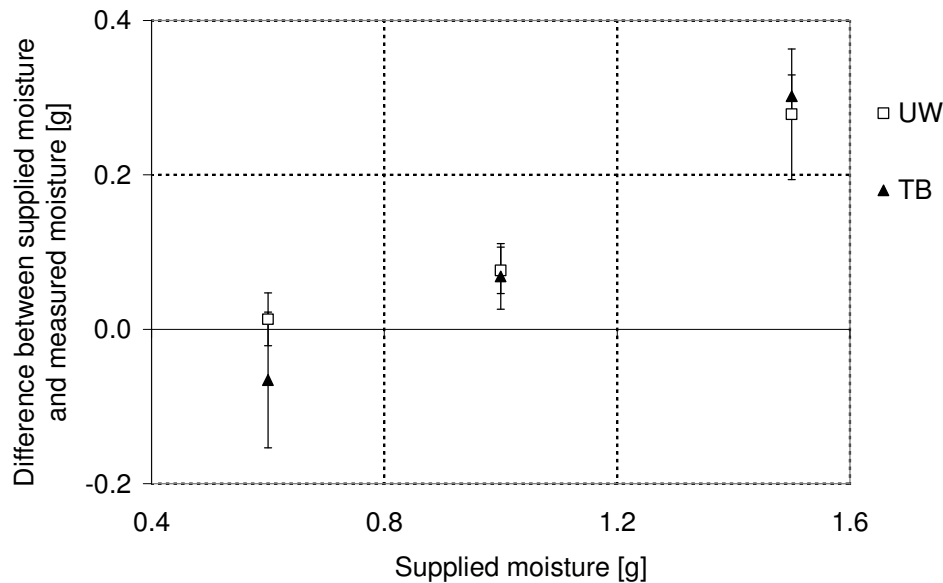
Figure 5.14: Correlation of the difference between supplied moisture and moisture contents measured by X-ray radiography and the supplied amount of moisture at the beginning of the measurements (R^2=0.98).

The results of the measurement spread strongly. Mean standard deviations of the different conditions ranged up to 0.07 g.

The difference between the supplied moisture and the initial moisture content measured by X-ray radiography is shown in Figure 5.14. For 0.6 g supplied moisture the moisture content of the initially wet underwear was 0.59 +/-0.03 g and in the initial wet thermal barrier 0.67 +/-0.09 g. But the higher the initial moisture content, the bigger the difference between the supposed and the measured moisture content. For UW 1.0 only 0.92 +/-0.03 g moisture was detected, for TB 1.0 the detected amount was 0.93 +/-0.04 g, for UW 1.5 it was 1.22 +/-0.08 g and for TB 1.5 it was only 1.20 +/-0.03 g.

Start of evaporation

Figure 5.15 shows the decrease of the moisture contents within the initially wet layers. The point at which evaporation starts is not clearly visible. We defined the start of evaporation by the time when the decrease of the moisture content rose over 0.05 g per 3 s. For UW conditions (i.e. water initially supplied to the underwear) a starting point of the evaporation could be determined (Figure 5.15). The moisture content stayed constant in the beginning for

about 30 s to 60 s. Those values were spreading strongly with standard deviations up to 34 s. At TB conditions (i.e. water initially located in the thermal barrier 2) the moisture content decreased right from the beginning for 1.0 g and 1.5 g initial moisture. Only for TB 0.6 there was a starting point at 33 +/-17 s visible. In the measurement without an air gap, evaporation started with a delay of 103 +/-31 s for UW conditions and of 33 +/-21 s for TB conditions.
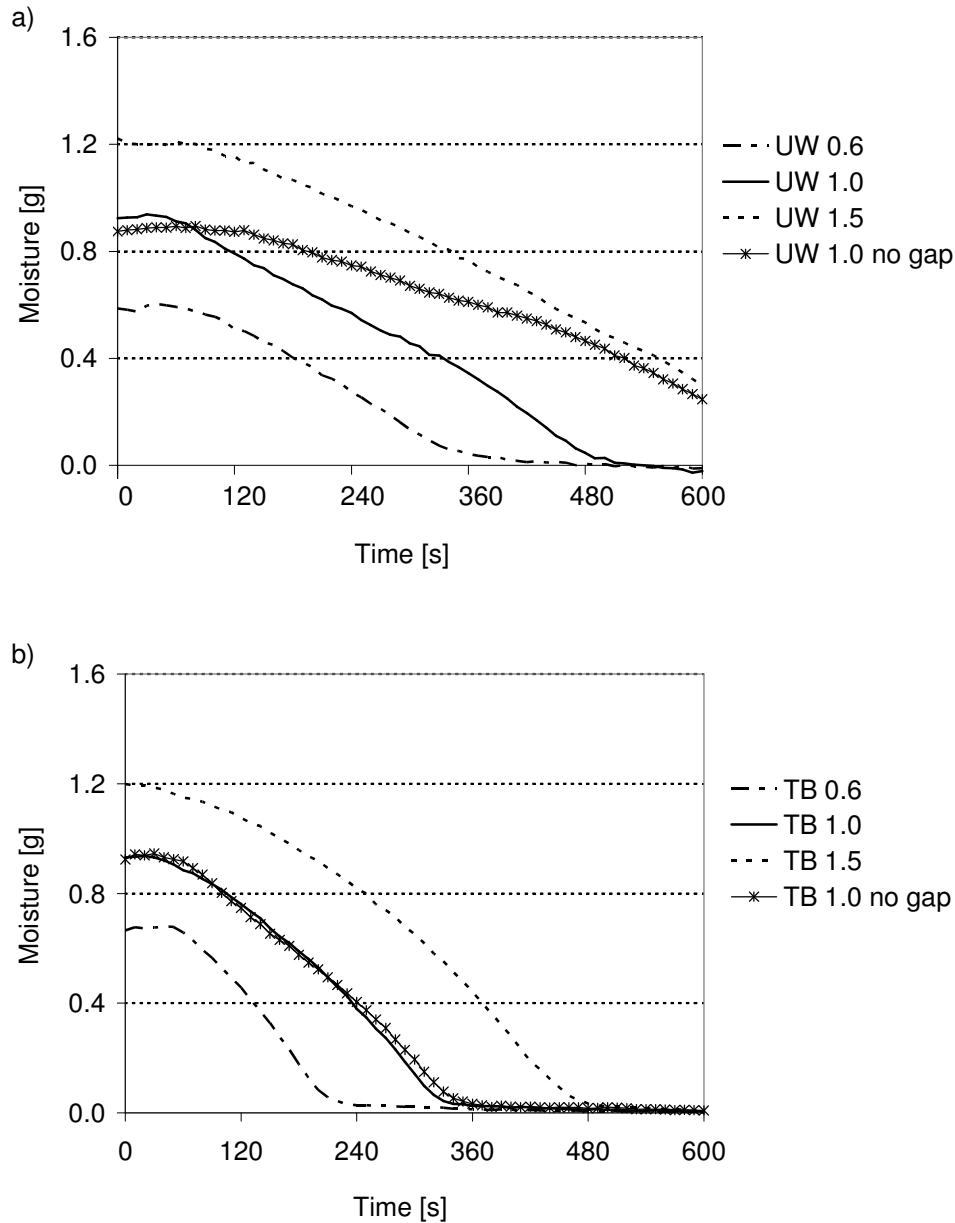

Figure 5.15: Change of the moisture content with time in the initially wet layer for a) UW conditions and b) TB conditions.

Evaporation rate

The moisture decrease in the UW conditions (i.e. water initially in the underwear) was linear with time and the curves ran parallel during evaporation. In TB conditions (i.e. water initially in the thermal barrier 2) the decrease of moisture was not linear throughout the evaporation process. The curves were more or less parallel which means that they were not dependent on the different amounts of moisture.

The moisture content decreased slower for UW conditions than for TB conditions. The air gap had no influence on the evaporation rate for TB conditions. But for UW conditions evaporation was slower in measurements with an air gap.

In order to determine the mean evaporation rate we divided the difference of moisture content from 0.5 g to 0.2 g moisture by the time it took to evaporate that amount of water. As in conditions UW 1.0 without an air gap and UW 1.5 the moisture content of 0.2 g was not reached at the end of the measurement, we calculated the evaporation rate for 0.8 g to 0.5 g instead.

Condition	Evaporation rate (SD) [g/s]	Evaporation rate per evaporating surface area (SD) [g/m²s]
UW 0.6	$2.1 (+/-0.14) \cdot 10^{-3}$	0.27 (+/-0.02)
UW 1.0	$2.1 (+/-0.01) \cdot 10^{-3}$	0.27 (+/-0.01)
UW 1.5	$1.9 (+/-0.03) \cdot 10^{-3}$	0.24 (+/-0.01)
UW 1.0 without gap	$1.2 (+/-0.11) \cdot 10^{-3}$	0.30 (+/-0.03)
TB 0.6	$4.4 (+/-0.98) \cdot 10^{-3}$	0.58 (+/-0.13)
TB 1.0	$3.8 (+/-0.41) \cdot 10^{-3}$	0.49 (+/-0.05)
TB 1.5	$4.0 (+/-0.20) \cdot 10^{-3}$	0.52 (+/-0.03)
TB 1.0 without gap	$3.3 (+/-0.29) \cdot 10^{-3}$	0.43 (+/-0.04)

Table 5.3: Mean evaporation rates for different conditions; absolute and per evaporating surface.

The results are shown in Table 5.3. The evaporation rates from the initially wet underwear were smaller than the ones from the initially wet thermal barrier (TB 2). However, spreading was very large. The evaporation rate of the condition UW 1.0 without an air gap was about

half of the evaporation rate of the same condition with an air gap. In this condition the underwear was lying directly on the lid of the measurement cell. Thus, evaporation was only possible in one direction. The surface from which evaporation could take place and following the evaporation rate was halved.

In order to normalize the evaporation rate in terms of evaporating surface we divided it by the evaporating surface of 77 cm^2 and 38 cm^2 respectively for condition UW 1.0 without an air gap. The resulting evaporation rates are listed in Table 5.3.

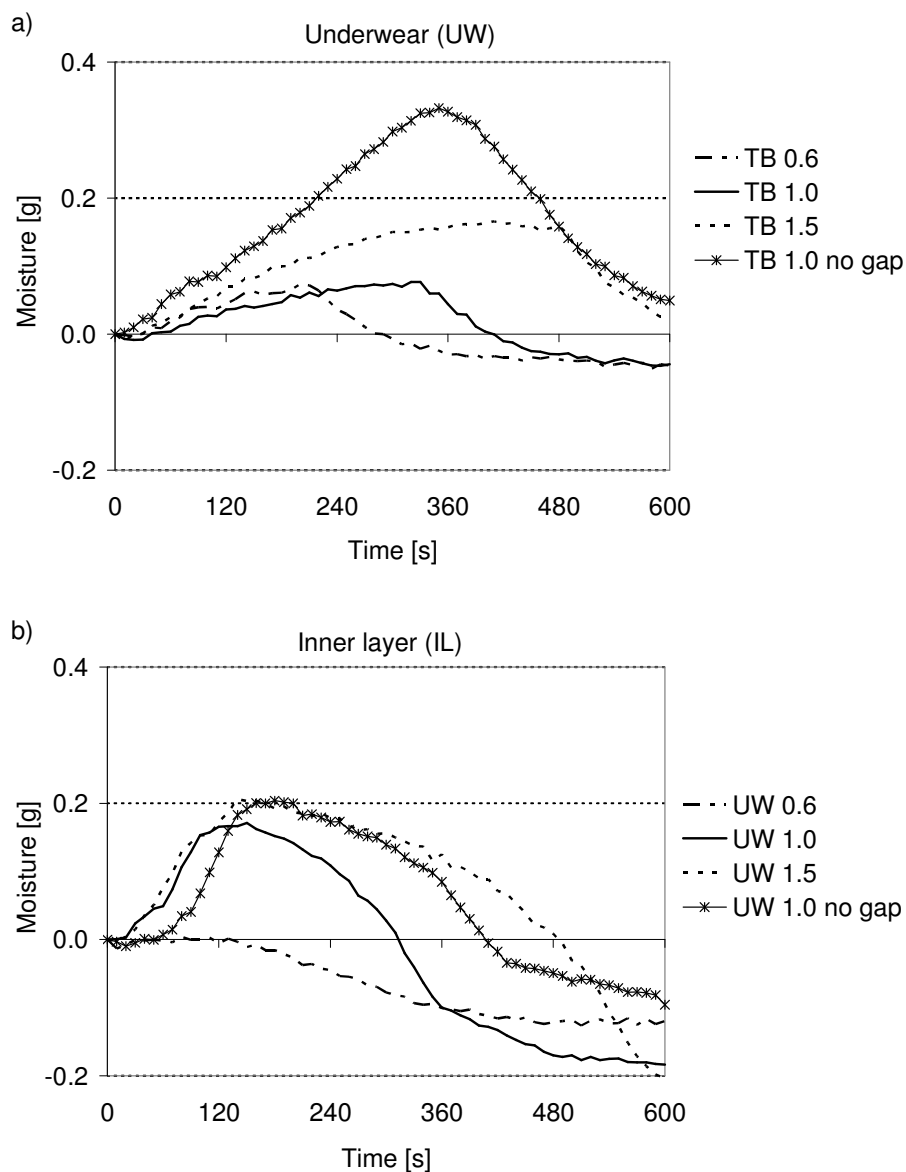**Moisture accumulation in the inner layers**

Figure 5.16: Changes of moisture contents with time in a) the underwear of TB conditions and b) the liner of UW conditions for different initial moisture contents and measurements with and without an air gap.

The moisture accumulation in the underwear of TB conditions (i.e. water initially located in the thermal barrier 2) is shown in Figure 5.16 a. During evaporation the underwear absorbed up to 0.18 g water. Standard deviations of 0.01 g to 0.07 g appeared. Moisture continuously increased until it reached a maximum and then decreased again. The higher the initial moisture content was, the later the maximal moisture content was reached. The moisture accumulation in the liner of UW conditions is shown in Figure 5.16 b. In UW conditions the initial moisture increase was much steeper than in TB conditions. Maximal moisture contents of 0.2 +/-0.7 g were reached all at about the same time, independently on the amount of the initial moisture content.

At the end of the measurement the moisture content of the liner of all UW conditions reached a negative value (Figure 5.16). As the moisture contents of all layers which were not wetted initially were set to zero, a negative amount of moisture at the end of the measurement indicates that this amount of moisture must have been present within the layer at the beginning of the measurement. The samples were kept at room conditions prior to the test. Therefore, an initial amount of water corresponding to their moisture regain was present in all layers.

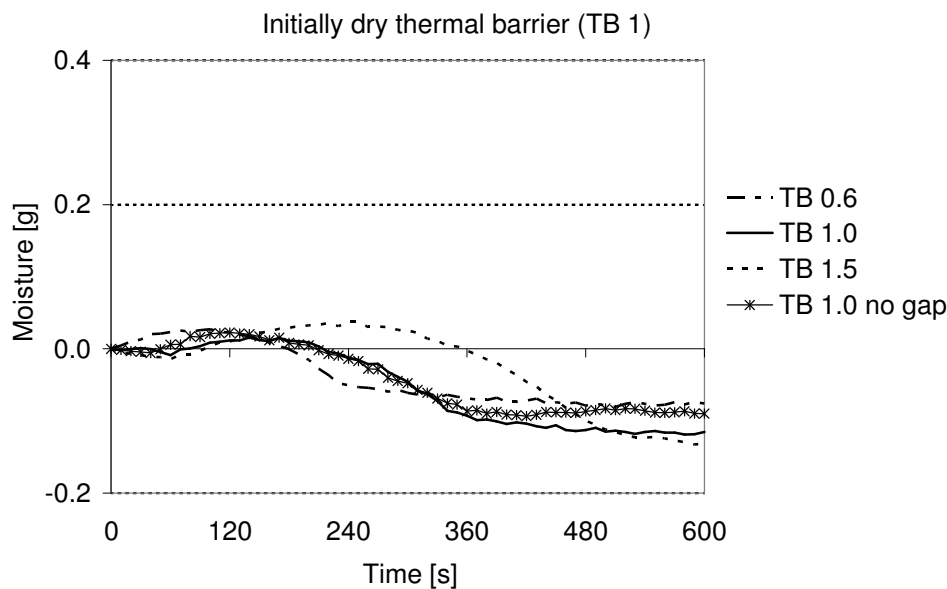Figure 5.17: Changes of moisture contents with time in the initially dry thermal barrier 1 of TB conditions for different initial moisture contents and measurements with and without an air gap.

The thermal barrier 1 neighbouring the initially wet thermal barrier 2 absorbed in the beginning moisture from the initially wet thermal barrier 2 as it reached a negative moisture value during the measurement (Figure 5.17).

The maximal moisture content absorbed by the liner depended on the initial amount of moisture in the systems (Figure 5.18). The maximal moisture absorption in the liner was for UW 0.6 only 0.01 +/-0.01 g while for UW 1.0 condition 0.18 +/-0.05 g and for UW 1.5 even 0.22 +/-0.06 g moisture was measured maximally. The maximal moisture content for TB conditions was the same in the underwear and the liner. 0.08 +/-0.06 g was accumulated maximally in the underwear and the liner of condition TB 0.6 and TB 1.0. The moisture content spread more for the liner with a standard deviation of 0.06 g than for the underwear with a standard deviation of 0.02 g. A maximal moisture content of 0.17 +/-0.09 g was measured in the underwear and liner of condition TB 1.5.
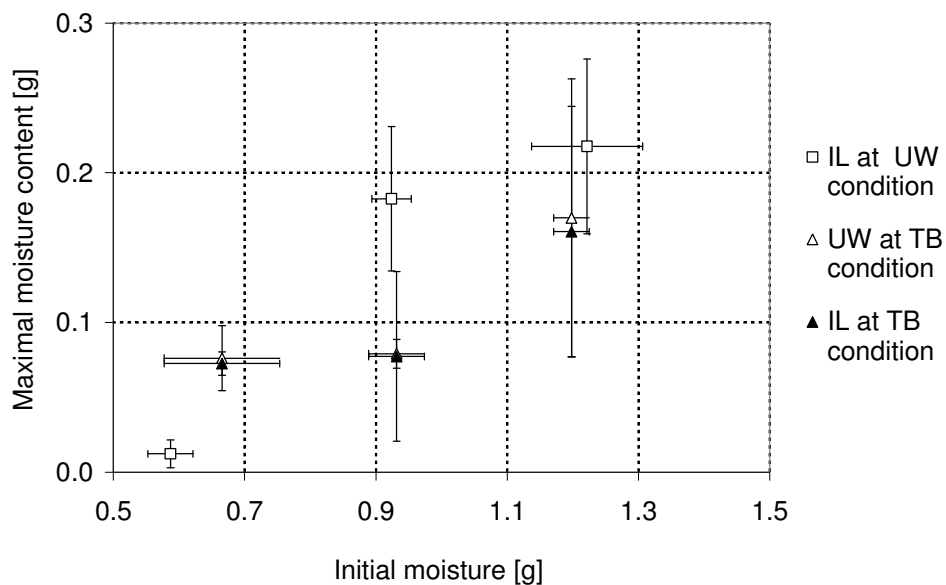
Figure 5.18: Maximal moisture contents in the underwear and the liner for TB and UW conditions.

We get a good correlation between the time to reach the maximal moisture content in the inner layers (i.e. underwear and liner) and the time at which evaporation stopped in the initially wetted layer; for the underwear it amounts to $R^2 = 0.991$ and for the liner to $R^2 = 0.995$ for TB conditions (Figure 5.19). The maximal moisture content was reached about the same time as evaporation stopped. The end of evaporation was defined by the time when the decrease of the moisture content in the initially wet layer got smaller than 0.05 g per 3 s. In conditions with moisture initially located in the underwear (UW conditions) it was not possible to make this correlation due to missing evaporation end points of UW 1.0 and UW 1.5. Maximal moisture contents were reached for all conditions at about the same time (127-167 +/-29 s) except for UW 0.6 where the maximal moisture content was reached after 47 +/-34 s. This was more than 300 s earlier than evaporation stopped.
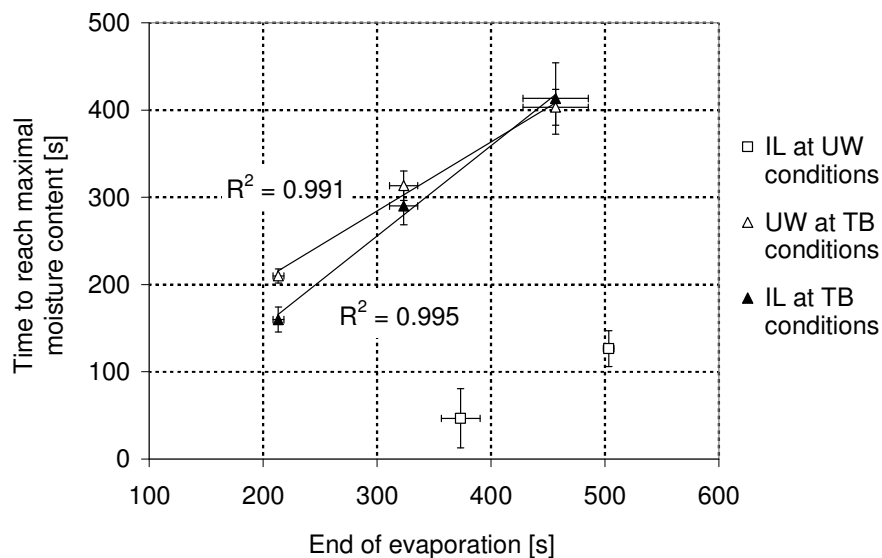
Figure 5.19: Comparison between the time at the end of evaporation and the time of the maximal moisture content in the underwear and liner of TB conditions with an air gap.

The maximal moisture content in the underwear in condition TB 1.0 (i.e. 1 g water initially located in the thermal barrier 2) was 3.5 +/-0.5 times higher for the measurement without an air gap than for the measurement with an air gap (Figure 5.20). On the contrary, for the liner in condition UW 1.0 (i.e. 1 g water initially located in the underwear) the difference between the maximal moisture content of the measurement with an air gap and the measurement without an air gap was not significant.
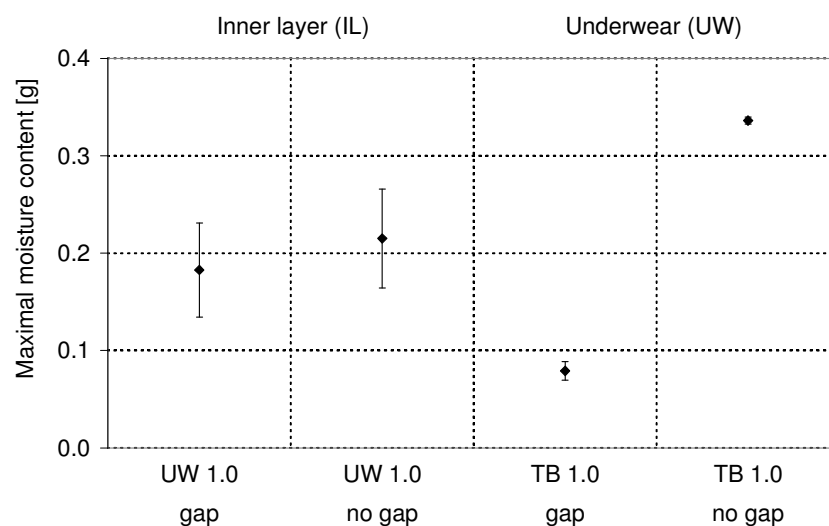
Figure 5.20: Comparison of the maximal moisture absorbed in the underwear when 1 g moisture was supplied to the thermal barrier 2 (condition TB 1.0) and in the liner when 1 g moisture was supplied to the underwear (condition UW 1.0) in each case with and without an air gap.

No significant moisture increase in the other layers was observed. The outer layer even dried out during the measurement when heating up. We suppose that this resulted from a measurement error. The fibres of the upper support of the measurement setup stretched at the high temperatures during the measurement. The outer layer was sagging in the beginning and was straightened during the measurement. Furthermore, as the horizontal line was adjusted to the lower surface of the samples, we suppose that geometric errors appeared at the upper surface of the samples.

Comparison of the results of the X-ray radiography and temperature measurements
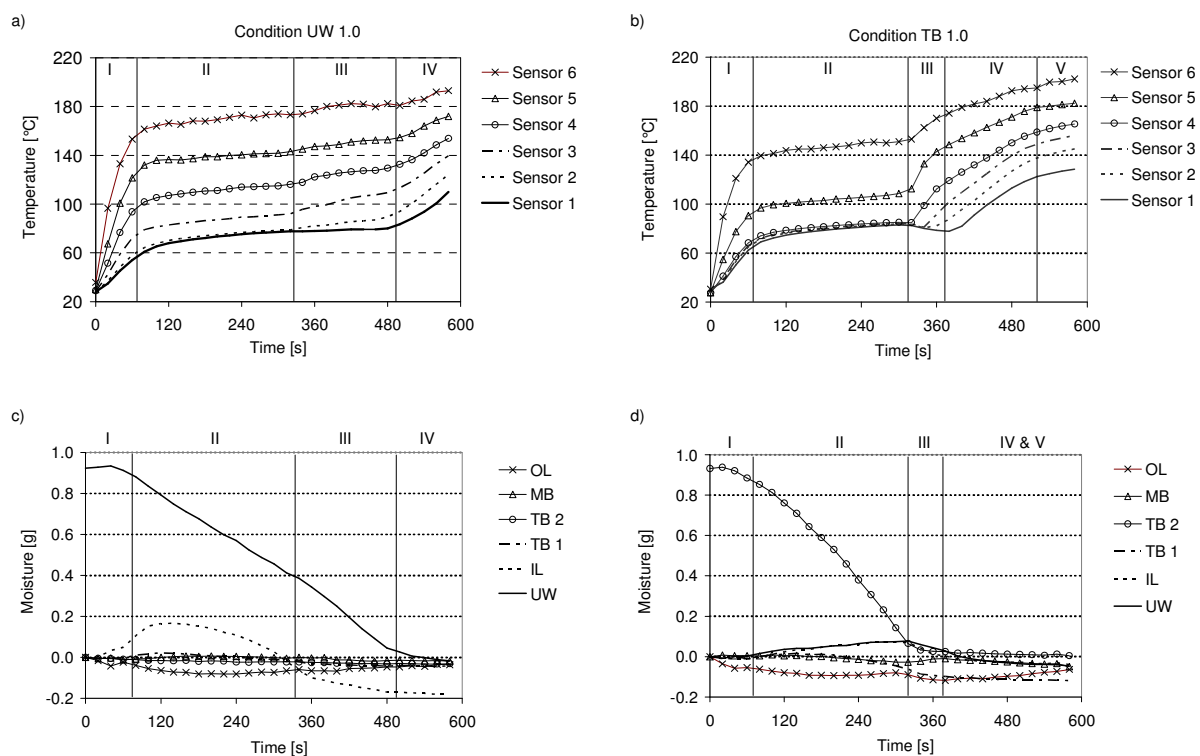
Figure 5.21: Comparison between temperatures within the clothing layers (Chapter 5.1) and the moisture content. a) Temperatures of UW 1.0, b) temperatures of TB 1.0, c) moisture contents of UW 1.0, d) moisture contents of TB 1.0.

The temperature distribution within the clothing system for the same setup has been described in Chapter 5.1. Figure 5.21 shows the temperature curves of the sensors placed between the single layers of conditions a) UW 1.0 and b) TB 1.0 as well as the moisture content in the different layers for the same conditions c) UW 1.0 and d) TB 1.0 respectively. Comparing the temperatures within the clothing layers and the moisture contents shows that evaporation ended at the same time as the temperature plateau of the temperature measurement ended,

which were end of phase III for UW conditions and end of phase II for TB conditions. At the end of phase II of UW conditions the slight temperature rise in the liner corresponds to the decrease of the evaporation rate in the liner.

The temperature drop in the inner layers (i.e. underwear and liner) at the end of phase II of condition TB 1.0 (Figure 5.21 b) also corresponds to the findings that moisture has accumulated in those layers, which was evaporating after the end of evaporation of the initially wet thermal barrier 2 (Figure 5.21 d).

5.2.3 Discussion

The analysis of the moisture content and distribution of the different textile layers with X-ray radiography was hampered by the non-ideal geometry of the samples. The horizontal alignment of the samples was not possible for all layers. Especially the upper layers were supposed to be erroneous due to geometric shifts, which resulted in an overlay of about 1 mm of the layers traversed by X-ray. Furthermore, even when two supports on both sides of the samples and an additional loading should ensure the flatness of the samples, a certain wrinkling of the samples could not be avoided. The fibres of the upper support stretched during heat exposure and thus changed the geometry of the upper layers. Shifts of the samples were considered in the evaluation process. But not all geometric errors could be avoided and results of the moisture measurements spread strongly.

The measured initial moisture content was less than the supplied moisture especially at the higher initial moisture contents. Moisture started to wick to the neighbouring layers as soon as the assemblies were put together. Therefore, initial moisture was also present in the neighbouring layers of the wet layer. Wicking can only appear when a threshold value of moisture content in the wet layer is transgressed [31, 64, 70]. Thus, at UW 0.6 (i.e. 0.6 g water initially located in the underwear) this threshold value was not reached and therefore no moisture wicked to the liner.

Evaporation in the wet thermal barrier 2 started earlier than in the wet underwear which can be explained by higher temperatures in the thermal barrier 2 than in the underwear (Chapter 5.1). Therefore evaporation started with increasing rate right from the beginning at TB conditions while a delay of the start of evaporation appeared in UW conditions.

Evaporation rates were not depending on the initial amount of moisture, but on the location of the moisture. Evaporation was slower in UW conditions than in TB conditions.

In the measurements without an air gap, the evaporation rate of condition TB 1.0 did not differ from the evaporation rate measured with an air gap. But the evaporation rate of condition UW 1.0 was lower without an air gap than with an air gap. If the air gap was missing, the underwear was lying directly on the cap of the measurement cell. Thus, moisture could only evaporate in one direction. The evaporation surface was half of the evaporation surface of conditions with an air gap. Thus, the evaporation rate was halved.

During evaporation, moisture was detected in the inner layers (i.e. underwear and liner). In TB conditions (i.e. water initially supplied to the thermal barrier 2) moisture accumulated in the liner and the underwear continuously during evaporation. Only when all moisture had evaporated from the initially wet thermal barrier 2, the moisture content of the inner layers started to decrease. Only little moisture was accumulated in the initially dry thermal barrier 1 (Figure 5.17). Thus, wicking from the initially wet thermal barrier 2 to the inner layers (i.e. underwear and liner) might not have taken place or at least only to a small extent. The moisture accumulated in the underwear and the liner rather resulted from condensation of moisture that evaporated from the initially wet thermal barrier 2 and moved to the inside. Condensed water also appeared on the cap of the measurement cell during evaporation.

In UW conditions moisture started to wick to the liner as soon as the assembly was piled up. Thus, moisture was already present in the inner layers when the measurement started. The moisture content in the liner strongly increased with rising temperature. The wicking process seemed to accelerate with increasing temperature. After around 127-167 +/-29 s the wicking stopped and moisture started to evaporate from the liner. This maximal moisture content was reached in all layers at about the same time. One can suppose that wicking (transfer of liquid moisture) only took place until the initially wet layer reached a lower humidity threshold after which the concentration of water was too low to get a transfer between the layers.

Findings of the X-ray radiography measurements agreed well with the findings of the temperature measurements of Chapter 5.1. The duration of evaporation was the same in both measurement methods. In the temperature analysis we concluded that moisture must have accumulated in the inner layers of the TB conditions. X-ray radiography affirmed those findings. In the underwear and the liner of the TB conditions maximal amounts of moisture up

to 0.17 +/-0.09 g were found in each of those layers. For measurements without an air gap this amount reached even up to 0.34 +/-0.01 g. Condensed moisture was also found on the cap of the measurement cell at the end of the measurement. In the temperature measurements the moisture in the innermost two layers caused a temperature drop in the sensors neighbouring those layers (sensor 1 - 3 according to Figure 5.21) at the end of the evaporation phase.

5.2.4 Conclusions

X-ray radiography proved to be a very valuable tool to study qualitatively the distribution of moisture and the evaporation processes within clothing layers. However, with the elaborated data set, the evaluation was quite tricky and results spread a lot.

We showed that upon exposure to thermal radiation, moisture accumulated in the inner layers (i.e. underwear and liner) of the protective clothing. This moisture accumulation derived from steam that evaporated in the outer layer and re-condensed in the inner layers. Moisture wicking to those inner layers is not probable as the moisture content of the layer between the initially wet layer and the liner was quite low.

6 PHYSICAL MODELLING AND COMPARISON WITH THE EXPERIMENTAL RESULTS

A thorough physical model of the heat and mass transfer in firefighting protective clothing systems would allow checking and comparing new textile combinations with respect to thermal protection, physiological properties and moisture management. Such a model would help to save time and money for laboratory and subject tests as only the most promising solutions have to be tested. Such a model, considering dry heat transfer by conduction, convection, radiation, moisture phase change with the associated heat release or uptake, as well as the presence of liquid water was implemented in this chapter.

6.1 Survey about existing models

The first mathematical simulation of heat and moisture transfer in textiles came from the drying technology [110]. A theory of drying had to be developed in order to build up efficient drying processes to save huge amounts of energy. As these theories described the basics of heat and moisture transfer in porous media, they were adapted to different related fields like thermal physiological properties of clothing and the influence of moisture on protective clothing.

Most of the research was made in physiology to predict the thermal comfort of clothing [11, 57, 111-114]. Farnworth [57] developed a physiological model including the transport of heat by conduction and radiation and vapour transport by diffusion. In his model he neglected the heat and mass transfer by forced convection as for example by wind or body motion and the

presence and transport of liquid by wicking. Lotens [114] adapted parts of this model to implement a whole body model to simulate the heat exchange between the human body and the environment. This model consists of cylinders of different sizes which represent the different body parts. Rossi [11] also carried on the model of Farnworth [57]. Additionally to the human body as heat source, he also considered the changing environment. But he also neglected the presence and transport of liquid water.

Li and Holcombe [115, 116] implemented a two-node model of the dynamic heat and moisture transport behaviour of clothing. In a series of further studies, Li improved this model [51, 107, 113, 117, 118] by considering the water content in the textile layers and its influence on the effective thermal conductivity, radiative heat transfer, vapour diffusion, fibre moisture sorption, condensation, evaporation and liquid transport by capillary actions.

Fan also worked on a series of models [50, 74, 106, 111, 119] based on the work by Li and Holcombe [115, 116] which they improved by adding evaporation in the textile layers, mobile condensates, moisture movement induced by the pressure gradient and the movement of liquid condensates.

All these studies mainly considered physiological properties at moderate environmental conditions. In firefighting, environmental temperatures and humidity exceed these conditions. Especially at extreme situations (for example flashover), fabric thermal properties change and nonlinear thermal transfer characteristics appear. Such complex dynamic fabric properties have to be considered in a simulation of firefighting protective clothing [34].

Different simulations on heat and mass transfer at hot thermal environments were performed so far [8, 34, 46, 120]. Torvi et al. [121] used a different approach to simulate measurements on a copper calorimeter plate. His model considered convection, conduction and radiation in the fabric, between fabric and burner and in the air gap as well as thermochemical reactions within the fabric. Moisture transfer was not considered in this model. Song [36] implemented a model based on Torvi et al. [121] in order to simulate heat and mass transfer during flash fire exposure. Song et al. [120] used this model in order to be able to predict skin burn injuries based on Henriques [24] damage integral. Chitrphiromsri [34] further improved this model in order to analyse thoroughly the coupled heat and moisture transfer through protective clothing during flash fire exposure. Thanks to this model, different parameters such as temperature,

moisture content, fibre regain, relative humidity, vapour density and fabric weight per unit area were analysed.

The most accurate model for our considerations is the one of Prasad et al. [8]. They implemented a one-dimensional model of transient heat and moisture transfer through protective clothing layers exposed to thermal radiation. The model is based on energy and mass continuity equations. They assumed the local moisture content to be in equilibrium at all times. Capillary action and volume changes of the fibres due to the changing moisture content were neglected.

6.2   Implementation of the model of heat and mass transfer processes within protective clothing layers exposed to thermal radiation

In order to implement a one-dimensional physical model of the evaporation process of a defined amount of moisture inside textile clothing layers, we assume a textile combination consisting of 2 different layers of thicknesses d_1 and d_2. The layers are surrounded by air with a temperature T_{amb} of 20 °C. The front surface of the dry layer is exposed to thermal radiation Q_{rad}. Figure 6.1 shows a diagram of the setup of the simulation.
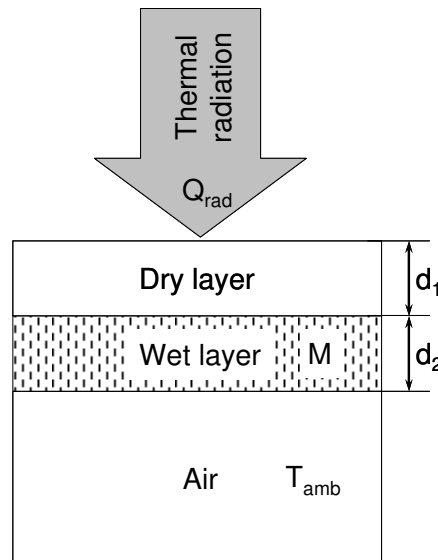
Figure 6.1: Setup of the model: two textile layers of thicknesses d_1 and d_2. The wet layer contains a defined amount of moisture m_{liq} with corresponding local moisture content M. The outer surface of the dry layer is exposed to the thermal radiation Q_{rad}.

One of the layers contains a defined amount of moisture m_{liqu}. The local moisture content M of the wet layer is defined by:

$$M = \frac{m_{liqu}}{m_{fab}}$$

(6.1)

M	Local moisture content	[kg/kg]
m_{liqu}	Mass of the liquid water	[kg]
m_{fab}	Mass of the dry fabric	[kg]

In experimental measurements of temperatures within multilayer textile combinations including a wet layer exposed to thermal radiation it was shown that temperature curves can be divided into five different phases; an initial rising phase, a stagnation phase, a temperature drop in the inner layers, a final rising phase and a second stagnation phase (Chapter 5.1.2). As not all of those phases were visible in each of the experiments and in order to simplify the physical model, we assume three phases for the evaporation process:

- Phase 1: The textile combination including the wet layer is heated up
- Phase 2: The moisture inside the textile combination is evaporating at constant temperature
- Phase 3: The temperatures of the dry textile layers increase again

Figure 6.2 shows the assumed temperature curves for the simulation.

Figure 6.2: Assumed temperatures within the layers at the three different phases of the process: heating up, evaporation and temperature increase in the dry sample.

We implemented a one dimensional model of the described system. In order to simplify the model, evaporation during the first phase is neglected in a first approach. Temperatures in all layers are assumed to be constant during the evaporation (phase 2).

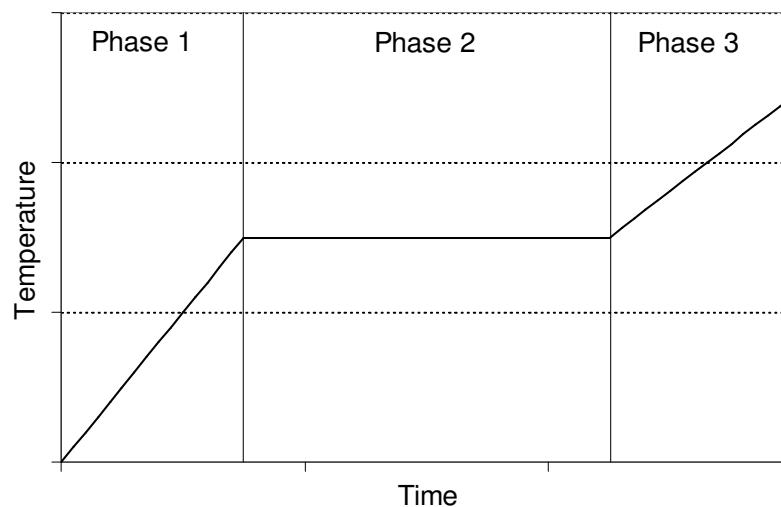We define the transient energy continuity for the two layers for all three phases. Only at the end of phase 3, steady state is reached.

$$\Delta Q_{fib} + \Delta Q_{liqu} + \Delta Q_{air} + \Delta Q_{evap} - \Delta Q_{sorp} - \Delta Q_{cosa} = Q_{rad-in} - Q_{rad-out} - Q_{cove} \qquad (6.2)$$

ΔQ_{fib}	Energy absorbed by the fibres	[W/m^2]
ΔQ_{liqu}	Energy absorbed by liquid water	[W/m^2]
ΔQ_{air}	Energy absorbed by air	[W/m^2]
ΔQ_{evap}	Heat of evaporation	[W/m^2]
ΔQ_{sorp}	Heat of sorption	[W/m^2]
ΔQ_{cosa}	Heat of condensation	[W/m^2]
Q_{rad-in}	Thermal radiation inward heat flow	[W/m^2]
$Q_{rad-out}$	Thermal radiation outward heat flow	[W/m^2]
Q_{cove}	Convective heat transfer	[W/m^2]

In a first approach we neglect condensation during the whole process. Therefore Q_{cond} is equal to zero. Heat of sorption is only emitted if water vapour is absorbed by the fibres [114]. As we assume non-hygroscopic materials, heat of sorption Q_{sorp} is also neglected.

The energy absorbed by the material, the air and the water is defined by:

$$\Delta Q_{fib} = m_{fib} \cdot \Delta T \cdot C_{fib} \qquad (6.3)$$

$$\Delta Q_{air} = m_{air} \cdot \Delta T \cdot C_{air} \qquad (6.4)$$

$$\Delta Q_{liqu} = m_{liqu} \cdot \Delta T \cdot C_{liqu} \qquad (6.5)$$

m_{fib}	Mass of the fibres	[kg]
m_{air}	Mass of the air	[kg]
m_{liqu}	Mass of the liquid water	[kg]
C_{fib}	Heat capacity of the fibres	[J/kg·K]
C_{air}	Heat capacity of the air	[J/kg·K]
C_{liqu}	Heat capacity of the liquid water	[J/kg·K]
ΔT	Temperature difference	[K]

The textiles are assumed to be exposed to a constant thermal radiation heat flux Q_{rad} of 5 kW/m^2. The inward heat flow thus follows from:

$$Q_{rad-in} = \varepsilon Q_{rad} \tag{6.6}$$

Q_{rad-in}	Thermal radiation inward heat flow	[W/m^2]
ε	Absorption coefficient of the textile surface	-
Q_{rad}	Energy emitted from the heat source	[W/m^2]

The emitted thermal radiative heat transfer is defined as:

$$Q_{rad-out} = \varepsilon \sigma (T_{surf}^4 - T_{amb}^4) \tag{6.7}$$

$Q_{rad-out}$	Thermal radiation outward heat flow	[W/m^2]
σ	Stefan-Boltzmann constant	[W/m^{2}K^4]
T_{surf}	Surface temperature	[K]
T_{amb}	Ambient temperature	[K]

Thermal radiation within the textile layers is neglected. And no forced convective heat transfer is assumed to take place. But natural convection heat transfer due to the temperature gradient between the hot surface of the sample and the environment occurs.

$$Q_{cove} = h \cdot (T_{surf} - T_{amb}) \tag{6.8}$$

h	Natural convection heat transfer coefficient	[W/m^{2}K]

We can get the natural convection heat transfer coefficient using the definition of the Nusselt number [55]:

$$Nu_L = \frac{hL}{k} = \lambda Ra_L^n \tag{6.9}$$

h	Natural convection heat transfer coefficient	[W/m^{2}K]
L	Characteristic length	[m]
k	Thermal conductivity	[W/m·K]
λ	Geometric constant	-
Ra	Rayleigh Number	-
n	Constant depending on whether flow is laminar or turbulent	-

The Rayleigh number is given by [55]:

$$Ra_L = Gr_L Pr = \frac{g\beta(T_{surf} - T_{amb})L^3}{\nu\alpha} \tag{6.10}$$

Gr	Grashof number	-
Pr	Prandtl number	-
g	Gravitational acceleration	$[m/s^2]$
β	Volumetric thermal expansion coefficient	$[1/K]$
ν	Kinematic viscosity	$[m^2/s]$
α	Thermal diffusivity	$[m^2/s]$

For the upper surface of a heated plate the relations are given as follows [55]:

$$Nu_L = 0.54 Ra_L^{1/4} \qquad \left(10^4 \leq Ra_L \leq 10^7\right) \tag{6.11}$$

$$Nu_L = 0.15 Ra_L^{1/3} \qquad \left(10^7 \leq Ra_L \leq 10^{11}\right) \tag{6.12}$$

The natural convection heat transfer coefficient depends also on the relative humidity. Zhang et al. [122] found changes of the Nusselt number from 0.5% to 23% depending on relative humidity, surface temperature and geometry.

Phase 1:

Following these assumptions, the energy conservation for phase 1 reduces to following equation:

$$\Delta Q_{fib} + \Delta Q_{liqu} + \Delta Q_{air} + \Delta Q_{evap} = Q_{rad-in} - Q_{rad-out} - Q_{cove} \tag{6.13}$$

ΔQ_{fib}	Energy absorbed by the fibres	$[W/m^2]$
ΔQ_{liqu}	Energy absorbed by liquid water	$[W/m^2]$
ΔQ_{air}	Energy absorbed by air	$[W/m^2]$
ΔQ_{evap}	Heat of evaporation	$[W/m^2]$
Q_{rad-in}	Thermal radiation inward heat flow	$[W/m^2]$
$Q_{rad-out}$	Thermal radiation outward heat flow	$[W/m^2]$
Q_{cove}	Convective heat transfer	$[W/m^2]$

If we further simplify the model and assume that the textiles are homogeneous, we can average the density, the heat capacity and the conductivity for the fibres, the air and the moisture. We obtain the one dimensional heat transfer:

$$\rho_{tot} C_{tot} \frac{dT}{dt} = k_{tot} \frac{d^2T}{dx^2} \tag{6.14}$$

T	Temperature	[K]
C_{tot}	Total heat capacity of the fabric, the air and the liquid water	[J/kg·K]
ρ_{tot}	Total density of the dry fabric and the liquid water	[kg/m^3]
k_{tot}	Total thermal conductivity of the fabric, the air and the liquid water	[W/m·K]

This equation (6.14) is solved for both layers using following boundary (BC) and initial conditions (IC):

BC: $Q(x = 0) = Q_{rad-in} - Q_{rad-out} - Q_{conv}$ (6.15)

$Q(x = d_1 + d_2) = Q_{rad-out} + Q_{conv}$ (6.16)

IC: $T(t = 0) = T_{amb}$ (6.17)

T_{amb}	Ambient temperature	[K]
t	Time	[s]
d_1	Thickness of the 1st layer	[mm]
d_2	Thickness of the 2nd layer	[mm]

The total density of the system is given by:

$$\rho_{tot} = \frac{m_{tot}}{V_{fab}} = \frac{m_{liqu} + m_{fab}}{V_{fab}} \tag{6.18}$$

ρ_{tot}	Density of the whole system	[kg/m^3]
m_{tot}	Mass of the whole system	[kg]
m_{liqu}	Mass of the liquid water	[kg]
m_{fab}	Mass of the dry fabric	[kg]
V_{fab}	Volume of the whole system, (equal to the volume of the fabric)	[m^3]

Inserting the local moisture content M according to (6.1) we get:

$$\rho_{tot} = \rho_{fab}(1+M) \tag{6.19}$$

ρ_{tot}	Density of the whole system	[kg/m^3]
ρ_{fab}	Density of the dry fabric	[kg/m^3]
M	Local moisture content	[kg/kg]

The total heat capacity of a wet textile can be calculated by:

$$C_{tot}(m_{fab} + m_{liqu}) = C_{fab}m_{fab} + C_{liqu}m_{liqu} \tag{6.20}$$

C_{tot}	Total heat capacity of the wet textile	[J/kg·K]
C_{liqu}	Heat capacity of the liquid water	[J/kg·K]
C_{fab}	Heat capacity of the dry fabric	[J/kg·K]

Dividing by m_{fab} we get:

$$C_{tot}\left(1 + \frac{m_{liqu}}{m_{fab}}\right) = C_{fab} + C_{liqu}\frac{m_{liqu}}{m_{fab}} \tag{6.21}$$

Adding the definition of the local moisture content M leads to:

$$C_{tot} = \frac{C_{fab} + M\dfrac{c_{liqu}}{W_{H_2O}}}{(1+M)} \tag{6.22}$$

c_{liqu}	Molar heat capacity of liquid water	[J/mol·K]
M	Local moisture content	[kg/kg]
W_{H2O}	Molecular weight of water vapour	[g/mol]

The total thermal conductivity of a wet textile is given by:

$$k_{tot} \cdot d_{tot} = k_{fab} \cdot d_{fab} + k_{liqu} \cdot d_{liqu} \tag{6.23}$$

k_{tot}	Total thermal conductivity	[W/m·K]
k_{fab}	Thermal conductivity of the dry fabric	[W/m·K]
k_{liqu}	Thermal conductivity of liquid water	[W/m·K]
d_{tot}	Total thickness of the wet fabric	[m]
d_{fab}	Thickness of the fabric	[m]
d_{liqu}	Thickness of liquid water	[m]

where the thickness d is defined by:

$$d = \frac{V}{A}$$

(6.24)

The area A is the same for all terms and cancels out.

As the total volume of the wet fabric V_{tot} contains the volume of the liquid water V_{liqu} and is the same as the volume of the dry fabric V_{fab}, the factor $k_{fab} \cdot V_{liqu}$ has to be subtracted from $k_{fab} \cdot V_{fab}$. Thereof the total thermal conductivity can be calculated by Prasad et al. [8]:

$$k_{tot} \cdot V_{fab} = k_{fab} \cdot V_{fab} - k_{fab} \cdot V_{liqu} + k_{liqu} \cdot V_{liqu}$$

(6.25)

V_{tot}	Volume of the wet fabric	[m³]
V_{fab}	Volume of the dry fabric (equal to V_{tot})	[m³]
V_{liqu}	Volume of liquid water	[m³]

Dividing by with V_{fab} leads to:

$$k_{tot} = k_{fab} - k_{fab} \frac{V_{liqu}}{V_{fab}} + k_{liqu} \frac{V_{liqu}}{V_{fab}}$$

(6.26)

If we replace the volumes by mass and density, we get:

$$k_{tot} = k_{fab} - k_{fab} \frac{\rho_{fab} m_{liqu}}{\rho_{liqu} m_{fab}} + k_{liq} \frac{\rho_{fab} m_{liqu}}{\rho_{liqu} m_{fab}}$$

(6.27)

ρ_{fab}	Density of the dry fabric	[kg/m³]
ρ_{liqu}	Density of liquid water	[kg/m³]
m_{liqu}	Mass of the liquid water	[kg]
m_{fab}	Mass of the dry fabric	[kg]

With equation (6.1) we finally get:

$$k_{tot} = k_{fab} + \left(k_{liqu} - k_{fab}\right)\left[\frac{\rho_{fab} M}{\rho_{liqu}}\right]$$

(6.28)

M	Local moisture content	[kg/kg]

Phase 2:

End of phase 1 is reached, when a temporary equilibrium is reached und temperatures stop increasing. All energy is now used to evaporate the water. During the evaporation of the water in the textile layer, temperatures stay constant. Therefore ΔQ_{fib}, ΔQ_{liqu} and ΔQ_{air} are equal to zero. The energy conservation equation (6.2) reduces to:

$$\Delta Q_{evap} = Q_{rad-in} - Q_{rad-out} - Q_{cove} \tag{6.29}$$

ΔQ_{evap}	Heat of evaporation	[W/m²]
Q_{rad-in}	Thermal radiation inward heat flow	[W/m²]
$Q_{rad-out}$	Thermal radiation outward heat flow	[W/m²]
Q_{cove}	Convective heat transfer	[W/m²]

The energy used for evaporation is given by [11]:

$$\Delta Q_{evap} = \varphi \, \dot{m}_{evap} \tag{6.30}$$

φ	Latent heat of evaporation	[J/g]
$\dot{m}_{evap}$	Evaporation rate	[g/m²s]

As the system is open, we assume that pressure and volume inside the textile layers stays constant. The volume of evaporated steam is immediately escaping out of the textile layers. We further assume that the volume of the evaporating liquid water replaced by steam is negligible. Thus, the mass flux of steam out of the textile layers is equal to the mass flux due to evaporation of steam.

$$\dot{m}_{out} = \dot{m}_{evap} \tag{6.31}$$

$\dot{m}_{out}$	Mass flux out of the system	[g/m²s]
$\dot{m}_{evap}$	Evaporative mass flux	[g/m²s]

The evaporation speed is defined by the Hertz-Knudsen-Schrage equation (6.32) [73].

$$\dot{m}_{evap} = E \sqrt{\frac{W_{H_2O}}{2\pi R}} \left[\frac{p_{sat}\left(T_{surf}\right)}{\sqrt{T_{surf}}} - \frac{p_{vap}}{\sqrt{T_{vap}}} \right] \tag{6.32}$$

$\dot{m}_{evap}$	Evaporative mass flux	[kg/m^{2}s]
E	Evaporation coefficient	-
T$_{surf}$	Liquid surface temperature	[K]
p$_{sat}$(T$_{surf}$)	Saturation pressure at the liquid surface	[Pa]
p$_{vap}$	Partial pressure of water vapour	[Pa]
T$_{vap}$	Temperature in the vapour above the liquid surface	[K]
W$_{H2O}$	Molecular weight of water vapour	[g/mol]
R	Universal gas constant	[J/mol·K]

$$p_{vap} = p_{sat} RH \tag{6.33}$$

RH	Relative humidity	-

Equation (6.32) defines the rate of evaporation in a partial vacuum. According to Krischer [72] the evaporation rate from a wet surface at a certain depth d of a drying medium is defined as:

$$\dot{m}_{evap} = \frac{1}{R_{H_2O}T_{surf}} \frac{1}{\dfrac{1}{b}+\dfrac{\delta d}{D}} \left(p_{sat}(T_{surf}) - p_{vap} \right) \tag{6.34}$$

R$_{H2O}$	Specific gas constant of water vapour	[J/kg·K]
b	Mass transfer coefficient	[m/s]
d	Thickness of the textile layers above the evaporation surface	[m]
δ	Diffusion resistance factor	-
D	Diffusion coefficient	[m^2/s]

Steam can flow into both directions, either directly to the adjacent air of the wet layer or through the dry textile layer.

Phase 3:

We assume that all the moisture has evaporated out of the textile layer at the end of phase 2. We further assume that the amount of water vapour that has not diffused out of the layers is negligible and does not influence the dry heat transfer.

Following those assumptions and according to the first phase, energy conservation reduces to (6.35):

$$\Delta Q_{fib} + \Delta Q_{air} = Q_{rad-in} - Q_{rad-out} - Q_{cove} \tag{6.35}$$

ΔQ_{fib}	Energy absorbed by the fibres	[W/m^2]
ΔQ_{air}	Energy absorbed by air	[W/m^2]
Q_{rad-in}	Thermal radiation inward heat flow	[W/m^2]
$Q_{rad-out}$	Thermal radiation outward heat flow	[W/m^2]
Q_{cove}	Convective heat transfer	[W/m^2]

In analogy to the first phase we simplify the model and assume that the textile is homogeneous. We obtain the one dimensional heat conduction equation (6.36):

$$\rho_{fab} \, C_{fab} \frac{dT}{dt} = k_{fab} \frac{d^2T}{dx^2} \tag{6.36}$$

T	Temperature	[K]
C_{fab}	Heat capacity of the dry fabric	[J/kg·K]
ρ_{fab}	Density of the dry fabric	[kg/m^3]
k_{fab}	Thermal conductivity of the dry fabric	[W/m·K]

This equation (6.36) is solved for the two dry layers using following boundary (BC) and initial conditions (IC):

BC:
$$Q(x = 0) = Q_{rad-in} - Q_{rad-out} - Q_{conv} \tag{6.37}$$

$$Q(x = d_1 + d_2) = Q_{rad-out} + Q_{conv} \tag{6.38}$$

IC:
$$T(t_{p3} = 0) = T(t_{p2} = end) \tag{6.39}$$

t_{p2}	Time of phase 2	[s]
t_{p3}	Time of phase 3	[s]
T	Temperature	[K]
d_1	Thickness of the 1st layer	[mm]
d_2	Thickness of the 2nd layer	[mm]

6.2.1   Comparison of the model with experimental results

Using those relations the heat transfer equation (6.14) can be solved for the two layers during the first and the second phase. For most of the fabrics a thermal conductivity of 0.04 W/m·K can be assumed. Exceptions are low density battings or down [57]. Thermal capacities of textiles are around 1500 J/kg·K [11].

The constants used for the simulation are listed in Table 6.1:

b_1	$3.0 \cdot 10^{-3}$	[m/s]	Q_{rad}	5000	[W/m^2]
b_2	$1.7 \cdot 10^{-3}$	[m/s]	R	8.31	[J/mol·K]
C_{air}	1005	[J/kg·K]	RH	60	[%]
C_{fab}	1500	[J/kg·K]	R_{H2O}	462	[J/kg·K]
c_{liqu}	75.4	[J/mol·K]	d	0.7	[mm]
D	$0.02 \cdot 10^{-3}$	[m^2/s]	T_{amb}	293	[K]
d_1	0.7	[mm]			
d_2	1.4	[mm]	**Greek**		
h	17	[W/m^{2}K]	ε	0.98	-
k_{air}	0.024	[W/m·K]	δ	1.1	-
k_{fab}	0.04	[W/m·K]	ρ_{fab1}	300	[kg/m^3]
k_{liqu} (at 80 °C)	0.67	[W/m·K]	ρ_{fab2}	101	[kg/m^3]
L	0.07	[m]	ρ_{liqu} (at 80 °C)	971	[kg/m^3]
M	0.7	[kg/kg]	σ	$5.67 \cdot 10^{-8}$	[W/m^{2}K^4]
W_{H2O}	18	[g/mol]	φ (at 100 °C)	2272	[J/g]

Table 6.1: Constants used for the simulation.

The mass transfer coefficients can be related to the heat transfer coefficient of the textile layers [72]. The mass transfer coefficients as well as the natural convection heat transfer coefficient were estimated for the simulation.

Phase 1 and 2:

Figure 6.3 shows a comparison between simulated temperatures (straight lines) and measured temperatures (dotted lines) during the heating up and evaporation phase (phase 1 and 2).
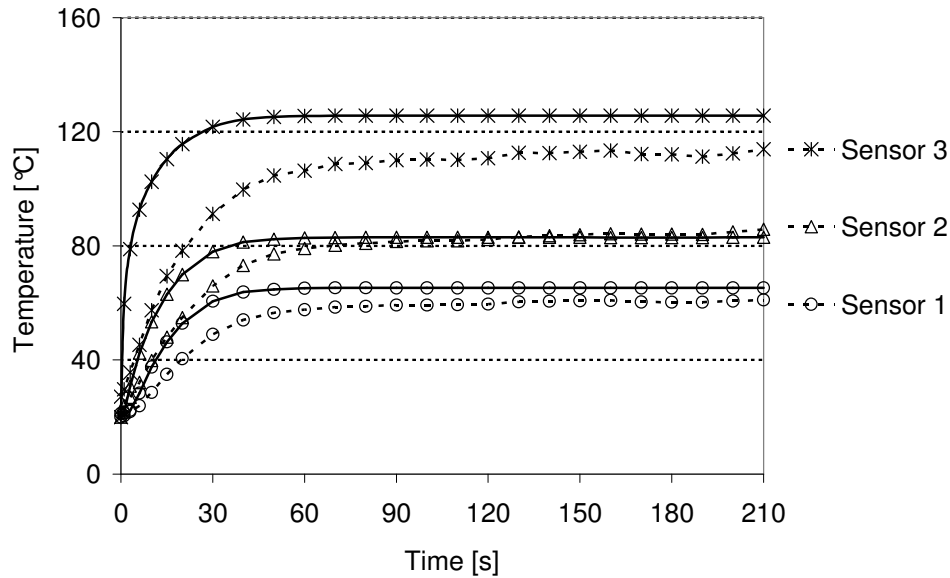
Figure 6.3: Temperatures within the textile layers (on the inner surface of the textile layer, between the two textile layers and on the outer surface of the textile layers) during heating up and evaporation of the moisture. Comparison between simulated (straight lines) and measured (dotted lines) results.

Comparing the results of the simulation with the experimental results, we find that the initial temperature increase and the temperatures at the outer surface of the sample was overestimated by the model. In consideration of the simplicity of the physical model, the simulated temperatures are still a good approach to the experimental results.

Phase 3:

Figure 6.4 shows a comparison between simulated temperatures (straight lines) and measured temperatures (dotted lines) within the dry textile layers when all moisture has evaporated out of the layers (phase 3).

The temperature increases in the dry samples were also overestimated by the physical model. But temperatures reached at the equilibrium state agree well with the experimental findings.
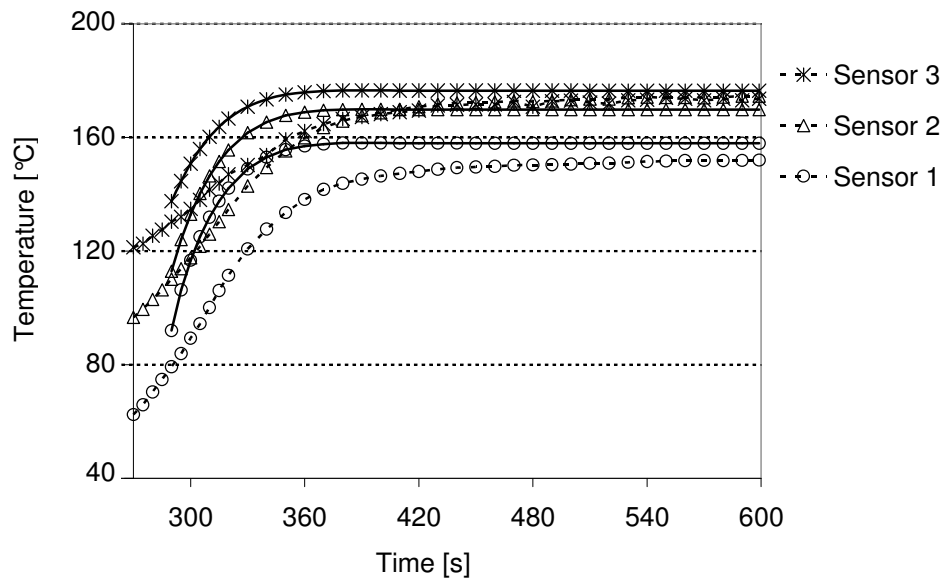
Figure 6.4: Increase of temperature after all moisture has evaporated out of textile layers. Comparison between simulated (straight lines) and measured (dotted lines) results.

6.2.2 Conclusions

Even though the temperature increase in the beginning of phase 1 and phase 3 was overestimated, and in spite of the simplicity of the model, the results corresponded well with the findings of the experiments.

Further improvements of the model will allow predicting evaporation and steam movement within clothing combinations containing wet layers exposed to thermal radiation. The enhanced model should consider the steam transfer and the condensation within the clothing layers as well as evaporation right from the beginning of phase 1. It should also be possible to calculate optional setups with different numbers and kinds of textile layers or without an air gap, which appears when the clothing combination is touching the skin. Especially the amount of moisture condensing on the skin and the resulting temperature within the skin are of particular interest.

Using such an advanced physical simulation would allow comparing different kinds of clothing combinations with regard to their heat protection as well as comfort properties. Expensive and time consuming laboratory tests could be minimised.

PART III: FUTURE PERSPECTIVES

7 INNOVATIVE SUGGESTIONS

Different innovative suggestions for firefighter protective clothing systems in order to avoid steam movement towards the skin and the development of steam burns are proposed in this chapter. Superabsorbing polymers can be used as water storage and cooling system in the firefighter protective clothing system. A drainage system handles the moisture in the underwear, drains off surplus amount of water and avoids moisture transfer to the firefighter jacket.

7.1 Superabsorbing polymers for the use as water storage and cooling device

Superabsorbing polymers (SAP) can be used as water storage or even as cooling system in firefighter protective clothing. Surplus of water is absorbed and stored by the SAPs and only released at a low rate. Due to the heat of evaporation taken from the superabsorbing layer, the clothing is cooled down, what produces a cooler microclimate within the protective clothing.

Additional moisture stored within the protective clothing bears the risk of fast evaporation and thus of causing steam burns. Therefore, we investigated the moisture evaporation rate from a superabsorbing polymer compared to a textile surface.

7.1.1   Drying of nonwoven fabrics containing superabsorbing polymers

Samples with a diameter of 8 cm consisting of a cotton rip knit fabric respectively superabsorbing polymer nonwoven (75% superabsorbing polymer and 25% PET) were soaked with distilled water and left in a closed jar at 20 +/-2 °C during 8 hours. The samples were dabbed off on a paper towel without additional pressure in order to remove surplus of water just before the start of the measurement. Three cotton samples contained 2.70 +/-0.13 g and three SAP 24.81 +/-0.66 g water at the beginning of the measurement. The samples were dried on a heated scale at 80 °C. Each measurement was repeated three times with different samples of the same material.

The drying curves are shown in Figure 7.1. The drying rate increases faster in the beginning for cotton samples than for SAP fabrics. As the SAP contains initially 9 times more water than the cotton fabric, it takes longer until the wet sample is heated up. But as soon as the maximal evaporation rate was reached, both fabrics dried at the same rate with a drying rate of 0.178 g/min for cotton and 0.174 g/min for SAP.
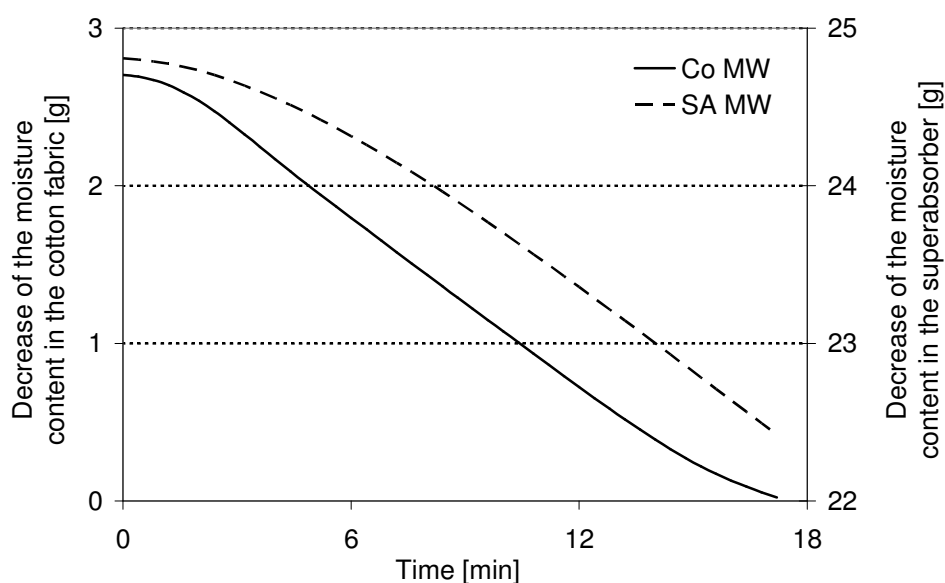

Figure 7.1: Drying behaviour of a cotton rip knit and of a superabsorbing polymer-PET nonwoven.

SAPs are able to store large amounts of moisture, but once heated up, the moisture evaporates from SAPs with the same evaporation rate as from other textiles. Therefore, superabsorbing polymers bear a similar risk for steam burns as other hydrophilic or hygroscopic textiles.

7.1.2 Vests containing superabsorbing polymers

Vests containing superabsorbing polymers are used in hot environments for the cooling of the body. The evaporation of the moisture from the vest withdraws energy from the adjacencies near the body which results in a cooler microclimate near the body.

Tests with superabsorbing vests on the thermal manikin were performed to study the risk of steam burns due to the moisture storage in the vest. Apart from the SAP vest, we used cotton T-shirts as underwear as well as state-of-the-art firefighter protective jackets and trousers. The SAP vest was worn between the underwear and the protective jacket.

We measured three different clothing combinations: firefighter protective clothing without SAP vest, with a dry SAP vest and with a SAP vest soaked with water.

Each of the combinations was measured at:
- $5\ kW/m^2$ thermal radiation during 4 min
- $10\ kW/m^2$ thermal radiation during 2 min
- Flashover test with a total heat flux of $84\ kW/m^2$ during 8 s and 112 s post flashover according to EN ISO/DIS 13506.3 [90]

The underwear, the SAP vest for the dry measurement, the firefighter jacket and the trousers were conditioned for at least 24 hours at standard climatic conditions of 20 +/-2 °C and 65 +/-5% relative humidity. The SAP vest for the wet measurement was soaked with water 8 hours prior to the test and then conditioned at standard climatic conditions of 20 +/-2 °C and 65 +/-5% relative humidity. The wet vest contained 265 +/-26 g water at the beginning of the measurement.

All samples were weighed before and after the measurements in order to determine the evaporated amounts of moisture and a possible moisture transfer from the vest to the other layers.

Behaviour of SAP vest exposed to thermal radiation

In the thermal radiation test, the manikin was exposed frontally to thermal radiation of $5\ kW/m^2$ during 4 min respectively to $10\ kW/m^2$ during 2 min. The manikin was clothed with underwear, SAP vest and firefighter protective jacket and trousers. Temperatures on the chest were recorded throughout the measurement.

Temperature increase on the chest [°C]		
	5 kW/m^2	**10 kW/m^2**
Without SAP vest	5.4	8.0
With dry SAP vest	3.0	3.3
With soaked SAP vest	2.0	1.4

Table 7.1: Mean temperature increase [°C] on the chest at the exposure to 5 kW/m^2 during 4 min respectively to 10 kW/m^2 during 2 min.

The temperature increase on the surface of the thermal manikin was found to be smaller if measured with the soaked vest than if measured with the dry vest or without vest (Table 7.1). If measured with the SAP vest the difference between the temperature increase on the chest at 5 kW/m^2 and at 10 kW/m^2 was very small (0.3 °C with the dry and 0.6 °C with the soaked vest). Only for the measurement without the vest, the temperature increased at 10 kW/m^2 in average 2.6 °C more than at 5 kW/m^2. It has to be considered, that the exposure time at 5 kW/m^2 was twice as long as the exposure time at 10 kW/m^2.

The vest seemed to exert a positive influence on the thermal insulation, which is obvious, as an additional clothing layer was added to the clothing combination. However, the water within the soaked vest also seemed to improve the insulation of the vest due to the higher heat capacity.

If the vest was soaked with water, the weight of the T-shirt increased during the measurement (Table 7.2). In the other measurements (i.e. with dry vest or without the vest) the weight of the T-shirt decreased. Therefore, a slight moisture transfer towards the body took place in the measurement with soaked vest.

Furthermore, less moisture evaporated out of the jacket during the measurements including SAP vests than in the measurements without vest. And in the measurement with wet SAP vest, less moisture evaporated from the jacket than in the measurement with dry vest, while more moisture evaporated from the wet vest than from the dry one. Another possibility could be that in the measurements with wet SAP vest the moisture evaporating from the firefighter jacket was substituted by moisture evaporating from the vest and condensing in the firefighter jacket.

Difference of the moisture content [g]		
	5 kW/m^2	**10 kW/m^2**
Without SAP vest		
Jacket	-37.3	-34.3
T-shirt	-0.6	-0.8
With dry SAP vest		
Jacket	-31.7	-33.5
Vest	-2.5	-2.2
T-shirt	-0.5	-0.4
With soaked SAP vest		
Jacket	-30.1	-30.6
Vest	-6.2	-6.1
T-shirt	0.6	0.6

Table 7.2: Difference of the moisture content before and after the exposure to 5 kW/m^2 during 4 min respectively to 10 kW/m^2 during 2 min.

Behaviour of SAP vest in a flashover

In a third measurement series, the manikin (clothed the same way as in the former measurements) was exposed to a laboratory flashover test during 8 s and 112 s post flashover according to EN ISO/DIS 13506.3 [90]. The heat flux was recorded by sensors distributed over the body of the thermal manikin. Only the sensors covered by the vest at the chest and the upper back were considered for the evaluation. Times to pain respectively times to 1st to 3rd degree burns were calculated according to Henriques damage integral [24]. Thereof the total surface of burned areas was determined.

The areas covered by the SAP vest in which pain or 1st to 3rd degree burns were recorded are listed in Table 7.3. The percentage of the areas covered by the vest at which pain or 1st to 3rd degree burns appeared was bigger for measurements without the superabsorbing vest than for

measurements with vest. The percentage of burned areas was the same for dry and wet vest, but the areas at which pain appeared was smaller if the vest was soaked with water.

	Pain [%]	1st degree burn [%]	2nd degree burn [%]	3rd degree burn [%]
Without SAP vest				
Chest	20.0	0.0	20.0	30.0
Upper back	8.3	8.3	33.3	41.7
With dry SAP vest				
Chest	10.0	0.0	0.0	0.0
Upper back	50.0	8.3	0.0	0.0
With soaked SAP vest				
Chest	0.0	0.0	0.0	0.0
Upper back	16.7	8.3	0.0	0.0

Table 7.3: Percentage of the surface at the chest and the upper back reaching pain level and 1st to 3rd degree burns.

During the flashover more moisture accumulated in the T-shirt than during the exposure to thermal radiation. No statistical evaluation could be made as each setup was measured only once. Even in the measurement without the vest and with dry vest, where the T-shirt dried out during the exposure to thermal radiation, moisture accumulated in the T-shirt during the flashover exposure. The decrease of moisture within the SAP vest was also strongly increased.

Difference of the moisture content [g]			
	Without SAP vest	With dry SAP vest	With soaked SAP vest
Vest	---	-6.2	-14.1
T-shirt	0.0	0.9	1.3

Table 7.4: Difference of the moisture content before and after exposure to the flashover.

The superabsorbing vest increased the protection against thermal radiation and exposure to flashover. This increase comes from the additional textile layer increasing the thickness and therefore the insulation of the clothing system. Aside from the increase of insulation due to the additional textile layer, the additional moisture within the superabsorbing vest also increased the protection against thermal radiation as well as against flashover situations. The temperature increase at the chest during exposure to thermal radiation was less with soaked vest than with dry vest and the percentage of surface areas at which pain appeared was smaller with the addition of moisture.

Nevertheless, a moisture transfer towards the body took place, as moisture accumulated in the T-shirt. As only temperature on the manikin surface was measured during the experiments, the development of steam burns due to the condensation of steam could not be screened out.

7.1.3 Conclusions

Superabsorbing polymers are able to absorb huge amounts of water. Surplus of sweat can be absorbed by superabsorbing polymers and a damp feeling on the skin can be avoided. Additionally, vests containing superabsorbing polymers could be used as cooling system adapting evaporative cooling.

In drying experiments we found that the surface water evaporated at the same rate from a fleece containing superabsorbing polymers as from other textiles. This means that superabsorbing polymers do not decrease the evaporating rate at their surface. The amounts of water stored in the superabsorbing polymers thus could still bear the risk of evaporation and causing steam burns.

In flashover measurements with vests containing superabsorbing polymers no negative impact on the heat protection could be found. Protection was even increased due to the additional clothing layer and the thereby increased thickness of the clothing combination. During the measurement moisture transfer to the underwear took place. This means that moisture evaporated from the superabsorbing vest and condensed in the underwear or at the surface of the manikin. However it was not possible to detect any significant temperature increase due to energy transferred during condensation.

7.2   Drainage system

In order to control the distribution of moisture within protective clothing, to avoid moisture accumulation in the firefighter jacket and to remove surplus of sweat out of the underwear, we invented a novel moisture management system for the underwear. This system consists of a two-layer textile combination containing embroideries at the outer layer cross connected with the inner layer by seams. It is worn as underwear in direct contact with the skin and works as drainage system in order to lead off surplus of sweat.

7.2.1   Ability of embroideries to drain water

In a first step we investigated whether it is possible to drain water into defined directions using embroideries. Therefore we performed measurements on the sweating cylinder. The samples were embroidered with stripes of straight embroideries. We fixed the samples in two different directions on the cylinder, a) the embroideries in vertical direction and b) the embroideries in horizontal direction.

The measurements on the sweating cylinder were run in three different phases:

- **Acclimatization phase:** 1 h at constant surface temperature of 35 °C
- **Sweating phase:** 30 min of sweating with a sweating rate of 30 g/h and constant power of 25 W
  (corresponds to 600 g/h sweating and a physical activity of 500 W for a human)
- **Drying-up phase:** 1 h at constant power of 5 W
  (corresponds to a physical activity of 100 W for a human)

During the measurements the samples on the sweating cylinder were monitored by an infrared camera in order to visualise the moisture distribution. The IR-pictures are shown in Figure 7.2. As the sweating cylinder was heated, the dry areas of the textile were visible as hot areas (bright) while the wet areas were cooler due to the evaporative cooling (dark). It can be seen that the water was drained in the direction of the embroidery. As the sweating cylinder contains two levels of water outlets, only two stripes along those outlets were visible in the horizontal alignment, while in the vertical position the stripes started at the water outlets and ran vertically downwards.
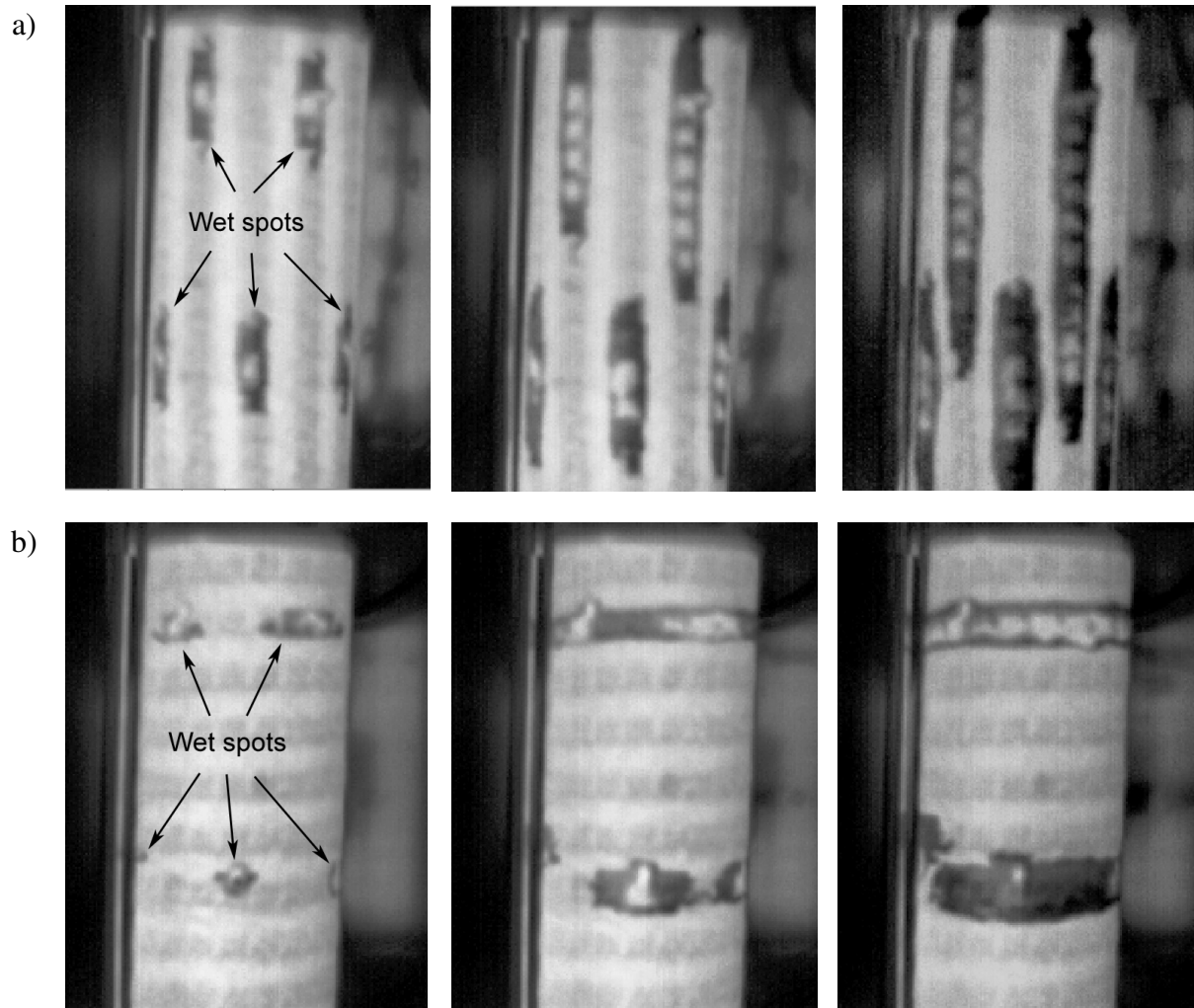
Figure 7.2: Spreading of the moisture in textiles containing embroideries. a) Vertical alignment of the embroideries and b) horizontal alignment of the embroideries.

7.2.2 Two-layer drainage system

In a further step, we tested whether it was possible to lead surplus moisture away from the body by a two layer drainage system. This system consists of a layer containing embroideries cross connected by seams with a second layer without embroideries worn in contact to the skin.

We studied if moisture was led through the cross connections to the outer layer containing embroideries. The setup consisted of stripes of this two-layer drainage system hanging vertically (Figure 7.3), the upper end of the inner layer without embroideries dipped into water while the lower ends of the two layers of the drainage system were put separately into two different pots in order to collect dripped off moisture.
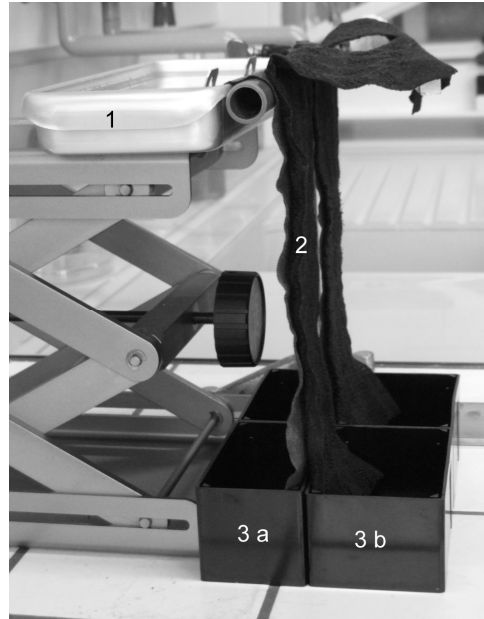
Figure 7.3: Setup of experiment: (1) water tank, (2) two-layer sample containing embroideries on the outer layer, cross connected with the inner layer by seams, (3) water collectors a) of the inner layer without embroideries, b) of the outer layer with embroideries

We observed that water was led from the inner layer without embroideries to the outer layer containing embroideries and dripped off at the ends of the embroideries (Figure 7.4). The amount of water collected in the two pots widely spread and therefore no reliable statements about the ability to wick water from the inner layer to the outer layer could be made using this method.
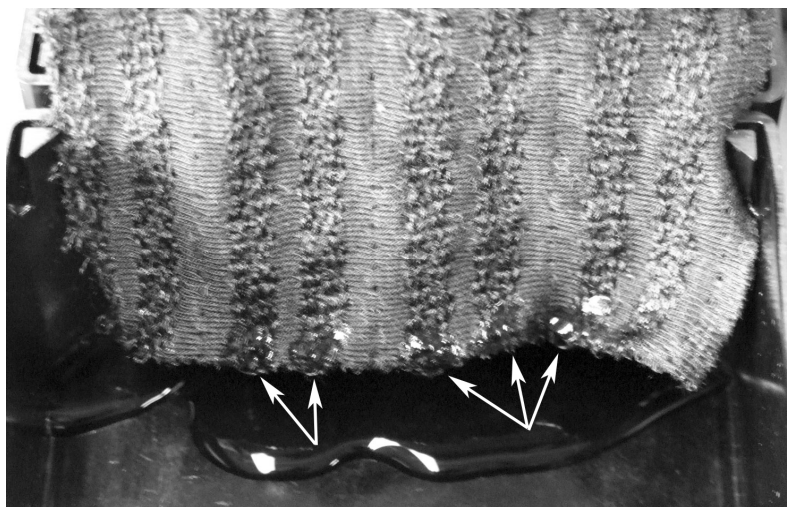
Figure 7.4: If we dip the upper end of the layer without embroideries into water, we observed that the water was led to the other layer containing embroideries, along the embroideries and dripped off at the ends of the embroideries.

In further measurements on the sweating cylinder, we measured how the system coped with heavy sweating. Therefore we attached two plastic bags containing blotting paper to the lower ends of the layers in order to collect the moisture that dripped off each layer separately. Then we fixed the two-layer drainage system with plastic bags on the sweating cylinder. Only one phase was run on the sweating cylinder. In order to maximize dripped off moisture, we chose the maximal possible sweating rate of the cylinder (~110-120 g/h) during 1 hour. The power was set to 25 W, corresponding to a physical activity of 500 W for a human.

We measured three different combinations of hydrophilic and hydrophobic underwear knits:

- Phil-Phil: Two layers of hydrophilic treated aramid rip knit.
- Phob-Phil: The inner layer consisting of hydrophobic aramid rip knit and the outer layer of hydrophilic treated aramid rip knit.
- Phil-Phob: The inner layer consisting of hydrophilic aramid rip knit and the outer layer of hydrophobic aramid rip knit.

In order to evaluate the influence of the embroideries to the moisture distribution, we also measured the mentioned textile combinations without embroideries.

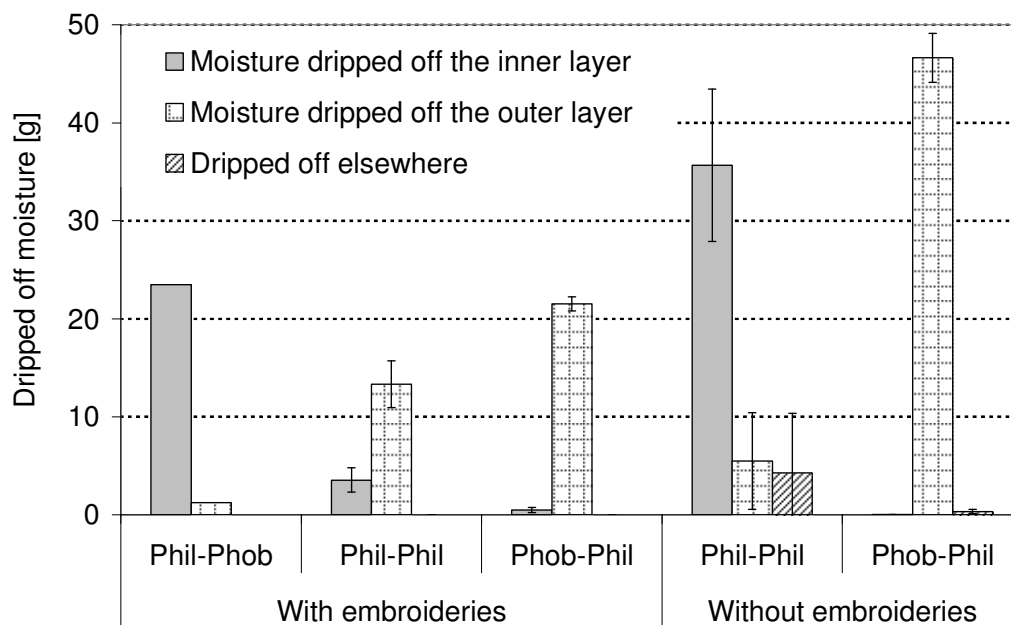Figure 7.5: Distribution of dripped off moisture from different textile combinations containing embroideries on the outer layer, cross connected to the inner layer by seams and from combinations without embroideries.

The results of the measurements are shown in Figure 7.5. In the combination of a hydrophilic inner layer with a hydrophobic outer layer, moisture was sparely transported by the cross connection to the outer layer and therefore only about 1.2 g water dripped off at the outer layer. We concluded that the outer layer has to be hydrophilic in order to achieve a wicking effect to the embroideries.

If the outer layer was hydrophilic, in both cases, in combination with a hydrophilic respectively with a hydrophobic layer, moisture was transported to the outer layer and more moisture dripped off from the outer layer than from the inner one. If both layers were hydrophilic 3.5 +/-1.3 g, moisture dripped off from the inner layer and 13.3 +/-2.4 g moisture from the outer layer. In the combination of a hydrophobic inner layer with a hydrophilic outer layer even 21.5 +/-0.7 g water dipped off from the outer layer while only 0.5 +/-0.3 g moisture dripped off from the inner layer. If we compared these results with the results of the measurements with the same combination of hydrophobic and hydrophilic layers but without the embroideries, we see that without the embroideries even more moisture was transported to the outer layer, as 46.6 +/-2.5 g water dripped off from the outer hydrophilic layer while less than 0.5 g dripped off from the inner hydrophobic layer.

The only real improvement could be found for the combination of two hydrophilic layers, where without the embroideries 35.7 +/-7.8 g water dripped off from the inner layer and only 5.5 +/-5.0 g water from the outer layer.

The combination of two hydrophilic layers promises to be the best solution due to comfort aspects. A hydrophilic layer next to the skin is more comfortable than a hydrophobic one. Furthermore, the cooling of the body due to the evaporation of sweat close to the skin is assured due to the higher moisture content in the hydrophilic layer than in the hydrophobic layer.

7.2.3 Conclusions

It is possible to drain moisture in arbitrary downwards directions or even horizontally using a drainage system. Surplus water can be collected and led out of the clothing or for example into a water reservoir. Using a two layer drainage system, surplus sweat can be drained away from the skin to an outer layer and then along the drainage out of the clothing. This would

allow managing all sweat directly in the underwear. Moisture accumulation in the firefighter jacket or trousers could be avoided using such a drainage system.

The drainage system consisting of embroideries only works properly with the right combination of hydrophilic properties of the samples. The outer layer of the system containing the embroideries has to be hydrophilic. The best effect was reached with a hydrophobic inner layer in combination with a hydrophobic outer layer. In order to have a comfortable system for the wearer a system consisting of two hydrophilic layers promises to be the best solution.

8   CONCLUSIONS AND OUTLOOK

Aim of this thesis was to investigate the transfer and the absorption of moisture within protective clothing layers and its effect on heat transfer. The main emphasis was put on conditions for the formation of steam burns. In a first part the distribution of moisture in textile layers was studied using the sweating torso in order to simulate real physical exercise with sweating. The evaporation of moisture within textile layers exposed to low level thermal radiation was investigated by analysing the temperature distributions within the layers as well as by X-ray radiography in the second part of the thesis. A model simulating evaporation of moisture within protective clothing layers exposed to thermal radiation and the heat and moisture transfer through the layers was implemented and compared with experimental results. Finally new solutions for a moisture management system and a moisture storage system to reduce the risk of steam burns were proposed and evaluated.

8.1   Conclusions

Evaporation was faster and took place at higher temperatures if the moisture was located in the outer layers of the clothing system than if it was located in the inner layers. In the X-ray measurements, an inwards steam flow and condensation of steam in the inner layers of the clothing combinations was found. As heat of evaporation is released during condensation, burns may occur due to this energy transfer to the skin. Furthermore, if steam is adsorbed by the skin and heat of sorption is released in the inner layers of the skin, this might lead to second degree steam burns. Therefore, moisture accumulation in the outer layers of the firefighter protective clothing has to be avoided. This can be reached for example by hydrophobic treatment of the whole firefighter jacket and trousers.

In contrast to the assumptions about the development of steam burns, we found that temperatures in wet clothing combinations were not higher than temperatures reached with measurements of dry combinations. Temperatures measured in clothing combinations containing a wet layer were found to be always lower than temperatures measured in the corresponding dry combinations. A sudden and fast evaporation was not found to take place. Evaporation occurred at constant temperature and at constant evaporation rate. A sudden blast of steam is therefore not likely to appear.

Analysing the moisture distribution within firefighter protective clothing, we found that moisture mainly accumulated in the inner layers of the clothing combination, which were the underwear, the station uniform layer or the liner of the firefighter jacket. Temperatures in those inner layers cannot be very high, because otherwise burns would appear just due to those high temperatures. On the other hand, no burns appear for example in a steam bath, where temperatures reach up to 55 °C at saturated steam. Temperatures have to be higher than this in order to cause burns. Assuming a microclimate of 100% relative humidity within the protective clothing layer, the firefighter should be able to easily bear temperatures up to 50 °C. As it needs less energy to heat up steam than to evaporate water, steam burns may appear due to heating up the saturated microclimate inside the clothing. Is the clothing suddenly exposed to a more intense external heat source, the temperature increase of the steam within the clothing may cause burns by stewing the skin in this hot steam.

Another burning scenario could be due to conductive heat transfer. Air is a very good insulator. But as soon as the air layer is removed, for example by compressing the firefighter protective garment, a high energy transfer to the skin could take place due to the high thermal conductivity of the water. This could also lead to burns, even to scalds as the clothing is sucked with water.

8.2 Outlook

Still a lot of questions concerning the development of steam burns are unsolved. The exact mechanism leading to steam burns is not yet clear. Further investigations about the evaporation at different kinds of thermal exposures and the steam transfer have to be done in further studies.

8.2.1   Further research

In this thesis only the influence of moisture in protective clothing layers exposed to low level thermal radiation was considered. A thorough study about the impact of the amount and the location of moisture in protective clothing exposed to different kinds and intensities of heat exposures shall give further insight into conditions at which the influence of the moisture in the protective clothing is either positive or negative

By improving the physical model, evaporation and steam movement through different kinds of textile layers could be predicted. Liquid moisture transfer as well as steam movement through the textile combinations depending on the porosity of the materials have to be considered. The heat of condensation cannot be neglected. In a further step, the model shall be expanded to two or three dimensions. Such a model will help to analyse the influence of different parameters on the evaporation rate and the steam transfer within the clothing layers without performing extensive laboratory tests.

In order to further investigate the development of steam burns, the evaporation of moisture within protective clothing layers has to be studied systematically for all kinds and intensities of thermal exposures. Especially the moisture moving towards the skin hast to be quantified and the energy released due to condensation of the steam has to be determined. The development of a sensor able to predict burns not only by skin temperature, but also due to the condensation of steam on the skin, respectively the absorption of hot steam into the skin would help to predict the occurrence of steam burns. In order to be able to develop such a sensor, the processes leading to scalds of the skin have to be studied thoroughly.

Determination of the steam transfer into the skin

No clear answer exists to the question whether steam penetrates the skin into deeper layers, where it can cause second degree burns.

In a small and exploratory study, we wanted to find out if the skin is able to absorb steam at a fast rate. Therefore, we compared the water uptake of the skin after immersion into liquid water and after exposure to steam. The moisture content of the right forearm of some friends was measured before and after the moisture exposure by means of a corneometer (Figure 8.1).
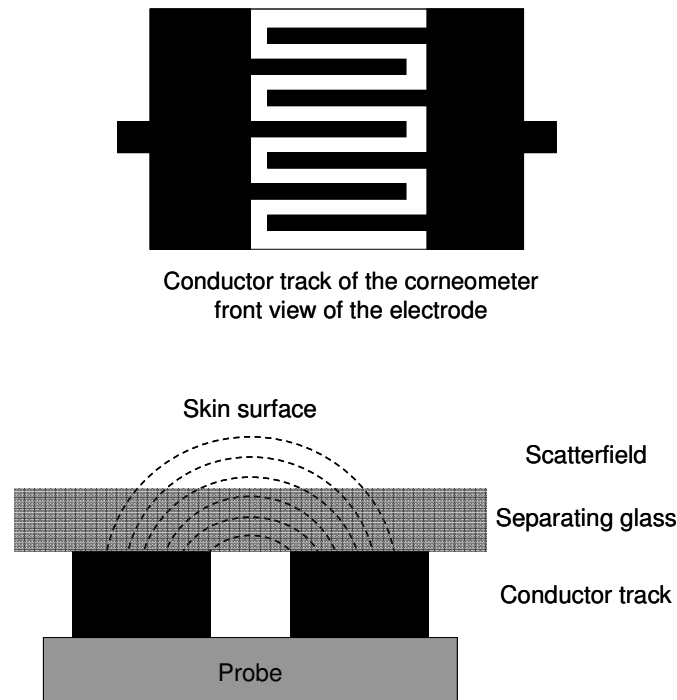
Figure 8.1: Functionality of the corneometer: A capacitor formed by two meshing gold combs induces a scatterfield. The change of dielectric constant of the skin is measured, whereof the moisture content of the skin can be determined.

The corneometer is an instrument to measure the stratum corneum hydration [123]. Hereby, the change of the capacity of a capacitor formed by two meshing gold combs is measured. The capacitor is pushed against the skin, which acts as a dielectric. The dielectric constant of the skin changes depending on its moisture content (dielectric constant of water $\varepsilon=81$).

CM arbitrary units	Skin type
< 30	Very dry skin
30-40	Dry skin
> 40	Normal skin

Table 8.1: Capacitive measurement of the humidity of the skin (CM arbitrary units) of different skin types using a corneometer.

The output of the corneometer (CM) is given in CM arbitrary units, which are linearly correlated with the moisture content of the skin [123]. The definition of the CM arbitrary units for the different skin types is given in Table 8.1.

7 members of our department (4 males and 3 females) agreed to take part in our study. Two different measurements were performed at different days, which were the measurement of the stratum corneum hydration after immersion of the skin into water at 35 °C and the stratum corneum hydration after the exposure of the skin to steam.

In the first test, the moisture content of the dry skin of the right forearm was measured with the corneometer. Afterwards, the forearm was immersed into a water bath of 35 +/-1 °C during 5 minutes. Thereafter, the arm was dabbed with a towel and the stratum corneum hydration was measured 30-45 s after the end of immersion.

For the second test, the stratum corneum hydration was measured again first of the dry skin of the right forearm. Afterwards, the participants held the inner side of their right forearm during 5 minutes over a water bath with a temperature of 75 +/-1 °C at a distance of about 10 cm (Figure 8.2). The arm and the bath were covered with a cardboard box in order to avoid effects due to air movements. The box did not contain any openings for steam transfer. Therefore a high humidity environment developed within the box, resulting in a steam temperature of 55 +/-5 °C. By lifting the box, an exchange of the air within the box and the environment took place, resulting in a temperature and humidity decrease whereby the participants could regulate the temperature in order to feel comfortable during the measurement.
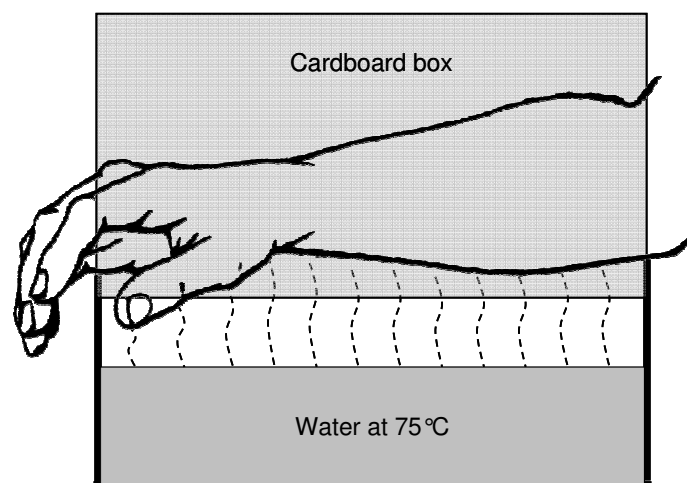

Figure 8.2: Setup of the experiment: The right forearm was held over a bath with water at 75 +/-1 °C. The arm and the bath were covered by a cardboard box in order to avoid effects due to air movements.

The difference between the wet and dry measurement of the stratum corneum hydration was calculated for both measurements. The results are shown in Figure 8.3.

Statistical analysis was performed using the Wilcoxon Signed Rank Test. The stratum corneum hydration was significantly higher after the exposure to steam than after immersion into a water bath, which strengthens the assumption that steam is absorbed by the skin. The impact of the temperature was not considered in this study, as it was not possible to immerse the skin into water of 55 °C. But the temperature is assumed to have a significant influence on the water absorption behaviour of the skin.
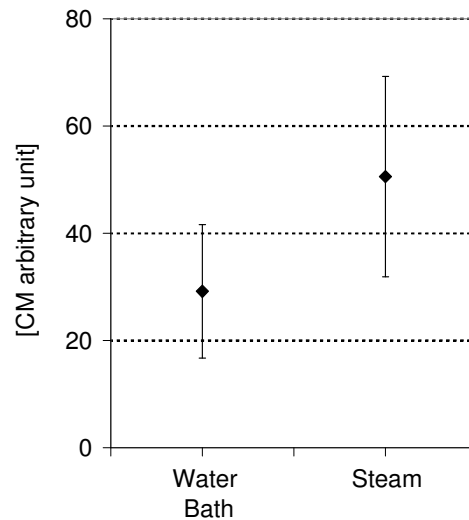
Figure 8.3: Stratum corneum hydration after 5 min immersion into a water bath of 35 °C versus 5 min exposure to steam of 55 °C.

In this exploratory study we wanted to find out whether hot steam is penetrating the skin and causing burns in deeper skin layers. The findings indicate that the water content of the skin increases more after exposure to hot steam than after immersion into temperate water. The impact of the higher temperature of the steam was not considered in this study. In a further survey the effect of the temperature on the penetration of liquid water respectively steam into the skin has to be investigated in more detail.

8.2.2 Future trends

Different new approaches to the problems concerning firefighting protective clothing are in development, for example phase change materials (PCM) [126, 127] or active cooling systems [128].

Phase change materials (PCM)

During the phase change of a material energy is absorbed or released respectively. If this phase change takes place at about environmental temperatures, this effect can be used for the storage of energy and especially in clothing technology to improve comfort applications [68, 126, 127, 129, 130]. In a study Rossi et al. [129] checked the applicability of this principle for firefighting environments. The PCM for this purpose consisted of paraffin with a melting point at around 50 °C. Slightly higher phase change temperatures would be necessary in order to improve the performance [129]. Furthermore, according to EN 469 [47], materials used for firefighter protective clothing must not melt. Therefore, further studies are necessary to improve the system in order to make it adaptable to firefighting environment.

Active cooling system

Active cooling systems were initially developed for astronauts in aerospace environments. Cao et al. [131] adapted this principle to the use in hot environments. They developed an active cooling system consisting of tubes within the garment in which cold liquid circulates. The body is cooled due to the circulation of this cold liquid. Batteries and a pump are necessary in order to keep the system running.

Another approach was used by Chitrphiromsri et al. [128]. They investigated the feasibility of a water-injection system. Hereby water is injected into the outer layer of the clothing at a sudden high thermal heat flux. The evaporation of this moisture absorbs a large amount of the impinging energy and temperatures within the clothing will not rise as high as without injection system. In order to prevent steam movement towards the skin, they propose the use of a moisture barrier with low vapour permeability.

8.2.3 Development of new solutions

Two possible new solutions for the improvement of firefighter protective clothing systems in order to prevent steam burns were proposed in this thesis. It needs still more work on those new solutions in order to be able to present a novel clothing concept for firefighters.

Superabsorbing polymers (SAP)

An additional layer containing superabsorbing polymers within the protective clothing could work as moisture storage. Furthermore, if soaked with water, it can work as cooling system due to the evaporation of water [124, 125]. In tests, vests containing superabsorbing polymers soaked with water provided a better protection against thermal radiation of 5 kW/m², 10 kW/m² and flashover situations. However, moisture transfer towards the skin was observed and therefore the risk of the appearance of steam burns cannot be excluded.

The sorption and evaporation behaviour of superabsorbing polymers have to be studied thoroughly in order to estimate the risk of steam burns due to the additional moisture present in the protective clothing system.

Drainage system

A two-layer drainage system was proposed in this thesis to collect moisture in the underwear, and lead it out of the clothing by stripes of embroideries. This system turned out to work well for the combination of two hydrophilic underwear knit layers. Further improvements of the system considering wicking properties of the yarn and lightness and flexibility of the textiles have to be done in order to make this system marketable. Furthermore, the effectiveness and the comfort of the system have to be studied thoroughly.

Finally, the proposed drainage system has to be worked out in more details in order to provide an efficient moisture management system for the prevention of steam burns.

REFERENCES

1. Barker, R. L., Guerth-Schacher, C., Grimes, R. V., et al., Effects of moisture on the thermal protective performance of firefighter protective clothing in low-level radiant heat Exposures. Textile Research Journal, 2006. **76**(1): p. 27-31.

2. Lawson, J. R., Fire fighter's protective clothing and thermal environments of structural fire fighting. In: Performance of Protective Clothing, 1997. American Society for Testing and Materials, West Conshohocken, PA: ASTM STP.

3. Lee, Y. M. and Barker, R. L., Effect of moisture on the thermal protective performance of heat-resistant fabrics. Journal of Fire Sciences, 1986. **4**(5): p. 315-331.

4. Mäkinen, H., Smolander, J. and Vuorinen, H., Simulation of the effect of moisture content in underwear and on the skin surface on steam burns of fire fighters. In: Performance of Protective Clothing, 1988. American Society for Testing and Materials, West Conshohocken, PA: ASTM STP.

5. Stull, J. O., The effect of moisture on firefighter protective clothing thermal insulation. In: 4th NRIFD Symposium, 2005. National Research Institute of Fire and Disaster, Mitaka, Tokyo, Japan.

6. Veghte, J. H., Functional integration of fire fighters' protective clothing. In: Performance of Protective Clothing, 1886. American Society for Testing and Materials, West Conshohocken, PA: ASTM STP.

7. Stull, J. O., The effect of moisture on firefighter protecting clothing thermal insulation: A review of industry research. In: Performance of Protective Clothing, 2000. American Society for Testing and Materials, West Conshohocken, PA: ASTM STP.

8. Prasad, K., Twilley, W. and Lawson, J. R., Thermal performance of fire fighters protective clothing. 1. Numerical study of heat and water vapour transfer. 2002,

National Institute of Standards and Technology, Fire Research Division: Gaithersburg, MD.

9. Lawson, J. R., Fire fighter's protective clothing and thermal environments of structural fire fighting. 1996, National Institute of Standards and Technology, Fire Research Division: Gaithersburg, MD.

10. Krasny, J. F., Apparel flammability - accident simulations and bench-scale tests. Textile Research Journal, 1986. **56**(5): p. 287-303.

11. Rossi, R., Experimentelle Untersuchung zur Wechselwirkung von Schutz und Physiologie bei Feuerwehrschutzkleidung Ph.D. thesis, Swiss Federal Institute of Materials Testing and Research (Empa) and Swiss Federal Institute of Technology (ETH), Zurich, 1999.

12. Holcombe, B. V., The evaluation of protective clothing. Fire Safety Journal, 1981. **4**(2): p. 91-101.

13. Schoppee, M. M., Welsford, J. M. and Abbott, N. J., Protection offered by lightweight clothing materials to the heat of a fire. In: Performance of Protective Clothing, 1986. American Society for Testing and Materials, West Conshohocken, PA: ASTM STP.

14. Hoschke, B. N., Standards and specifications for firefighters clothing. Fire Safety Journal, 1981. **4**(2): p. 125-137.

15. Abbott, N. J. and Schulmann, S., Protection from fire: Non flammable fabrics and coatings. Journal of Coated Fabrics, 1976. **6**: p. 48-64.

16. LeBlanc, P. R. and Fahy, R. F., Firefighter fatalities in the United States - 2003. 2004, National Fire Protection Association: Quincy.

17. Nunneley, S. A., Heat-stress in protective clothing - interactions among physical and physiological factors. Scandinavian Journal of Work Environment & Health, 1989. **15**: p. 52-57.

18. Schopper-Jochum, S., Schubert, W. and Hocke, M., Vergleichende Bewertung des Trageverhaltens von Feuerwehreinsatzjacken (Phase 1). Arbeitsmedizin, Sozialmedizin und Umweltmedizin, 1997. **32**(4).

19. Holmer, I., Protective clothing in hot environments. Industrial Health, 2006. **44**(3): p. 404-413.

20. Holmer, I. and Gavhed, D., Classification of metabolic and respiratory demands in fire fighting activity with extreme workloads. Applied Ergonomics, 2007. **38**(1): p. 45-52.

21. Taylor, N. A. S., Challenges to temperature regulation when working in hot environments. Industrial Health, 2006. **44**(3): p. 331-344.

22.   Clarke, J. A., A colour atlas of burn injuries. 1992. London: Chapman & Hall Medical.

23.   Moritz, A. R. and Henriques, F. C., Studies of thermal injury II: The relative importance of time and surface temperature in the causation of cutaneous burns. American Journal of Pathology, 1947. **23**(5): p. 695-720.

24.   Henriques, F. C., Studies of thermal injury V: The predictability and the significance of thermally induced rate processes leading to irreversible epidermal injury. Archives of Pathology, 1947. **43**(5): p. 489-502.

25.   Henriques, F. C. and Moritz, A. R., Studies of thermal injury I: The conduction of heat to and through skin and the temperatures attained therein - a theoretical and an experimental investigation. American Journal of Pathology, 1947. **23**(4): p. 531-&.

26.   Moritz, A. R., Henriques, F. C., Dutra, F. R., et al., Studies of thermal injury IV: An exploration of the casualty-producing attributes of conflagrations - local and systemic effects of general cutaneous exposure to excessive circumambient (air) and circumradiant heat of varying duration and intensity. Archives of Pathology, 1947. **43**(5): p. 466-488.

27.   Hardy, J. D., Stolwijk, J. A., Hammel, H. T., et al., Skin temperature and cutaneous pain during warm water immersion. Journal of Applied Physiology, 1965. **20**(5): p. 1014-&.

28.   Stoll, A. M. and Chianta, M. A., Method and rating system for evaluation of thermal protection. Aerospace Medicine, 1969. **40**(11): p. 1232-&.

29.   Rossi, R., Indelicato, E. and Bolli, W., Hot steam transfer through heat protective clothing layers. International Journal of Occupational Safety and Ergonomics, 2004. **10**(3): p. 239-245.

30.   Brans, T. A., Dutrieux, R. P., Hoekstra, M. J., et al., Histopathological evaluation of scalds and contact burns in the pig model. Burns, 1994. **20**: p. 48-51.

31.   Spencer-Smith, J. L., The physical basis of clothing comfort, Part 4: The passage of heat and water through damp clothing assemblies. Clothing Research Journal, 1977c. **5**(3): p. 116-128.

32.   Morris, A. M. and Rai, S., Sauna bath burn. British Medical Journal, 1978. **1**(6117): p. 894-895.

33.   Papp, A., Sauna-related burns: A review of 154 cases treated in Kuopio University Hospital Burn Center 1994-2000. Burns, 2002. **28**(1): p. 57-59.

34.   Chitrphiromsri, P., Modelling of thermal performance of firefighter protective clothing during the intense heat exposure. Ph.D. thesis, North Carolina State University, Raleigh, 2004.

35. Crown, E. M., Dale, J. D. and Bitner, E., A comparative analysis of protocols for measuring heat transmission through flame resistant materials: Capturing the effects of thermal shrinkage. Fire and Materials, 2002. **26**(4-5): p. 207-213.

36. Song, G., Modeling thermal protection outfits for fire exposures. Ph.D. thesis, North Carolina State University, Raleigh, 2002.

37. Veghte, J. H., Functional integration of fire fighters' protective clothing. In: Performance of Protective Clothing, 1986. American Society for Testing and Materials, West Conshohocken, PA: ASTM STP.

38. Torvi, D. A. and Hadjisophocleous, G. V., Research in protective clothing for firefighters: State of the art and future directions. Fire Technology, 1999. **35**(2): p. 111-130.

39. Barker, R. L. and Song, G., The effect of clothing air layers on thermal protective performance in single layer garments. In: 4th NRIFD Symposium, 2005. National Research Institute of Fire and Disaster, Mitaka, Tokyo, Japan.

40. Chitrphiromsri, P. and Kuznetsov, A. V., Modelling heat and moisture transport in firefighter protective clothing during flash fire exposure. Heat and Mass Transfer, 2005. **41**(3): p. 206-215.

41. Crown, E. M., Lawson, L. K., Dale, J. D., et al., Moisture effects in heat transfer through clothing systems: Implications for performance standards. In: 4th NRIFD Symposium, 2005. National Research Institute of Fire and Disaster, Mitaka, Tokyo, Japan.

42. Havenith, G. and Heus, R., Ergonomical properties of firefighter clothing: Assessment using human subject testing. In: 4th NRIFD Symposium, 2005. National Research Institute of Fire and Disaster, Mitaka, Tokyo, Japan.

43. Rossi, R. and Weder, M., Untersuchung des Wärme- und Feuchtetransfers bei mehrschichtigen Schutzkleidungen. In: 5. Dresdner Textiltagung, 2000. Dresden, Germany.

44. Shinohara, M. and Yanai, E., Effects of moisture barrier on the thermal performance of firefighters' protective clothing. In: 4th NRIFD Symposium, 2005. National Research Institute of Fire and Disaster, Mitaka, Tokyo, Japan.

45. Song, G., Clothing air gap layers and thermal protective performance in single layer garment. Journal of Industrial Textiles, 2007. **6**(3): p. 193-205.

46. Torvi, D. A. and Threlfall, T. G., Heat transfer model of flame resistant fabrics during cooling after exposure to fire. Fire Technology, 2006. **42**(1): p. 27-48.

47. EN 469: 2003, Schutzkleidung für die Feuerwehr - Laborprüfverfahren und Leistungsanforderungen für Schutzkleidung für die Brandbekämpfung.

48. Rossi, R., Sweatmanagement - Optimale Feuchte- und Wärmetransporteigenschaften von Textilschichten. In: 39. Internationale Chemiefasertagung: Feuchtigkeitsaufnahme verschiedener Textilschichten in Kombination mit verschiedenen Textilkombinationen, 2000. Dornbirn, Austria.

49. Dias, T. and Delkumburewatte, G. B., The influence of moisture content on the thermal conductivity of a knitted structure. Measurement Science & Technology, 2007. **18**(5): p. 1304-1314.

50. Fan, J. and Cheng, X. Y., Heat and moisture transfer with sorption and phase change through clothing assemblies. Part I: Experimental investigation. Textile Research Journal, 2005. **75**(2): p. 99-105.

51. Li, Y. and Zhu, Q. Y., A model of coupled liquid moisture and heat transfer in porous textiles with consideration of gravity. Numerical Heat Transfer Part a-Applications, 2003. **43**(5): p. 501-523.

52. Rossi, R. M. and Zimmerli, T., Influence of humidity on the radiant, convective and contact heat transmission through protective clothing materials. In: Performance of Protective Clothing, 1995. American Society for Testing and Materials, Philadelphia: ASTM STP.

53. Lawson, L. K., Crown, E. M., Ackerman, M. Y., et al., Moisture effects in heat transfer through clothing systems for wildland firefighters. International Journal of Occupational Safety and Ergonomics, 2004. **10**(3): p. 227-238.

54. Bejan, A., Heat transfer. 1993. New York: John Wiley & Sons, Inc.

55. Incropera, F. P. and DeWitt, D. P., Introduction to heat transfer, 4 ed. 2002. New York: John Wiley & Sons, Inc.

56. Cussler, E. L., Diffusion: Mass transfer in fluid systems, 2 ed. 2000. Cambridge: Cambridge University Press.

57. Farnworth, B., A numerical model of the combined diffusion of heat and water vapor through clothing. Textile Research Journal, 1986. **56**(11): p. 653-665.

58. Barnes, J. C. and Holcombe, B. V., Moisture sorption and transport in clothing during wear. Textile Research Journal, 1996. **66**(12): p. 777-786.

59. Chen, X. M., Kornev, K. G., Kamath, Y. K., et al., The wicking kinetics of liquid droplets into yarns. Textile Research Journal, 2001. **71**(10): p. 862-869.

60. Crow, R. M. and Osczevski, R. J., The interaction of water with fabrics. Textile Research Journal, 1998. **68**(4): p. 280-288.

61. VanLangenhove, L. and Kiekens, P., Textiles and the transport of moisture. Textile Asia, 2001: p. 32-34.

62. Woodcock, A. H., Moisture transfer in textile systems, Part I. Textile Research Journal, 1962. **8**(32): p. 628-633.

63. Zhuang, Q., Harlock, S. C. and Brook, D. B., Transfer wicking mechanisms of knitted fabrics used as undergarments for outdoor activities. Textile Research Journal, 2002. **72**(8): p. 727-734.

64. Kissa, E., Wetting and Wicking. Textile Research Journal, 1996. **66**(10): p. 660-668.

65. Kim, S. H., Lee, J. H., Lim, D. Y., et al., Dependence of sorption properties of fibrous assemblies on their fabrication and material characteristics. Textile Research Journal, 2003. **73**(5): p. 455-460.

66. Lewandowski, M., Perwuelz, A. and Vroman, P., Influence of porosity on capillary flow in textiles. In: 3rd Autex Conference, 2003. Lodz.

67. Yoo, S. and Barker, R. L., Moisture management properties of heat-resistant workwear fabrics - Effects of hydrophilic finishes and hygroscopic fiber blends. Textile Research Journal, 2004. **74**(11): p. 995-1000.

68. Zhu, Q. Y. and Li, Y., Effects of pore size distribution and fiber diameter on the coupled heat and liquid moisture transfer in porous textiles. International Journal of Heat and Mass Transfer, 2003. **46**(26): p. 5099-5111.

69. Rajagopalan, D., Aneja, A. P. and Marchal, J. M., Modeling capillary flow in complex geometries. Textile Research Journal, 2001. **71**(9): p. 813-821.

70. Adler, M. M. and Walsh, W. K., Mechanisms of transient moisture transport between fabrics. Textile Research Journal, 1984. **54**(5): p. 334-343.

71. Marek, R. and Straub, J., Analysis of the evaporation coefficient and the condensation coefficient of water. International Journal of Heat and Mass Transfer, 2001. **44**(1): p. 39-53.

72. Krischer, O., Die wissenschaftlichen Grundlagen der Trocknungstechnik. 1992. Berlin: Springer-Verlag.

73. Jones, F. E., Evaporation of water: With emphasis on applications and measurements. 1992. Lewis cop.: Chelsea, Michigan.

74. Fan, J. T., Cheng, X. Y., Wen, X. H., et al., An improved model of heat and moisture transfer with phase change and mobile condensates in fibrous insulation and comparison

with experimental results. International Journal of Heat and Mass Transfer, 2004. **47**(10-11): p. 2343-2352.

75. Agache, P. and Humbert, P., Measuring the skin. 2004. Berlin: Springer-Verlag.

76. Bromley, L. A., Properties of seawater and its concentrates and related solutions at temperatures up to 400°F. 1972, United States Department of the Interior: Berkeley, California.

77. Kerslake, D. M., The stress of hot environments. 1972. Cambridge: Cambridge University Press.

78. Zimmerli, T. and Weder, M. S., Protection and comfort - A sweating torso for the simultaneous measurement of protective and comfort properties of PPE. In: Performance of Protective Clothing, 1997. American Society for Testing and Materials, West Conshohocken, PA: ASTM STP.

79. Richards, M. G. M. and Fiala, D., Modelling fire-fighter responses to exercise and asymmetric infrared radiation using a dynamic multi-mode model of human physiology and results from the Sweating Agile thermal Manikin. European Journal of Applied Physiology, 2004. **92**(6): p. 649-653.

80. Camenzind, M. A., Dale, J. D. and Rossi, R. M., Manikin test for flame engulfment evaluation of protective clothing: Historical review and development of a new ISO standard. Fire and Materials, 2006, published online (in press).

81. Holmer, I., Thermal manikin history and applications. European Journal of Applied Physiology, 2004. **92**(6): p. 614-618.

82. EN 31092: 1993, Physiologische Wirkungen: Messung des Wärme- und Wasserdampfdurchgangswiderstandes unter stationären Bedingungen (sweating guarded hot plate test).

83. McCullough, E. A., Kwon, M. and Shim, H., A comparison of standard methods for measuring water vapour permeability of fabrics. Measurement Science & Technology, 2003. **14**(8): p. 1402-1408.

84. DIN 53814: 1974, Bestimmung des Wasserrückhaltevermögens von Fasern und Fadenabschnitten.

85. DIN 53923: 1978, Bestimmung des Wasseraufnahmevermögens von textilen Flächengebilden.

86. DIN 53924: 1997, Bestimmung von Sauggeschwindigkeit von textilen Flächengebilden gegenüber Wasser (Steighöhenverfahren).

87. Hu, J. Y., Yi, L., Yeung, K. W., et al., Moisture management tester: A method to characterize fabric liquid moisture management properties. Textile Research Journal, 2005. **75**(1): p. 57-62.

88. Morton, W. E. and Hearle, J. W. S., Physical properties of textile fibres, 3 ed. 1993. Manchester, UK: The Textile Institute.

89. ISO 6942: 2002, Protective clothing - Protection against heat and fire - Method of test: Evaluation of materials and material assemblies when exposed to a source of radiant heat.

90. ISO/DIS 13506.3: 2003, Protective clothing against heat and flame – Test method for complete garments – Prediction of burn injury using an instrumented manikin.

91. Crow, R. M. and Dale, J. D., Evaluation of flash fire protective clothing using an instrumented mannequin. 1992, University of Alberta: Edmonton, Alberta, Canada.

92. Göpel, W., Hesse, J. and Zemel, J. N., Sensors - A comprehensive survey, Part II: Chemical and biochemical sensors. Vol. 3. 1992. New York: John Wiley & Sons, Inc.

93. Tränkler, H. R. and Obermeier, E., Sensortechnik: Handbuch für Praxis und Wissenschaft, ed. Obermeier, E. 1998. Berlin: Springer-Verlag.

94. Mitter, H., Uncertainty of humidity measurement of gases. Tm-Technisches Messen, 2005. **72**(5): p. 334-346.

95. Heber, K. V., Humidity measurement at high temperatures. Sensors and Actuators, 1987. **12**(2): p. 145-157.

96. Reusch, W., Virtual textbook of organic chemistry: Polymers. http://www.cem.msu.edu/~reusch/VirtualText/polymers.htm, 14/07/2006 [cited 2007].

97. GmbH, M. S., FLUITEX-Gewebe: Thermische Eigenschaften und chemische Beständigkeit. http://www.muehlen-sohn.de/ms_file/downloads/9910-062-Thermeigenschaft.pdf [cited 2007].

98. Limited, G. C., Polyaramid polymetaphenylene isophthalamide (Nomex) – properties and applications. http://www.azom.com/Details.asp?ArticleID=1994, 11/7/2002 [cited 2007].

99. Brandrup, J., Immergut, E. H. and Grulke, E. A., Polymer handbook, Fourth ed. Vol. 1. 1999. New York: John Wiley & Sons, Inc.

100. Umbach, K. H., Optimization of the wear comfort by suitable fibre, yarn and textile construction. In: 40. Internationale Chemiefasertagung: Feuchtigkeitsaufnahme

verschiedener Textilschichten in Kombination mit verschiedenen Textilkombinationen, 2001. Dornbirn, Austria.

101. Selic, E., Synthese und Charakterisierung von Superabsorbern für Wasser und wässrige Lösungen. Ph.D. thesis, Gerhard-Mercator-Universität, Duisburg, 1999.

102. Kaltenecker, O., Superabsorbierende Beschichtungen auf Vliesstoffen: Herstellung und Eigenschaften. Ph.D. thesis, Universität Stuttgart, Stuttgart, 1996.

103. Weder, M., Bruhwiler, P. A. and Laib, A., X-ray tomography measurements of the moisture distribution in multilayered clothing systems. Textile Research Journal, 2006. **76**(1): p. 18-26.

104. Aschoff, J., Günther, B. and Kramer, K., Energiehaushalt und Temperaturregulation. Physiologie des Menschen. Vol. 2. 1971. München: Urban & Schwarzenberg.

105. Hüsler, J. and Zimmermann, H., Statistische Prinzipien für medizinische Projekte. 2001. Bern: Verlag Hans Huber.

106. Fan, J. T. and Cheng, X. Y., Heat and moisture transfer with sorption and phase change through clothing assemblies. Part II: theoretical modelling, simulation, and comparison with experimental results. Textile Research Journal, 2005. **75**(3): p. 187-196.

107. Li, Y. and Zhu, Q. Y., Simultaneous heat and moisture transfer with moisture sorption, condensation, and capillary liquid diffusion in porous textiles. Textile Research Journal, 2003. **73**(6): p. 515-524.

108. Roels, S. and Carmeliet, J., Analysis of moisture flow in porous materials using microfocus X-ray radiography. International Journal of Heat and Mass Transfer, 2006. **49**(25-26): p. 4762-4772.

109. Krawiz, A. D., Introduction to diffraction in materials science and engineering. 2001. New York: John Wiley & Sons, Inc.

110. Whitaker, S., Simultaneous heat, mass, and momentum transfer in porous media: A theory of drying. Advances in heat transfer, ed. Hartnett, J. P. and Irvine, T. F. J. Vol. 13. 1977. New York: Academic Press.

111. Fan, J. T., Luo, Z. X. and Li, Y., Heat and moisture transfer with sorption and condensation in porous clothing assemblies and numerical simulation. International Journal of Heat and Mass Transfer, 2000. **43**(16): p. 2989-3000.

112. Fohr, J. P., Couton, D. and Treguier, G., Dynamic heat and water transfer through layered fabrics. Textile Research Journal, 2002. **72**(1): p. 1-12.

113. Li, Y. B. and Fan, J. T., Transient analysis of heat and moisture transfer with sorption/desorption and phase change in fibrous clothing insulation. Numerical Heat Transfer Part a-Applications, 2007. **51**(7): p. 635-655.

114. Lotens, W. A., Heat transfer from humans wearing clothing. Ph.D. thesis, TNO, Soesterberg, 1993.

115. Li, Y. and Holcombe, B. V., Mathematical simulation of heat and moisture transfer in a human-clothing-environment system. Textile Research Journal, 1998. **68**(6): p. 389-397.

116. Li, Y., Holcombe, B. V. and Apcar, F., Moisture buffering behavior of hygroscopic fabric during wear. Textile Research Journal, 1992. **62**(11): p. 619-627.

117. Li, Y. and Luo, Z., An improved mathematical simulation of the coupled diffusion of moisture and heat in wool fabric. Textile Research Journal, 1999. **69**(10): p. 760-768.

118. Li, Y., Zhu, Q. Y. and Yeung, K. W., Influence of thickness and porosity on coupled heat and liquid moisture transfer in porous textiles. Textile Research Journal, 2002. **72**(5): p. 435-446.

119. Fan, J. T. and Wen, X. H., Modelling heat and moisture transfer through fibrous insulation with phase change and mobile condensates. International Journal of Heat and Mass Transfer, 2002. **45**(19): p. 4045-4055.

120. Song, G. W., Barker, R. L., Hamouda, H., et al., Modeling the thermal protective performance of heat resistant garments in flash fire exposures. Textile Research Journal, 2004. **74**(12): p. 1033-1040.

121. Torvi, D. A. and Dale, J. D., Heat transfer in thin fibrous materials under high heat flux. Fire Technology, 1999. **35**(3): p. 210-231.

122. Zhang, J. H., Gupta, A. and Baker, J., Effect of relative humidity on the prediction of natural convection heat transfer coefficients. Heat Transfer Engineering, 2007. **28**(4): p. 335-342.

123. Khazaka, G., Assessment of stratum corneum hydration: corneometer CM 825. Bioengineering of the skin: Water and stratum corneum, ed. Fluhr, J., Elsner, P., Berardesca, E., et al. 2005. Boca Raton: CRC Press.

124. Bartkowiak, G., Liquid sorption by nonwovens containing superabsorbent fibres. Fibres & Textiles in Eastern Europe, 2006. **14**(1): p. 57-61.

125. Sadikoglu, T. G., Effect on comfort properties of using superabsorbent fibres in nonwoven interlinings. Fibres & Textiles in Eastern Europe, 2005. **13**(3): p. 54-57.

126. Shim, H., McCullough, E. A. and Jones, B. W., Using phase change materials in clothing. Textile Research Journal, 2001. **71**(6): p. 495-502.

127. Weder, M. and Hering, A., How effective are PCM materials? Experience from laboratory measurements and controlled human subject tests. In: 39. Internationale Chemiefasertagung: Feuchtigkeitsaufnahme verschiedener Textilschichten in Kombination mit verschiedenen Textilkombinationen, 2000. Dornbirn, Austria.

128. Chitrphiromsri, P., Kuznetsov, A. V., Song, G., et al., Investigation of feasibility of developing intelligent firefighter-protective garments based on the utilization of a water-injection system. Numerical Heat Transfer Part a-Applications, 2006. **49**(5): p. 427-450.

129. Rossi, R. M. and Bolli, W. P., Phase change materials for improvement of heat protection. Advanced Engineering Materials, 2005. **7**(5): p. 368-373.

130. Wang, S. X., Li, Y., Hu, J. Y., et al., Effect of phase-change materials on energy consumption of intelligent thermal-protective clothing. Polymer Testing, 2006. **25**(5): p. 580-587.

131. Cao, H. T., Branson, D. H., Peksoz, S., et al., Fabric selection for a liquid cooling garment. Textile Research Journal, 2006. **76**(7): p. 587-595.

CURRICULUM VITAE

Name: Corinne Keiser

Born: January 26, 1978 in Stans (NW)

Nationality: Swiss

Education

06/2004 - 09/2007	Ph.D. thesis at the Laboratory for Protection and Physiology *Empa, Swiss Federal Laboratories of Material Testing and Research and ETH Zurich*
10/1998 - 02/2004	Diploma Studies in Mechanical Engineering, *ETH Zurich*
08/1991 - 06/1998	Matura, *Kollegium St. Fidelis, Stans (NW)*

Career development

08/2002 - 10/2002	Semester project at the Institute of Traffic Security *Chalmers, Technical University of Gothenburg, Sweden*
01/2002 - 06/2002	Internship at *Sulzer Medica, Winterthur (now: Zimmer GmbH)*
09/2001 - 11/2001	Internship at the Institute of Fluid Mechanics *National Technical University of Athens, Greece*
09/1998 - 10/1998	Internship at the *Lake Lucerne Navigation Company*

Publications

C. Keiser, C. Becker and R. M. Rossi, Analysis of the distribution of sweat in firefighter protective clothing layers. In 3rd European Conference of Protective Clothing ECPC, Gdynia, Poland (2006).

C. Keiser, C. Becker and R. M. Rossi, Moisture transport and buffering in multilayer protective clothing fabrics. Textile Research Journal (2007).

C. Keiser and R. M. Rossi, Temperature analysis for the prediction of steam formation and transfer in multilayer thermal protective clothing at low level thermal radiation. Textile Research Journal, submitted (2007).

C. Keiser, P. Wyss and R. M. Rossi, X-ray radiography used to determine evaporation and moisture transfer within firefighter protective clothing exposed to low thermal radiation. International Journal of Heat and Mass Transfer, submitted (2007).